The combined role of Nth and MutY DNA glycosylases in *Mycobacterium smegmatis*

Gadisi Nthambeleni (1016339)

A dissertation submitted to the Faculty of Health Sciences, University of the Witwatersrand, Johannesburg, in fulfilment of the requirements for the degree of Master of Science in Medicine.

Declaration

I declare that this dissertation is my own, unaided work. It is being submitted for the degree of Masters of Science at the University of the Witwatersrand, Johannesburg. It has not been submitted before for any degree or examination at any other University.

_____

(Gadisi Nthambeleni) _____ day of _____ 2016

Abstract

During infection, *Mycobacterium tuberculosis* (MTB) encounters hostile conditions such as nutrient starvation, hypoxia and low pH which results in the generation of host-derived reactive oxygen (ROS) and nitrogen species (RNS) as part of the immune response to control the infection. Exposure to these reactive radicals can lead to oxidative damage of DNA which ultimately creates genomic instability through the introduction of mutations. Mycobacterial species have a high G+C content and these bases are particularly prone to oxidative damage. To counter this, MTB possesses specialized DNA repair systems such as the multi-step, multi-enzyme base excision repair (BER) pathway, wherein repair of oxidative damage is initiated by DNA glycosylases. These DNA glycosylases include the endonuclease III (Nth*)*, endonuclease VIII (Nei) and formamidopyrimidine glycosylases (Fp*g*). In addition, MutY which acts together with Fpg (MutM) and MutT, forms part of the GO system, preventing mutations produced from 7,8-dihydro-8-oxoguanine (8-oxoG) lesions. Previously in our laboratory, we demonstrated a novel antimutator role for Nth and MutY DNA glycosylases in the BER pathway for the maintenance of mycobacterial genome stability. These data showed an increase in spontaneous mutation rate and decreased survival of *Mycobacterium smegmati*s when the *mutY* gene was disrupted together with the *fpg* DNA glycosylases. Additionally, deletion of the *nth* DNA glycosylase in *M. smegmatis* resulted in increased mutation rates under DNA damaging conditions and its inactivation in combination with *nei* resulted in reduced survival in an oxidative environment, with a heightened mutation frequency. In this study, we further investigated the combined role of Nth and MutY in an attempt to uncover the molecular mechanisms that protect mycobacterial DNA under hostile host environments. Double deletion mutants of *M. smegmatis* mc^2155 lacking both the *mutY* and *nth* genes (Δ*mutY*Δ*nth*, Δ*nth*Δ*mutY*) were generated by homologous recombination. Both mutants displayed no growth defects under normal culture conditions (7H9 media) when

compared to the wildtype mc^{2}155 or the respective single *M. smegmatis* Δ*nth* and Δ*mutY* mutants. Under *in vitro* oxidative stress conditions, as generated by hydrogen peroxide, both the double deletion mutants displayed reduced survival kinetics compared to mc^{2}155 after 6 hours of exposure to hydrogen peroxide. As previously observed, loss of the *nth* gene resulted in increased DNA damage-induced mutation frequencies to rifampicin. In contrast, the *mutY* single deletion mutant and the double deletion mutants lacking both *nth* and *mutY* did not show increased DNA damage-induced mutagenesis compared to mc^{2}155. However, in the fluctuation assay, both double mutant strains, Δ*nth*Δ*mutY* and Δ*mutY*Δ*nth*, displayed an increase in spontaneous mutation rates to rifampicin when compared to wild type and the single Δ*nth*/Δ*mutY* deletion mutants. The Δ*nth*Δ*mutY* mutant demonstrated an exacerbated mutation rate when compared to the Δ*mutY*Δ*nth* mutant. Collectively, these data reinforce the previously observed antimutator role for the mycobacterial MutY and Nth DNA glycosylases. The exacerbated phenotype observed for Δ*nth*Δ*mutY* suggest that there is a functional hierarchy between the various DNA glycosylases in the BER pathway, with the Nth DNA glycosylase superseding MutY as an antimutator in mycobacterial genome maintenance.

Acknowledgements

I wish to convey my sincere gratitude to my supervisor, **Dr B.G. Gordhan** for the good job she has done. Your continuous support and encouragement throughout the study period have not gone unnoticed. Also, to **Prof B.D. Kana** for his patience, motivation and guiding my research for the past two years. I would like to thank all my **colleagues at the CBTBR**, who were willing to help and give me suggestions. It would have been a long difficult journey without you guys in the lab. I would also like to thank **Dr M. D. Chengalroyen** for her everyday support since day one. My research would not have been possible without your help. I would also like to thank **Tube** for helping me with the modelling and prediction of protein structures.

I would like to thank National Research Foundation (NRF) and the DST/NRF Centre of Excellence for Biomedical TB Research for financial assistance. The following grants were award to Dr.Bhavna Gordhan and Prof B.D. Kana, the South African Medical Research Council, the National Health Laboratory Service Research Trust, the South African Tuberculosis and AIDS Training (SATBAT) program under the National Institutes of Health/Fogarty International Centre, grant #1U2RTW007370/3 that facilitated this study.

Finally, I would like to thank my mom, three sisters, and my two lovely nieces, Rabeleni and Maanda Makwarela. They were always there supporting, cheering and encouraging me through good and bad times.

Presentations

This work was presented at the Molecular Biosciences Research Thrust (MBRT) post graduate research day on the 3rd of December 2015 (poster presentation).

Nthambeleni, S.G., Kana, B.D. and Gordhan, B. Is there a combined role for the Nth and MutY DNA glycosylases during DNA repair in *Mycobacterium smegmatis*?

Table of contents

Declaration……..……...1

Abstract……..……2

Acknowledgements……....4

Presentations……..…….....5

Table of Contents……...6

List of Figures……...…..…9

List of Tables……...……11

Nomenclature……...12

1. Introduction…..……16

1.1 Tuberculosis…….……..16

1.2 Tuberculosis Therapy…….…17

1.3 Tuberculosis infection……18

1.4 DNA damage caused by oxidative stress……..20

1.5 *Mycobacterium tuberculosis* defence against oxidative stress……..….21

1.6 DNA repair systems…….…..22

1.6.1 SOS repair system…….……..23

1.6.2 Recombination repair…….…….23

1.6.3 Nucleotide excision repair (NER) …….…….24

1.6.4 Base excision repair…….…....25

1.7 Glycosylase families involved in the base excision (BER) pathway…….……....26

1.8. Aim and objectives……30

1.8.1 Specific objectives……...31

2. Materials and Methods…….32

2.1 Bacterial strains and culture condition..…….32

2.2 Bacterial transformation conditions……..….....35

2.2.1 Preparation of chemically competent *E.coli* (DH5α) cells…….……35

2.2.2 Transformation of chemically competent *Escherichia coli* DH5α cells……35

2.3 Electroporation of *M. smegmatis*…….…….….36

2.4 Molecular biology techniques……....37

2.4.1 Mini-prep plasmid DNA extraction…….…...37

2.4.2 Maxi-prep plasmid DNA extraction……....37

2.4.3 Small scale genomic DNA extraction…….38

2.4.4 Large scale genomic DNA extraction…….38

2.4.5 Quantifying DNA……39

2.4.6 Polymerase chain reaction (PCR) …….…….39

2.4.7 Restriction endonuclease digestions……40

2.4.8 Agarose gel electrophoresis…….……40

2.4.9 DIG labelled probe synthesis…….…….40

2.4.10 Southern blot hybridizations……...…….…….41

2.5 Knockout vector construction……..…….43

2.5.1 Inactivation of the Nth and MutY DNA glycosylases to generate double deletion mutants…….45

2.5.2 Generation of SCO and DCO transformants…….……..46

2.5.3 Complementation of *M. smegmatis* mutants……..…….47

2.6 Phenotypic characterization of DNA glycosylase deficient mutant strains……...48

2.6.1 Growth kinetics under normal culture conditions……...48

2.6.2 Mutation frequency…….48

2.6.3 UV induced mutagenesis…….……....48

2.6.4 Sensitivity to H_2O_2…….….49

2.6.5 H_2O_2diffusion susceptibility test…….……....49

2.6.6 Mutation rate measurements……..…….50

2.6.7 Spectral analysis of rifampicin resistant mutants in the *rpoB* region……..52

3. Results……...……...……53

3.1 Bioinformatics of Nth and MutY DNA glycosylases……..…….……53

3.2 Confirmation of existing knockout constructs……...……57

3.3 Generation and identification of single crossover (SCO) and double crossover (DCO) mutants…….58

3.3.1 PCR confirmation of double mutants…….…….59

3.3.2 Southern Blot confirmation of double mutants…….…….….61

3.4 Complementation of the double deletion mutant strains……..…..66

3.4.1 PCR confirmation of complemented strains……...70

3.5 Phenotypic characterisation……....70

3.5.1 Growth kinetics……...70

3.5.2 Spontaneous mutation frequency……72

3.5.3 Effect of H_2O_2 on the survival of *M. smegmatis*……...……...73

3.5.4 H_2O_2 diffusion susceptibility test……....76

3.5.5 UV induced mutagenesis……77

3.5.6 Mutation rates of Nth and MutY DNA glycosylases……..81

3.5.7 Mutation spectrum……...83

4.0 Discussion……..87

4.1 Future studies…….94

5. Appendix……..95

5.1 Media preparation and solutions……95

5.1.1 *Mycobacterium smegmatis*…….…….95

5.1.2 *Escherichia coli*……...95

5.2 PCR and sequencing primers…….96

5.3 Vectors maps used in this study and previous studies……...97

5.4 Effect of hydrogen peroxide (H_2O_2) on the survival of *M. smegmatis* …….…….....100

5.5 DNA molecular weight markers……...102

6. References…….....103

List of Figures

Figure 1. The-multi-step, multi enzyme base excision repair (BER) pathway.…..……26

Figure 2.The GO pathway.....30

Figure 3. Strategy of generating combinational deletion of DNA glycosylase Nth and MutY in *M. smegmatis* 31

Figure 4. Schematic representation of the construction of knockout constructs using three way cloning. 44

Figure 5. Diagrammatic representation of allelic replacement by homologous recombination.. 46

Figure 6 .An example of the MSS-LC distribution graph/curve. 52

Figure 7. Predicted protein structure of the *M. smegmatis* Nth and MutY DNA glycosylases.. 54

Figure 8. Amino acid sequence alignments of the Nth and MutY DNA glycosylases from *M. smegmatis*, *M tuberculosis* and *E. coli*.,.....56

Figure 9. The p2NILΔ*nth*::pGOAL19 construct.....57

Figure 10. The p2NIL*mutY*::pGOAL17 construct. 58

Figure 11. PCR screen for identification of double gene knockout deleted mutant strains using *nth* primers.....60

Figure 12. PCR screen for identification of double gene knockout deleted strain using *mutY* primers.. 61

Figure 13. Genotypic characterization of mc^2155, Δ*mutY*, SCO and Δ*mutY*Δ*nth* by Southern blot analysis.. 63

Figure 14. Genotype characterization of mc^2155, Δ*mutY*, SCO and Δ*mutY*Δ*nth* by Southern blot analysis. 64

Figure 15. Genotypic characterization of mc^{2}155, Δ*nth*, SCO and Δ*nth*Δ*mutY* by Southern blot analysis. 65

Figure 16. Genotypic characterization of mc^{2}155, Δ*nth*, SCO and Δ*nth*Δ*mutY* by Southern blot analysis.. 66

Figure 17. Restriction mapping of pTWEETY::*nth.* 68

Figure 18. Restriction mapping of pTWEETY::*mutY*.. 69

Figure 19. PCR conformation of complemented strains..... 70

Figure 20. Growth curve of *M. smegmatis*mc^{2}155, single mutants, double mutants and complemented strains under normal culture conditions.. 71

Figure 21. Spontaneous rif^R mutation for single mutants, double mutants and complemented strains…. .. ……..…… 72

Figure 22. Rifampicin containing plates showing rif^R mutants from spontaneous mutation frequency assay.. 73

Figure 23. Assessment of mc^{2}155 with three different concentrations of H_2O_2.....74

Figure 24. Survival of mc2155, Δ*mutY*Δ*nth* , Δ*nth*Δ*mutY* and complemented strains under oxidative stress condition..... 76

Figure 25. H_2O_2 diffusion susceptibility assay of *M. smegmatis* and its derivative mutant and complemented strains.....77

Figure 26. Effect of different UV energies (25, 50, and 70 mJ/cm^2). (A) UV induced mutation frequency of *M. smegmatis* mc^2 155 to rifampicin..... 78

Figure 27. UV induced mutation frequency to rifampicin of mc^2 155, Δ*nth*, Δ*mutY*, Δ*nth*::*nth* and Δ*mutY*::*mutY*.....79

Figure 28. UV damaged induced mutation frequency of mc^{2}155, Δ*mutY*Δ*nth*, Δ*nth*Δ*mutY,* Δ*mutY*Δ*nth*::*nth* and Δ*nth*Δ*mutY*::*mutY* to rifampicin..... 81

Figure 29. The 81 bp RRDR region of the *rpoB* gene.. 85

Figure 30. pGEM3Zf(+). 97

Figure 31. p2NIL. 98

Figure 32. pGOAL17. 99

Figure 33. pGOAL19.. 99

Figure 34. pTWEETY. 100

Figure 35. Survival of the mc^{2}155, Δ*mutY*Δ*nth*, Δ*mutY*Δ*nth* and complemented strains under oxidative stress conditions.. 102

Figure 36. The DNA molecular weight markers. 102

List of Tables

Table 2.1: Bacterial strains used in this study.....33

Table 2.2: Bacterial vectors used in this study.....34

Table 3.1: Spontaneous mutation rates.....83

Table 3.2: Mutation patterns and percentage distribution of the rifampicin resistant mutations found in the RRDR region.....86

Table 5.1: Primers used in this study.....96

Nomenclature

A	Adenine
AIDS	Acquired Immune Deficiency Syndrome
Amp	Ampicillin
AP	Apurinic/Apyrimidinic
aph	Gene Encoding Kanamycin Resistance
BCG	Bacille Calmette-Guerin
BER	Base Excision Repair
BLAST	Basic Local Alignment Search Tool
bp	Base Pairs
BSA	Bovine Serum Albumin
C	Cytosine
CFU	Colony Forming Unit
CFZ	Clofazimine
CTAB	Cetyltrimethylammonium Bromide
DCO	Double Cross Over
DIG	Digoxigenin
DMSO	Dimethylsulphoxide
DNA	Deoxyribonucleic Acid
DNase	Deoxyribonuclease
DNTPs	Deoxynucleotide Triphosphate
DOTS	Directly Observed Treatment Short Course

DS	Downstream
EDTA	Ethylene Diamine Tetraacetic Acid
EMB	Ethambutol
EtOH	Ethanol
Fpg	Formamidopyrimidine DNA Glycosylase
g	Gram
G	Guanine
GFX	Gatifloxacin
G+C	Guanine and Cytosine
HIV	Human Immunodeficiency Virus
INH	Isoniazid
iNOS	Inducible Nitric Oxide Synthase
kan	Kanamycin
LA	Luria-Bertani Agar
lacZ	Gene Encoding β-galactosidase
LB	Luria-Bertani Broth
LTBI	Latent Tuberculosis Infection
m	Mili
M	Molar
MDR-TB	Multidrug-Resistant Tuberculosis
ml	Millilitre
MMR	Mismatch Repair
Min	Minutes

MutY	Adenine DNA Glycosylase
m-value	Number of Mutational Events
n	Nano
NaCl	Sodium Chloride
NaOH	Sodium Hydroxide
Nei	Endonuclease VIII
NER	Nucleotide Excision Repair
NOD	Nucleotide –Binding Oligmerazation Domain
Nth	Endonuclease III
OD_{600nm}	Optical Density at Wavelength of 600 nm
PAMP	Pathogen Associated Molecular Patterns
PCR	Polymerase Chain Reaction
PRR	Pattern Recognition Receptors
PTH	Prothionamide
PZA	Pyrazinamide
rif^R	Rifampicin Resistance
Rpm	Revolutions per minute
RRDR	Rifampicin Resistance Determining Region
SCO	Single Cross Over
sdH_20	Sterile Distilled Water
sacB	Gene Encoding Levansucrase
SDS	Sodium Dodecyl Sulphate
T	Thymine

TB	Tuberculosis
TDR-TB	Total Drug Resistance TB
TNF	Tumour Necrosis Factors
TLR	Toll Like Receptors
Tris	Tris (hydroxymethyl) aminomethane
Tween	Polyoxyethylene Sorbitan Monooleate
US	Up Stream
UV	Ultraviolet Light

1. Introduction

1.1 Tuberculosis

The genus *Mycobacterium* contains many important pathogenic bacteria such as *Mycobacterium leprae, Mycobacterium ulcerans* and *Mycobacterium bovis* which cause infections in both humans and animals. In humans, *Mycobacterium tuberculosis* (MTB) is the causative agent of tuberculosis (TB) which primarily infects the respiratory system. Robert Koch discovered the link between MTB and TB in 1882. Mycobacterial species are representative of both Gram-negative and Gram-positives (more related to Gram-negative), rod shaped bacteria with a diameter of between 0.2 -0.6 µm and length of 2-5 µm (Fu and Fu-Liu, 2002, Stoops *et al*., 2010). However, the gram classification of mycobacteria is problematic as it does not consider the mycolic acid layer in mycobacterial cell wall, which acts an outer membrane but is not comprised of phospholipids.

TB accounts for an estimated 1.4 million deaths and 9.6 million new cases of infection annually (WHO, 2015). In 1993, the World Health Organization (WHO) declared TB a global health emergency (WHO, 1993). Sub-Saharan Africa has the highest prevalence of TB worldwide and it is estimated that 254 000 adults and children died from TB related cases per year (Keugoung *et al*., 2014, Zumla, 2015). Moreover, people with compromised immune systems are more susceptible to TB hence, this opportunistic pathogen has consistently been one of the main causes of death in people living with Human Immunodeficiency Virus (HIV) or Acquired Immunodeficiency Syndrome (AIDS) (Rana *et al*., 2000, Corbett *et al*., 2003,Karim *et al*., 2009), with 15 % of TB incident cases being those co-infected with HIV/AIDS (WHO, 2009). This situation is further worsened by the rapid emergence of multi-drug resistant (MDR) forms of TB strains, which have acquired resistance against commonly used first line drugs such as rifampicin and isoniazid, extensively-drug resistant (XDR)

strains that are MDR but have also developed resistance to fluroquinolones and aminoglycosides. Totally drug resistant (TDR) strains of MTB are resistant to all first line and second line drugs (Zignol *et al*., 2006, Andrews *et al*., 2007, Hall *et al*., 2009, Calver *et al*., 2010, Gandhi *et al.*, 2010).

1.2 Tuberculosis Therapy

The only available and licensed vaccine for TB is *M .bovis* BCG (Bacille Clammete–Guerin), made from an attenuated strain of *Mycobacterium bovis.* BCG is usually given to new-born babies immediately after birth. However, the limitation of BCG is its varying efficacy against pulmonary tuberculosis in different settings, ranging from 60% to 80% in both infants and children (Colditz *et al*., 1994, Rodrigues *et al*., 1993, Fine, 1995). The reasons for this variation in efficacy include genetic variation in strains, genetic variation in human populations and geographical location (Brewer, 2000, Rowland and McShane, 2011).

The currently available first line TB drugs are more than 40 years old. Hence, there is a dire need for novel drugs for the treatment of TB, particularly for the treatment of MDR, XDR and TDR strains. The first line TB drug regimen includes a four-drug cocktail comprising of rifampicin, isoniazid, pyrazinamide and ethambutol for 6 months for the treatment of drug susceptible strains (McIlleron *et al*., 2006, Ma *et al*., 2010). As mentioned previously, the rapid emergence of drug resistant strains has rendered many of these treatments ineffective, thus requiring prolonged treatment of approximately 18 months and the use of second line drugs such as cycloserine, ethionamide, *p*-aminosalicylic acid (PAS), kanamycin and fluoroquinolones (Chhabra *et al*., 2012, Singh *et al.*, 2012). This lengthy treatment creates two major challenges which includes, managing the toxicity of the drugs and making sure that the patient is compliant until the end of treatment (Longo *et al*., 2015). Countries, like

Bangladesh and Cameron, have shortened the time for the treatment of MDR-TB from 20 to 9 months with the use of a seven drug regimen, with a cure rate of 85 to 89% (Aung *et al*., 2014, Kuaban *et al*., 2015). The 9 month regimen includes high dosage of ethambutol (EMB), gatifloxacin (GFX), clofazimine (CFZ), pyrazinamide (PZA), prothionamide (PTH) followed by a 4 month intensive phase with, kanamycin (kan) and isoniazid (INH) (Aung *et al*., 2014).

Directly Observed Treatment Short Course (DOTS) is a highly recommended approach by WHO for fighting TB. It involves observation of the patient for 6 to 18 months by a health care worker to ensure that the patient swallows each of the anti-TB drugs prescribed, at each dosing interval (Mitchison, 1985, Sagbakken *et al*., 2013). The main goals of DOTS are to improve the cure rate, to monitor patient compliance and to prevent relapses due to MDR-TB (Cox *et al.*, 2006, Frieden and Sbarbaro, 2007).

1.3 Tuberculosis infection

The lung alveolar macrophages are the first line of defence against TB infection and phagocytose the bacilli. Monocytes and neutrophils are also recruited to the site of infection to assist with clearance of the pathogen. The membrane bound pattern recognition receptors (PRR)s such as Toll-like receptors (TLRs) and C-type lectins (TLRs) or cytoplasmic receptors such as the nucleotide-binding oligomerization domain-(NOD) containing proteins recognize the pathogen via the pathogen-associated molecular patterns (PAMPs) (Akira *et al*., 2006, Harding and Boom, 2010). The interaction between PPR and PAMPs triggers the innate immune response, leading to mild inflammation, initiating the antimicrobial response (Mogensen, 2009, Ahmad, 2010). Antimicrobial responses activate the transcription factor (NF)-κB and the production of cytokines such as tumor necrosis factor (TNF)-α, interleukin

(IL)-1, IL-12, chemokines and nitric oxide (Caamano and Hunter, 2002, Ahmad, 2010). An important mechanism that enables MTB to survive in macrophages is the ability to prevent maturation of the phagosomes into phagolysosomes, which allow the bacteria to multiply in the phagosome (Ahmad, 2010). In addition, T-cell cytokines, chemokines and other host cells, such as dendritic cells and endothelial cells, are also deployed to the site of infection as part of the adaptive immune response (Sasindran and Torrelles, 2011, Silva Miranda *et al*., 2012). This results in the formation of granulomas, widely considered a hallmark of tuberculosis infection (Sasindran and Torrelles, 2011, Silva Miranda *et al*., 2012). Granulomas are a collection of immune cells which cluster around the bacteria, acting as a blockade, effectively restricting diseases spread to other parts of the lung and are clearly visible on a chest X-ray, serving as a good indication of TB disease (Woodworth and Behar, 2006, Ramakrishnan, 2012). However, during infection bacilli are able to escape this harsh immune assault generated by the host immune system by transitioning into a state of low metabolic activity, also known as bacterial persistence (Flynn and Chan, 2001, Gengenbacher and Kaufmann, 2012).

Latent TB infection which can be diagnosed by a tuberculin skin test, describes an individual who is infected with TB but displays no symptoms of TB disease and is consequently not contagious (Barry *et al.*, 2009, Chao and Rubin, 2010). It is estimated that more than one third of the humanity is latently infected with MTB and these individuals serve as a large reservoir for future active disease as they carry a 10% annual risk of developing active TB through the process of reactivation (Dooley Jr *et al.*, 1990, Corbett *et al*., 2003). Risk factors that contribute to reactivation of latent TB range from HIV co-infection, host genetics, malnutrition, indoor air pollution, smoking or diabetes (Jick *et al*., 2006, Lönnroth and Raviglione, 2008). Studies have shown that people infected with HIV have a higher risk of reactivation compared to non-infected individuals (Horsburgh Jr, 2004).

Another efficient method used by infected macrophages to control infection is the production of reactive oxygen species (ROS) such as hydroxyl radicals (•OH), singlet oxygen ($^1O_2$), hydrogen peroxide (H_2O_2) and reactive nitrogen species (RNS) (Zahrt and Deretic, 2002, Cadet and Wagner, 2014). ROS and RNS have the ability to cause damage to proteins, lipids and nucleotides (DNA), thus leading to either cell death or genomic instability. ROS and RNS are produced in activated macrophages by two enzymes namely NADPH oxidase (NOX2/gp91^{phox}) and inducible nitric oxide synthase (iNOS) respectively (Ehrt and Schnappinger, 2009). The superoxide anions ($O2^{\cdot-}$) produced by NOX2 serve as a catalyst for the production of ROS (Babior, 1999). ROS are formed when NOX2 assembles into an active enzyme complex that transports electrons across the membrane from NADPH to molecular oxygen, which results in the production of O_2^-, which dismutates into H_2O_2 and generates lethal hydroxyl radicals (Ehrt and Schnappinger, 2009). IFNγ induces iNOS and generates nitrite along with nitrate through metabolism of nitric oxide.

1.4 DNA damage caused by oxidative stress

As mentioned previously, ROS and RNS also have the ability to inflict damage on DNA, and such damage often results in cell death or alternatively in genetic instability leading to mutations. The hydroxyl radical (•OH) is one of the most reactive free radicals, resulting in damage to DNA such as single or double stranded breaks, mismatch base pairing, as well as apurinic and apyrimidinic (AP) sites (Demple and Harrison, 1994,Dos Vultos *et al.*, 2009, Bridge *et al.*, 2014). Mycobacteria are mostly susceptible to oxidative damage because of the high G+C content in their genomes (Dos Vultos *et al.*, 2009, van der Veen and Tang, 2015). Guanine is most vulnerable to oxidative DNA damage when compared to other bases due to its high oxidation potential, resulting in lesions such as 8-oxo-7,8-dihydroguanine (8-oxoG), which is pro-mutagenic and 2,6-diamino-4-hydroxy-5-formamido-pyrimidine (FapyG),

which is cytotoxic as it has the ability to block replication (Laval *et al*., 1998, David *et al*., 2007). The 8-oxoG lesion may result in G:C → T:A transversions, resulting in mispairing with adenine during replication if not repaired (Maki and Sekiguchi, 1992, Hazra *et al*., 2001). 8-oxoG can be further oxidized to spiroiminodihydrantoin and guanidinohydantoin (Luo *et al*., 2000, Hailer *et al*., 2005). Other base adducts caused by these hydroxyl radicals and free radicals are oxidation of cytosine to hypoxanthine, formed as a result of oxidation of the 5,6 double bond of cytosine, producing cytosine glycol (von Sonntag and Schuchmann, 1994, Cadet *et al*., 1999, Gros *et al*., 2002). Hydroxyl radical attacks on adenine generate oxidative adenine derived products such as 4, 6-diamino-5-formamidopyrimidine (FapyAde) and 8-oxo-7, 8-dihydroadenine (8-oxoAde), resulting in AT → GC mutations (Tudek, 2003). When thymine is exposed to oxidative stress, it results in changes in molecular structure and produces substrates such as 4,5 dihydroxyhydrothymine know as thymine glycol, 5-hydroxymethyluracil (hmU) and 5-formyluracil (fU),which is one of the major oxidative thymine lesions (Masaoka *et al*., 2001, Pfaffeneder *et al*., 2014).

1.5 *Mycobacterium tuberculosis* defence against oxidative stress

To defend themselves against damage caused by oxidative stress, pathogens have evolved several mechanisms responsible for resisting ROS and RNS, which involve the use of detoxifying molecules, the scavenging of ROS by certain vitamins and enzymes or protein regulation (Asad *et al*., 2004, Gutteridge and Halliwell, 2010). Detoxifying mechanisms against oxidative stress have been well characterized in *Escherichia coli* (*E. coli*) (Storz and Imlayt, 1999). When *E. coli* is exposed to oxidative stress, OxyR and SoxRS induces the expression of oxidative stress response genes (Zheng *et al*., 1998). OxyR stimulates the expression of a set of antioxidant genes which includes the catalases *katG*, *katE* and *katF*,

ahpCF (alkyl hydroperoxidase) and *oxyS* (a regulatory RNA) (Zheng *et al*., 1998, Zheng *et al*., 2001). The SoxRS regulon also triggered the expression of *sodA* and *sodB* which are superoxide dismutases (Touati, 1988, Bébien *et al*., 2002). Through redox-responsive 2Fe-2S clusters, SoxRS controls the expression of oxidative stress responsive genes by sensing nitrogen and oxidative stress (Green and Paget, 2004).

Interestingly in mycobacterial species the homologue for SoxR is missing, while OxyR is non-functional (Deretic *et al*., 1995, Chawla *et al*., 2012). Studies have proposed that in order to manage ROS/RNS stress during infection, mycobacteria sense redox changes and make use of the heme-based DosR/S/T system along with the thiol-based SigH/RshA system as a redox sensor (den Hengst and Buttner, 2008). In addition, the KatG catalase-peroxidase is a fascinating oxidative protective enzyme, which efficiently and effectively decomposes hydrogen peroxide (H_2O_2) into water and oxygen (Ng *et al*., 2004, Vlasits *et al*., 2007). Other important enzymatic defensive mechanisms against these intermediates are alkyl hydroperoxide reductases such as AhpC which scavenges H_2O_2 from the host (Chen *et al*., 1998, Springer *et al*., 2001).

1.6 DNA repair systems

DNA integrity is important for optimal cellular functioning and bioinformatics analysis of the sequenced MTB genome revealed the presence of homologs involved in several DNA repair pathways, namely nucleotide excision repair (NER), base excision repair (BER), SOS and recombination repair, which together detect and repair DNA damage to prevent cell lysis and mutation (Mizrahi and Andersen, 1998, Cole *et al.*, 1998, Güthlein *et al.*, 2009). Notably, in mycobacteria an important repair pathway is absent, the DNA mismatch repair system which may have serious repercussions (causing genome instability) for the repair system of this

genus (Mizrahi and Andersen, 1998). However, despite this the MTB genome is stable, suggesting that it is able to repair mispaired bases using other repair systems.

1.6.1 SOS repair system

The essential components of the SOS repair system are the LexA (dimer) and RecA proteins, which act as a repressor and inducer respectively by stalling DNA replication (Brent and Ptashne, 1981, Boutry *et al*., 2013). When there is no DNA damage LexA binds to a specific sequence known as the SOS box, upstream of the *recA* and *lexA* genes and represses their expression (Little *et al*., 1981, Davis *et al*., 2002). When DNA damage occurs, RecA coordinates and stimulates the expression of the genes required for survival by binding to the single-stranded DNA, resulting in the formation of a nucleoprotein filament. This action stimulates auto-cleavage, with LexA activating the SOS genes involved in recombination repair (Davis *et al*., 2002, Žgur-Bertok, 2013). Bioinformatics analysis has demonstrated that MTB possesses all the required genes needed for a functional SOS system (Cole *et al*., 1998, Mizrahi and Andersen, 1998). The main role of the SOS repair system is to induce genes involved in DNA repair, including base excision repair (BER), nucleotide excision repair (NER) and recombination DNA repair depending on which is suitable for the type of damage (Friedberg *et al*., 2005). All the known mycobacterial DNA repair systems will be discussed further below.

1.6.2 Recombination repair

Recombination is an important biological process wherein two DNA molecules combine or exchange genetic material. This process can be either homologous (exchange of DNA

molecules occurring between two identical molecules) or non-homologous (exchange of DNA molecules without sequence homology). Double stranded breaks caused by free radicals, radiation or replication errors are normally fixed by homologous recombination repair (Kuzminov, 1999). In mycobacteria and other bacteria, the main mediator of recombination repair system is the *recA* gene (Muttucumaru and Parish, 2004). Briefly, when a double stranded break is recognised in the genome, it causes RecB, RecC and RecD to form a three subunit complex, RecBCD, which is bifunctional with both helicase and nuclease activity (Dillingham *et al*., 2003). Once this complex attaches to the ends, it rapidly digests the DNA in a $3' \rightarrow 5'$ fashion. RecA assists specifically in pairing the single stranded DNA molecule with a homologous single stranded protein to repair the double stranded break (Dixon and Kowalczykowski, 1995, Dillingham *et al*., 2003). Also in MTB RecA contains an intein that has to spliced out for the protein to be functional (Davis *et al*., 2001, Sander *et al.*, 2001). In other pathogens such as *Salmonella typhimurium*, a *recA* deficient mutant showed enhanced sensitivity to the DNA damaging agent, hydrogen peroxide (H_2O_2) (Buchmeier *et al.*, 1995) indicating that RecA plays a significant role during DNA repair.

1.6.3 Nucleotide excision repair (NER)

One of the key DNA repair pathways is nucleotide excision repair (NER), which involves the excision of oligonucleotides that are approximately 30 base pairs long. The enzymes of the NER pathway recognize and eliminate bulky pyrimidine dimer lesions and 6,4 photoproducts caused by UV irradiation and genotoxic compounds (Van Houten *et al*.,2002, Rastogi *et al*., 2010). There are three main enzymes involved in the NER pathway in bacteria, these are UvrA, UvrB and UvrC (ABC complex), which are assisted by DNA polymerase I and DNA helicase II (UvrD) (Dos Vultos *et al*., 2009, Farnell, 2011). The NER pathway is a four step

system, which starts with the scanning and recognition of DNA lesions by protein trimmers, including two molecules of UvrA and UvrB (UvrAB machinery), followed by the release of the two UvrA molecules and pre-incision by UvrB, which splits the two DNA strands to validate the position of the lesion. UvrC binds to the site of the strand to be cleaved on the phosphodiester bond, and generates cuts several bases (4-5) away from the damaged site. The helicase UvrD, binds and displaces the segment of the damaged strand from the DNA molecule, followed by filling of the gap with the correct nucleotide by DNA polymerase I and sealing by DNA ligase (Sancar, 1996, Van Houten *et al*., 2002, Shuck *et al*., 2008, Kisker *et al*., 2013).

Interestingly, the mechanism of NER between eukaryotes and prokaryotes is similar however, there is a difference in the number of proteins involved, with more proteins required in eukaryotes compared to prokaryotes (Farnell, 2011). The main component of NER in bacteria is UvrB, which is responsible for damage recognition with two molecules of UvrA (Skorvaga *et al*., 2002). In *E. coli* K12, a *uvrB* mutant was more susceptible to psoralen (a photoactive chemical agent) when compared with *uvrA* and *uvrC* gene knockout mutants, indicative of a distinct role in the repair of adducts (Lage *et al*., 2010). In MTB, the UvrB mutant is highly sensitive to acid nitrite, used as a source of NOS (Darwin and Nathan, 2005). Additionally, the UvrB mutant of *Mycobacterium smegmatis* has increased sensitivity to UV, low pH, reactive oxygen species (ROS) and hypoxia when compared with the wildtype (Kurthkoti *et al*., 2008). Taken together, NER in mycobacteria appears to play an important role in protecting the bacterium from damage inflicted by the host immune system.

1.6.4 Base excision repair

Base excision repair (BER) is an important DNA repair pathway that deals mainly with oxidatively damaged bases (Lu *et al*., 2001, Kurthkoti and Varshney, 2011). DNA glycosylases are the first enzymes in the pathway that are responsible for the recognition and removal of damaged DNA, Figure 1 (Fromme *et al*., 2004, Guo *et al*., 2010, Jacobs and Schär, 2012). BER can be viewed in five basic steps shown in Figure 1: (I) the DNA glycosylase identifies and removes the oxidatively damaged or incorrect bases (shown in red), which results in (II) the formation of an AP (purinic/apyrimidinic site) site. (III), the AP endonuclease cleaves the sugar-phosphate backbone, creating a single stranded break, resulting in a 3′ hydroxyl group and 5'-terminal deoxyribosephosphate residue.(IV) deoxyribophosphodiesterase (dRpase) excises the 5'-terminal deoxyribose phosphate and converts the3′ termini to a hydroxyl group. (V) DNA polymerase then adds in the new correct nucleotide (shown in yellow) and DNA ligase seals the nick.

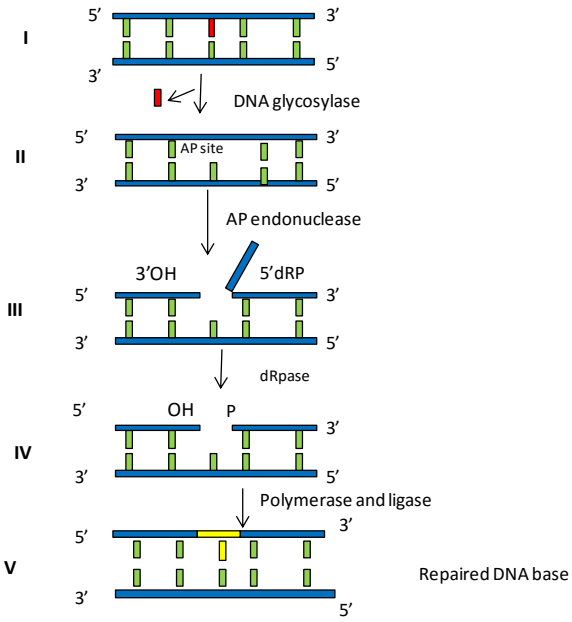

Figure 1. The-multi-step, multi enzyme base excision repair (BER) pathway showing the various steps involved in the repair of damaged bases. Modified from Kurthkoti and Varshney, 2011.

1.7 Glycosylase families involved in the base excision (BER) pathway

Glycosylases can be classified into families based on both sequence and structural homology. Even though structural and sequence homology may exists among members of the same family, these glycosylases can exhibit unique features and functions. In mycobacteria these glycosylases include the Endonuclease III (Nth) superfamily the formamidopyrimidine (Fpg/MutM/Fapy) and endonuclease VIII (Nei) DNA glycosylases which together form the Fpg/Nei family (Mizrahi and Andersen, 1998, Moolla *et al.*, 2014, Hassim *et al*., 2015).

Fpg and Nei glycosylases are categorized as the Fpg/Nei family as the sequence of these enzymes shares some common structural and biochemical features such as a helix-two-turn-helix motif (H2TH) and a zinc finger motif (Zharkov *et al*., 2003, Prakash *et al*., 2012). Additionally, it contains N- and C- terminal domains connected by a flexible hinge (Zharkov *et al.*, 2003). The N-terminal is composed of a β-sheet, whereas the α-helical C-terminal domain has a four cysteine zinc finger structure consisting of two anti-parallel β-strands, which are thought to be involved in DNA binding (Tchou *et al.*, 1993, Zharkov *et al*., 2003). Both Fpg and Nei are bi-functional glycosylases as they possess both glycosylase and AP activity, which allows for the cleavage of the phosphodiester bond. Notably, substrate preferences of Fpg and Nei are different; the main substrate for Fpg is oxidized purines such as highly mutagenic 8-oxoG, while Nei recognizes oxidized pyrimidines such as the thymine intermediate dihydrothymine (DHT) (Wallace *et al*., 2003, Zharkov *et al*., 2003, Prakash *et al*., 2012). In MTB and the non-pathogenic faster growing close relative of MTB, *Mycobacterium smegmatis* (*M. smegmatis*), two copies of Fpg (FpgI and FpgII) and Nei (NeiI and NeiII) exist (Mizrahi and Andersen, 1998, Cole *et al*., 1998). However, in MTB FpgI is non-functional as it is truncated at the 3' N-terminal and therefore, lacks the DNA binding domain required for glycosylase activity (Olsen *et al.*, 2009, Guo *et al.*, 2010).

The Nth and MutY DNA glycosylases are classified under the Nth super-family or Helix - hairpin-Helix (HhH) super-family (Thayer *et al*., 1995, Denver *et al*., 2003). Phylogenetic analyses indicates that the Nth protein is highly conserved in all phyla, with MutY found in only half of the Eukaryotes and less than half of the Archael species (Denver *et al*., 2003, Jacobs and Schär, 2012,). Sequence alignments of the *E.coli* Nth and MutY glycosylases indicate that they share some common features such as the Helix-turn Helix-hairpin motif involved in DNA binding, a glycine-proline-aspartate (GPD) motif and the 4Fe-4S cluster loop (FCL), which is not involved in either the binding or removal of damaged bases (Thayer *et al*., 1995, Zharkov and Grollman, 2002, Markkanen *et al*., 2013). In terms of activity the Nth DNA glycosylase is classified as a bi-functional enzyme as it possesses both glycosylase and AP activity that allows for the cleavage of the phosphodiester bond in the damaged DNA (Lomax *et al*., 2005, Hegde *et al*., 2008). The classification of MutY is controversial with some studies classifying it as mono-functional and others as bi-functional, with weak 3' AP lyase activity (Lu and Chang, 1988,Gogos *et al*., 1996, Corbett *et al*., 2003). Williams and David (1998) used an approach which traps the Schiff's base intermediate between DNA glycosylases and their substrates and demonstrated that MutY is a mono-functional glycosylase which lacks AP lyase activity (Williams and David, 1998).

Although Nth and MutY are sequence related, they are functionally different and do not share the same primary substrate specificity (Zharkov and Grollman, 2002). The main substrate for the Nth is oxidized pyrimidines (Bauche and Laval, 1999, Zharkov and Grollman, 2002) whilst MutY recognizes adenine mispaired with 8-oxo-7,8-dihydroguanine (8-oxoG) (Michaels *et al.*, 1990, Michaels and Miller, 1992). However, substrate overlap does exist between the Nth and Nei proteins as they share structural relatedness with Fpg and are able to recognize and repair oxidized purine lesions (Wallace, 1998, Prakash *et al.*, 2012). In *Salmonella typhimurium*, mutation phenotypes only became noticeable with the

combinatorial deletion of the *nth* and *fpg*/*nei g*enes, signifying an important antimutator role for *nth* (Suvarnapunya *et al.,* 2003). In support of this, a previous study conducted at the CBTBR has also demonstrated that lack of the Nth glycosylase in *M. smegmatis* results in increased DNA damage-induced mutations when bacteria are exposed to UV light and the combinatorial loss of Nth and Nei resulted in reduced survival when challenged with oxidative stress (Moolla *et al*., 2014). The increase in mutation rate upon deletion of Nth, individually or in combination with Nei, suggests an important antimutator role for Nth as well as a novel interaction between the Nth and Nei DNA glycosylases (Moolla *et al.*, 2014). In contrast, the combinational deletion of Nth and Fpg glycosylases did not result in increased mutation rates or reduced survival under oxidative stress (Moolla *et al*., 2014).

Organisms with G+C rich genomes like MTB are constantly at risk of being damaged by oxidative stress generated by the host, which may result in oxidative damage such as 8-oxoG (GO lesions) causing GC→TA and AT→CG mutations (Fraga *et al*., 1990, Steenken and Jovanovic, 1997). To counter such mutations, mycobacteria uses a DNA repair pathway known as the GO repair system, as shown in Figure 2 (Michaels and Miller, 1992, Kurthkoti and Varshney, 2012). The GO system involves the activity of three proteins, namely MutY, MutM (Fpg) and MutT, Figure 2 (Michaels and Miller, 1992, Tajiri *et al*., 1995). Briefly, (1) the guanine base is damaged by oxidative stress, forming an oxidized base 8-oxoG (red). (2) MutM/Fpg recognizes the damaged base pair, which is repaired by the BER pathway. (3) If replication takes place before the repair of the GO lesion by MutM/Fpg, this leads to the mis-incorporation of A with GO. (4) MutY binds to the mis-paired A against the GO lesion and offer a second chance to be repaired by Fpg. (5) The GO lesion is repaired by Fpgvia the BER pathway. If repair is not achieved this results in a GC→AT transversion (red box) (Michaels and Miller, 1992, Kurthkoti and Varshney, 2012). MutT eliminates oxidized dGTP

from the nucleotide pool, preventing insertion of damaged guanine bases during replication thus avoiding mismatches with adenine (Sakumi *et al*., 1993, Dos Vultos *et al*., 2009).

Sanders *et al.* (2009) investigated the consequence of the lack of the GO pathway in the GC rich bacterium *Pseudomonas aeruginosa*, by inactivating *mutM*, *mutY* and *mutT* and found that this resulted in increased mutations under oxidative stress conditions. Kurthkoti *et al*. (2010) investigated the role of *mutY* in *M. smegmatis*, and found that the loss of *mutY* did not result in phenotypic changes or increased mutation rates under an oxidative environment (Kurthkoti *et al*., 2010). In contrast, recent studies in our laboratory demonstrated an increase in spontaneous mutation rates and decreased survival of *M. smegmatis* when the *mutY* gene was disrupted together with the *fpg/nei* DNA glycosylases, suggestive of an antimutator role for MutY (Hassim *et al*., 2015).

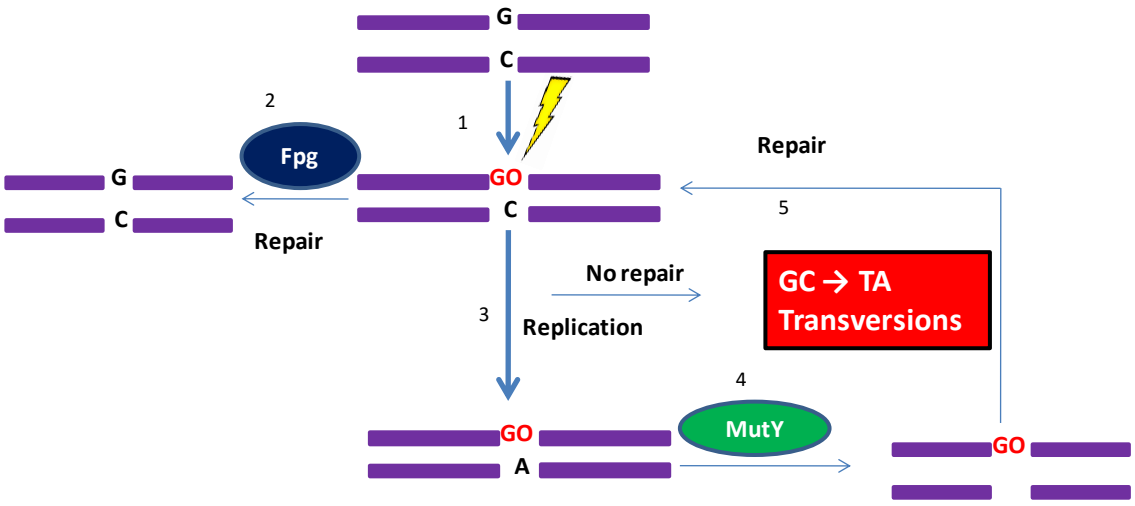

Figure 2. The GO pathway**.** Adapted from (de Oliveira et al., 2014).

1.8 Aim and objectives

The two previous studies at the CBTBR clearly demonstrated that the Nth and MutY DNA glycosylases are key enzymes of the BER pathway, responsible for preventing and or

reducing mutations in *M. smegmatis*. Hence, it is important to assess the combined role of these genes in maintaining mycobacterial genome integrity. In this study we aimed to assess the combinatorial role of these enzymes in BER. We hypothesize that the combined deletion of *nth* and *mutY* will lead to exaggerated mutation rates in *M. smegmatis*.

1.8.1 Specific objectives

Considering the above aims, the specific objectives were as follows:

- Generation of a *M. smegmatis* double deletion mutant strain by deleting the *mutY* gene in a Δ*nth* deletion mutant background and by deleting *nth* gene in a Δ*mutY*, using previously generated single deletion mutant strains and suicide vectors carrying inactivated copies of the *mutY* and *nth* genes respectively (Moolla *et al*., 2014, Hassim *et al*., 2015), Figure 3.

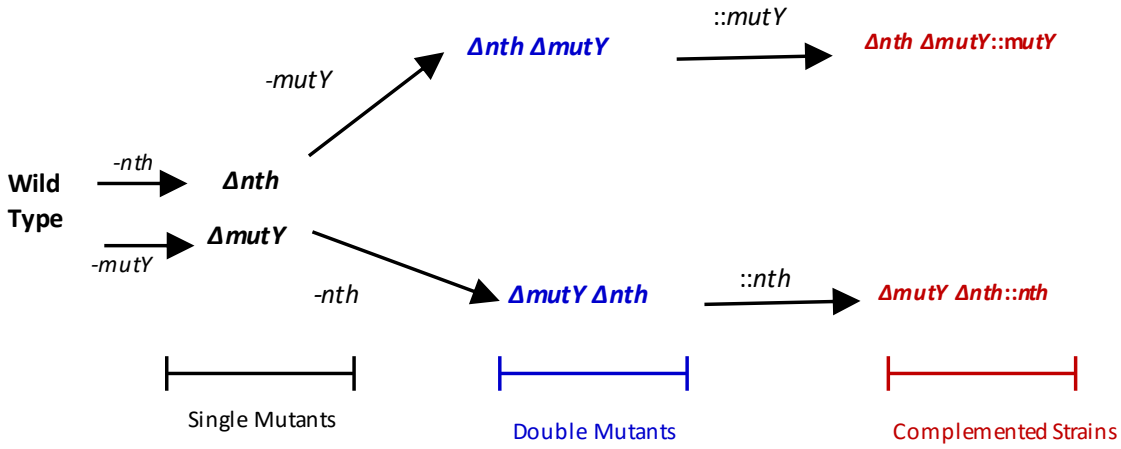

Figure 3. Strategy for generating combinatorialdeletion mutants of Nth and MutY DNA glycosylases in *M. smegmatis*

- Genotypic verification of the mutant and parental strains using PCR and Southern blot analysis.
- Complementation of mutant strains by reintroducing the respective functional gene into the mutant strain to confirm restoration of the observed phenotypes, Figure 3 red.

- Phenotypic characterization of the *M. smegmatis* mc^2155, single, double mutant and complemented strains by comparing the respective strains for:
    - Growth kinetics under normal growth conditions
    - Survival of the mutant and parental strains under oxidative stress conditions as generated by hydrogen peroxide.
    - Changes to rifampicin resistance.
    - Changes in spontaneous mutation rates as measured by the fluctuation assay.
    - Spectral assessment of the rifampicin resistant colonies isolated from the fluctuation assay to determine the genotype of the mutation that results in rifampicin resistance.

2. Materials and Methods

2.1 Bacterial strains and culture conditions

E.coli strains were grown overnight in a shaking incubator (Labcon shaking incubator) at 37°C in Luria-Bertani broth (1% tryptone, 1% NaCl, 0.5% yeast extract) (LB). LB media was supplemented with kanamycin (kan) at 50 µg/ml. *E. coli* strains transformed with large plasmids (>8kb) were grown at 30°C with shaking for two nights to prevent plasmid rearrangements. *M. smegmatis* and derivative strains were grown in Middlebrook 7H9 liquid medium (Difco) supplemented with 0.2% glycerol and 0.05% Tween80 (referred to hereafter as 7H9) with shaking or on Middlebrook 7H10 solid medium (Difco) supplemented with 0.085% NaCl, 0.2% glucose and 0.5% glycerol (referred to hereafter as 7H10). *M. smegmatis* complemented strains were grown in 7H9 supplemented with 25 µg/ml of kan.

Table 2.1. Bacterial strains used in this study.

Bacterial Strain	**Characteristics**	**Reference**
mc^2155	High frequency transformation mutant of *M. smegmatis* ATCC 607	(Snapper *et al*., 1990)
Δ*nth*	Derivative of *M. smegmatis* mc^2155 carrying an internal 570 bp deletion in *nth*	(Moolla *et al*., 2014)
Δ*mutY*	Derivative of *M. smegmatis* mc^2155 containing an internal 682 bp deletion in *mutY*	(Hassim *et al*., 2015)
Δ*nth*Δ*mutY*	Derivative of Δ*nth* carrying an internal 682 bp deletion in *mutY*	This study
Δ*mutY*Δ*nth*	Derivative of Δ*mutY* carrying and internal 570 bp deletion in Δ*nth*	This study
Δ*nth*::*nth*	Derivative of Δ*nth* carrying pTWEETY::*nth* integrated at the *attP*phage attachment site	(Moolla *et al*., 2014)
Δ*mutY*::*mutY*	Derivative of Δ*mutY*carrying pTWEETY::*mutY* integrated at the *attP*phage attachment site	(Hassim *et al*., 2015)
Δ*nth*Δ*mutY*::*mutY*	Derivative of Δ*nth*Δ*mutY* carrying pTWEETY::*mutY* integrated at the *attP*phage attachment site	This study
Δ*mutY*Δ*nth*::*nth*	Derivative Δ*mutY*Δ*nth* carrying pTWEETY:: *nth* integrated at the *attP*phage attachment site	This study
DH5α	*sup*E44 Δ*lacU*169 hsdR17 *recA*1 *endA*1 *gyrA*96 *thi*-1 *rel*A1	(Hanahan, 1983)

Table 2.2. Vectors used previously and in this study. Plasmid maps are shown in Appendix 5.3.

Plasmids	**Characteristics**	**Size(bp)**	**Reference**
pGEM3Zf(+)	*E. coli* cloning vector; amp^R; *lacZ*-alpha; *ori*E	3199	Promega
p2NIL	*E. coli* cloning vector and mycobacterial suicide plasmid; kan^R; *ori*E	4753	(Parish and Stoker, 2000)
pGOAL17	Plasmid carrying *lacZ* and *sacB* genes as a *Pac*I cassette; amp^R; *oriE*	8855	(Parish and Stoker, 2000)
pGOAL19	Plasmid carrying *lac*Z, *hyg* and *sacB* genes as a *Pac*I cassette; amp^R, *ori*E	10435	(Parish and Stoker, 2000)
p2NILΔ*mutY*::pGOAL17	p2NIL suicide vector carrying the deleted *mutY* gene and the selectable and counter selectable markers (*lacZ-sacB)* from pGOAL17, kan^R; *lacZ*; *sacB*; *oriE*	14508	(Hassim *et al*., 2015)
p2NILΔ*nth*::pGOAL19	p2NIL suicide vector carrying the deleted *nth* gene and the selectable and counter selectable markers (*hyg-lacZ-sacB)* from pGOAL19; kan^{R}hyg^R; *lacZ*; *sacB*; *oriE.*	14748	(Moolla *et al*., 2014)
pTWEETY	Mycobacterial integrating vector; kan^R, *ori*E, *int*	5835	(Pham *et al*., 2007)
pTWEETY::*mutY*	pTWEETY integrating vector carrying *mutY*: kan^R	7322	*(*Hassim *et al*., 2015)
pTWEETY:::*nth*	pTWEETY integrating vector carrying *nth*: Kan^R	6990	(Moolla *et al*., 2014)
pSE100	*E. coli*-Mycobacterium shuttle vector carrying Pmyc1*tetO*; Hyg^R	5538	Ehrt*et al*. 2005

amp^R–ampicillin resistance; *ori*E–origin of replication in *E.coli*; kan^R-Kanamycin resistance; hyg^R-hygromycin resistance.

2.2. Bacterial Transformation Conditions

2.2.1 Preparation of chemically competent *E.coli* (DH5α) cells

E. coli cells were inoculated in 50 ml of LB media and incubated at 37°C with shaking until the culture reached an optical density at a wavelength of 600nm (OD_{600nm}) of 0.5. The freshly grown cells were incubated on ice for 15 minutes (min) and centrifuged at 4500 revolutions per minute (rpm) for 5 min at 4°C. The cell pellets were re-suspended in 30 ml TfbI solution (30 mM potassium acetate, 100 mM rubidium chloride, 10 mM calcium chloride, 50 mM manganese chloride, and 15 % v/v glycerol - pH 5.8) and chilled on ice for 15 min. The cells were then harvested by centrifugation at 4000 rpm at 4°C. The pelleted cells were re-suspended in 10 ml TfbII solution (10 mM MOPS, 75 mM calcium chloride, 10 mM rubidium chloride and 15 % v/v glycerol), dispensed into 1 ml aliquots and stored at -80°C until required.

2.2.2 Transformation of chemically competent *Escherichia coli* DH5α cells

One hundred microlitres of chemically competent cells were chilled on ice for 15 min and mixed with 1-2 µg of plasmid DNA. The tubes were incubated in a heating block at 42°C for 90 seconds (heat shock) and then immediately transferred to ice for 2 min. Subsequently, 700 µl of 2XTY (2% tryptone, 1% NaCl, 1% yeast extract) was added to the cell mixture and incubated at 37˚C for 1 hour. Transformed cells were spread on LA agar plates containing the appropriate antibiotic and incubated at 37°C overnight to allow for growth of colonies. As a positive control to assess the transformation efficiency, chemically competent cells were transformed with 1 µg of a replicating plasmid pGEM3Zf(+) and 100 µl of a 10-fold dilution series was spread onto LA plates containing 100 µg/ml ampicillin. As a negative control competent cells were spread on LA plates containing ampicillin to ensure that the cells were

not contaminated. The plates were incubated at 37°C overnight or alternately at 30°C for two days when transforming large plasmids.

2.3 Electroporation of *M. smegmatis*

M. smegmatis cells were grown in 100 ml of 7H9 with shaking at 37°C to an OD_{600nm} of 0.6 - 0.8. The cells were harvested at 4000 rpm for 15 min at 4°C and washed three times by re-suspending the pellet in 20 ml of ice cold 10% glycerol. Washed cells were finally re-suspended in 900 µl of cold 10% glycerol and dispensed into three 300 µl aliquots in Eppendorf tubes. One-two µg of plasmid DNA was mixed with 300 µl of electro-competent *M. smegmatis* cells and then transferred to a cooled electroporation cuvette. The competent cells were exposed to an electrical pulse using the GenePulser™ electroporator (Bio-Rad) with the following parameters: 2.5 kV, 1000Ω and 25 µF. Subsequently, 800 µl of 7H9 was added to the cells and incubated for a minimum of 6 hours to overnight at 37°C to allow for recovery and replication of the transformants. The cells were then spread onto 7H10 plates supplemented with appropriate antibiotic/s and incubated at 37°C for 7-10 days. To determine the transformation efficiency, the replicating plasmid pSE100 (Table 2.2) was electroporated into an aliquot of competent cells, a 10-fold dilution series performed and plated onto7H10 plates containing 50 µg/ml of hygromycin. For the negative control, to ensure that the cells were not contaminated, no DNA was added to the cells and processed as described above.

2.4 Molecular biology techniques

2.4.1 Mini-prep plasmid DNA extraction

The mini-prep plasmid DMA extraction method was carried out using protocol described by Maniatis *et al*., 1982. *E. coli* clones carrying plasmid DNA were grown overnight at 37°C in 1 ml LB with shaking (250 rpm). One ml of the bacterial cells were harvested by centrifugation at 1300 rpm for 15 min and the pellets were re-suspended in 100 µl of solution I (0.5 M glucose,05 M EDTA, 0.1 M NaOH) followed by the addition of 200 µl of solution II (10 M NaOH, 10% SDS). After gentle inversion, 150 µl of solution III (5 M potassium acetate, 11.5% glacial acetic acid) was added and the tubes vigorously mixed. As a white precipitate formed, the tubes were incubated on ice for 10 min and centrifuged at 13000 rpm at room temperature for 10 minutes. The clear supernatant containing the plasmid DNA was precipitated with 500 µl of isopropanol by centrifugation at 13000 rpm for 10 min. The DNA pellet was washed with 70% ethanol and dried for 20 min in a SpeedVac concentrator (5301Eppendorf). The dried DNA pellet was re-suspended in 150 µl sterile distilled water (sdH_2O) to which 1µl of RNAse (10 mg/ml) was added and incubated at 42^oC for a further 15 min.

2.4.2 Maxi-prep plasmid DNA extraction

E. coli bulk plasmid DNA extraction was performed using the Nucleobond kit (Macherey Nagel) according to the manufacturer's specifications. *E. coli* clones were grown in 50 ml of LB broth with the appropriate antibiotics and the cultures were harvested by centrifugation at 4000 rpm for 10 min. The cells were re-suspended in 4 ml of buffer S1. Thereafter, 4 ml of buffer S2 was added followed by gentle inversion 5 times. Buffer S3 was added to the mixture, inverted till a white flocculent was visible and the suspension was centrifuged for 25

min at 4500 rpm. A Nucleobond column was equilibrated with 2.5 ml of buffer N2 and the clear supernatant was passed through the column. Thereafter, 10 ml of buffer N3 was added to wash the column and finally the DNA was eluted with 5 ml of buffer N5. The eluent was precipitated with 3.5 ml of isopropanol by centrifugation at 13000 rpm for 30 min. The pelleted DNA was washed with ice cold 70 % ethanol, air dried and dissolved in 200 µl of nuclease free water.

2.4.3 Small scale genomic DNA extraction

For small scale extraction of genomic DNA from *M. smegmatis*, the colony boil method was used. Briefly, a single colony was picked from solid media (7H10) and suspended in 50 µl of sdH_2O to which 50 µl of chloroform was added and boiled at 65˚C for 15 min. Thereafter, the mixture was centrifuged at 13000 rpm for 15 min and the supernatant containing the DNA was transferred into a fresh Eppendorf tube and used as DNA template for PCR reactions (Section 2.4.6).

2.4.4 Large scale genomic DNA extraction

The cetyltrimethylammonium bromide (CTAB) method (Doyle, 1987) was used for genomic DNA extraction from *M.* strains. Bacterial strains were spread onto solid media (7H10) and incubated at 37°C for two days. Cells were scraped off the plate using an inoculating loop and re-suspended in 500 µl of TE buffer (10 mM Tris-HCl, 10 mM EDTA, pH 8.0) and incubated at 65°C for 35 min. A 50 µl aliquot of lysozyme (10 mg/ml) was added and the mixture incubated at 37˚C for 60 min, followed by the addition of 6 µl of proteinase K (10 mg/ml) and 70 µl of 10% SDS. This mixture was incubated at 65°C for a further 120 min. Following the incubation, 100 µl of 5M NaCl and 80 µl of pre-warmed 10% CTAB was

added, mixed gently by inversion, and incubated at 65˚C for 10 min. Thereafter, 750 µl of chloroform: isoamyl alcohol (24:1) was added, gently inverted and centrifuged at 13000 rpm for 5 min. The top aqueous phase was transferred to a new tube and 600 µl of isopropanol was added. The DNA was concentrated by centrifugation for 25 min at 13000 rpm and the pellet was washed with 70% ethanol, air dried and dissolved in 500 µl of sdH2O.

2.4.5 Quantifying DNA

The Nanodrop ND-100 Spectrophotometer (NanoDrop technologies) was used to measure the concentration of nucleic acids at an absorbance of 260 nm (A_{260nm}). Water was used to blank the machine and 1µl of the DNA suspension was spotted onto the pedestal to measure the quantity and quality (A260/A at 280) of DNA.

2.4.6 Polymerase chain reaction (PCR)

PCR reactions were carried out using the FaststartTaq DNA Polymerase kit, (Roche Applied Science) following the manufacturer's instructions. All primers used in this study are listed in Appendix 5.2 and Table 5.1 (Moolla *et al,.* 2014; Hassim *et al.,* 2015). All PCR reactions were made up to a final volume of 50 µl, which contained 1-5 µl of template DNA, 2.5 µl each of the 10 mM forward and reverse primers, 10 µl of 10X GC rich buffer, 5 µl of Taq Buffer with 2 mM $MgCl_2$, 0.5 µl HotStartTaq and 8 µl 5XdNTPs(0.2 mM). Sterile distilled nuclease free water was used to adjust the reaction volume. Cycling conditions were carried out with the following parameters: denaturation at 95ºC at 5 min, followed by 30 cycles of denaturation at 94ºC for 30 seconds (sec), an annealing step at 61-67ºC (dependent on primers) for 30 sec and extension at 72ºC for 30 sec, ending with a final extension at 72ºC for 10 min.

2.4.7 Restriction endonuclease digestions

Restriction endonucleases and their respective buffers were purchased either from New England Biolabs, Roche Biochemicals or Fermentas and used according to the recommendations of the supplier. A standard restriction endonuclease digestion was carried out in a 20 µl reaction containing 0.5-1 µg of DNA and 1X restriction buffer. Bovine serum albumin (BSA) was added where necessary and an appropriate amount of sterile distilled water added to adjust the reaction volume. For plasmid digestions, the reactions were incubated at 37°C for 60 min (or for 30 min if the enzymes displayed star activity) and overnight for genomic DNA.

2.4.8 Agarose gel electrophoresis

DNA fragments were separated on 0.8% - 1%agarose gels. Generally, 5 µl of the DNA sample was mixed with 5µl of loading dye(1 ml 0.5 M Tris-HCl, 0.8 ml glycerol, 1.6 ml 10% SDS, 0.4 ml β-mercaptoethanol, 0.4 ml bromophenol blue and loaded into the wells of the agarose gel with an appropriate molecular weight marker (Roche Applied Science) for approximate size determination. The DNA fragments were separated in1X TAE buffer (1 mM EDTA, 40 mM Tris-acetic acid) at 90 V for 30 to 45 min depending on the size of the DNA fragments. For Southern blot analysis, the overnight genomic DNA digestion was separated for 2 to 3 hours on a 0.7% agarose gel at 80 V in cold TAE.

2.4.9 DIG labelled probe synthesis

To generate a labelled probe for Southern blot analysis, a PCR DIG Probe synthesis kit (Roche Applied Science) was used as per the manufacturer's instructions. Briefly,

approximately 1 µg of appropriate plasmid DNA was diluted to 50 ng with dH_2O. The PCR was carried out in a total volume of 50 µl with 1 mM forward and reverse primers added as listed in Table 5.1(Appendix 5.2) to amplify the upstream and downstream homologous regions. The positive PCR reaction was supplemented with 5 µl of DIG labelling mix and no DIG label was added to the negative control. The PCR product sizes were analysed on a 1% agarose gel to determine incorporation of the DIG label; the labelled product runs at a higher molecular weight on the gel compared to the unlabelled control, since incorporation of DIG increases the molecular size of the product. Five µl of the synthesized probe was added to 15 ml of DIG Easy Hyb solution (Roche Applied Science) for Southern blotting (Section 2.4.10) and the remaining labelled probe was stored at -20°C.

2.4.10 Southern blot hybridizations

The Southern blot technique enables a specific DNA sequence of interest to be identified from a complex mixture of DNA (Southern, 1975). This technique involves the separation of digested DNA by gel electrophoresis, transfer to a nitrocellulose membrane and labelling of the target DNA using a DIG labelled probe for visualization. Briefly, genomic DNA was prepared using the CTAB method (Section 2.4.4) from culture plate of *M. smegmatis* (mc^2155, Δ*nth*, Δ*mutY*, SCO strains, Δ*mutY*Δ*nth* and Δ*nth*Δ*mutY* Table 2.1). Approximately 2–3 µg of the genomic DNA was digested with appropriate enzymes and incubated overnight at 37°C. The digested DNA was separated on a 0.7% agarose gel as described in Section 2.4.8. The agarose gel was soaked in depurination buffer (0.2 M HCl) for 15 min at room temperature with gentle shaking, followed by two rinses with distilled water. The gel was then immersed in denaturation buffer (0.5 M NaOH, 1.5 NaCl) for 30 minutes, after which it was washed twice in distilled water and equilibrated in 1X TBE solution (89 mM Tris-Borate, 2 mM MEDTA, pH 8.3). The agarose gel was then covered with a Hybond

nitrocellulose membrane (Amersham) that was cut to size and sandwiched between two pieces of filter paper and two sponges. The assembled layers were enclosed in a plastic cassette and transferred to an electroblotting unit (OmniPAGEElectroblotting Unit, Cleaver Scientific Ltd CS-300 V) containing 1X TAE. The DNA was transferred onto the nitrocellulose membrane at 10 V for 2 hours at 4^{o}C. Subsequently, the DNA was UV cross-linked onto the nitrocellulose membrane at 2500 mJ/cm^2 in a UV-crosslinker for 2 minutes (UV Stratalinker 1800, Stratagene).

The membranes were pre-hybridized with 10 ml of DIG Easy-Hyb at 55°C for 15 min in a hybridizing oven (Hybrid Micro-4).The DIG Easy-Hyb solution with DIG labelled probe was heated to 95°C for 5 min and added to the hybridization bottle with the membranes. The membranes were hybridized overnight at 55°C in hybridizing oven. The following morning, the membranes were washed in 20 ml of pre-warmed 2X SSC wash solution I (300 mM NaCl, 30 mM sodium citrate and 0.1 % SDS), for 5 min at room temperature. Thereafter, the membranes were washed in solution II (0.5 × SSC and 0.1 % SDS) in the hybridizing oven at 65°C for 15 min. The above process was repeated twice after which the membranes were rinsed with wash buffer (0.1 M maleic acid buffer and 0.3 % Tween 20) for 10 min with gentle agitation at room temperature. Two microlitres of Anti-Digoxigenin-AP (Roche Applied Science) supplied with the kit was added to 20 ml of blocking solution and the membranes incubated for 30 min with gentle agitation. The membranes were then incubated in detection buffer for 5 min and placed inside a plastic hybridization bag (Roche Diagnostics; Mannheim, Germany) to which 1 ml CSPD (which emits a luminescent signal) was added. The hybridization bag was heat sealed and incubated for 10 min at 37°C. The membrane was then placed in an imaging cassette, exposed to X-ray film and placed in a dark

drawer for approximately 30-60 min. The X-ray film was developed using an automated developer (Axim).

2.5 Knockout vector construction

Plasmid constructs containing inactivated alleles of the *nth* and *mutY* genes were previously generated by PCR (Moolla, *et a*l., 2014; Hassim, *et al*., 2015). Briefly, as shown in Figure 4 (1) approximately 1500 bp upstream and downstream (red and green blocks respectively) of the genes of interest, containing residual 3' and 5' ends of the gene, were amplified by PCR using a high fidelity polymerase and primers that had appropriate restriction sites incorporated within the sequence. (2). The amplified upstream and downstream fragments were cloned into pGEM3Zf(+) (Appendix 5.3, Figure. 30) and sequenced to ensure mutations were not introduced during the PCR cycling. Subsequently, the upstream and downstream fragments were excised from pGEM3Zf(+)and (3) cloned by three way cloning into the suicide vector, p2NIL (Appendix 5.3, Figure31 [3]) which carries a kanamycin resistance marker. The Pac cassette from pGOAL17 (Appendix 5.3 Figure. 32) containing marker genes *sacB* and *lacZ* was inserted into the *Pac*I site of p2NIL (Figure. 4 [4]) to generate p2NILΔ*mutY*::pGOAL17 (map shown in Figure10) or the Pac cassette from pGOAL19 (Appendix 5.3 Figure. 33) with *sacB, lacZ, hyg* and was ligated into the *Pac*I site in p2NIL to generate p2NILΔ*nth*::pGOAL19 (map shown in Figure 9).

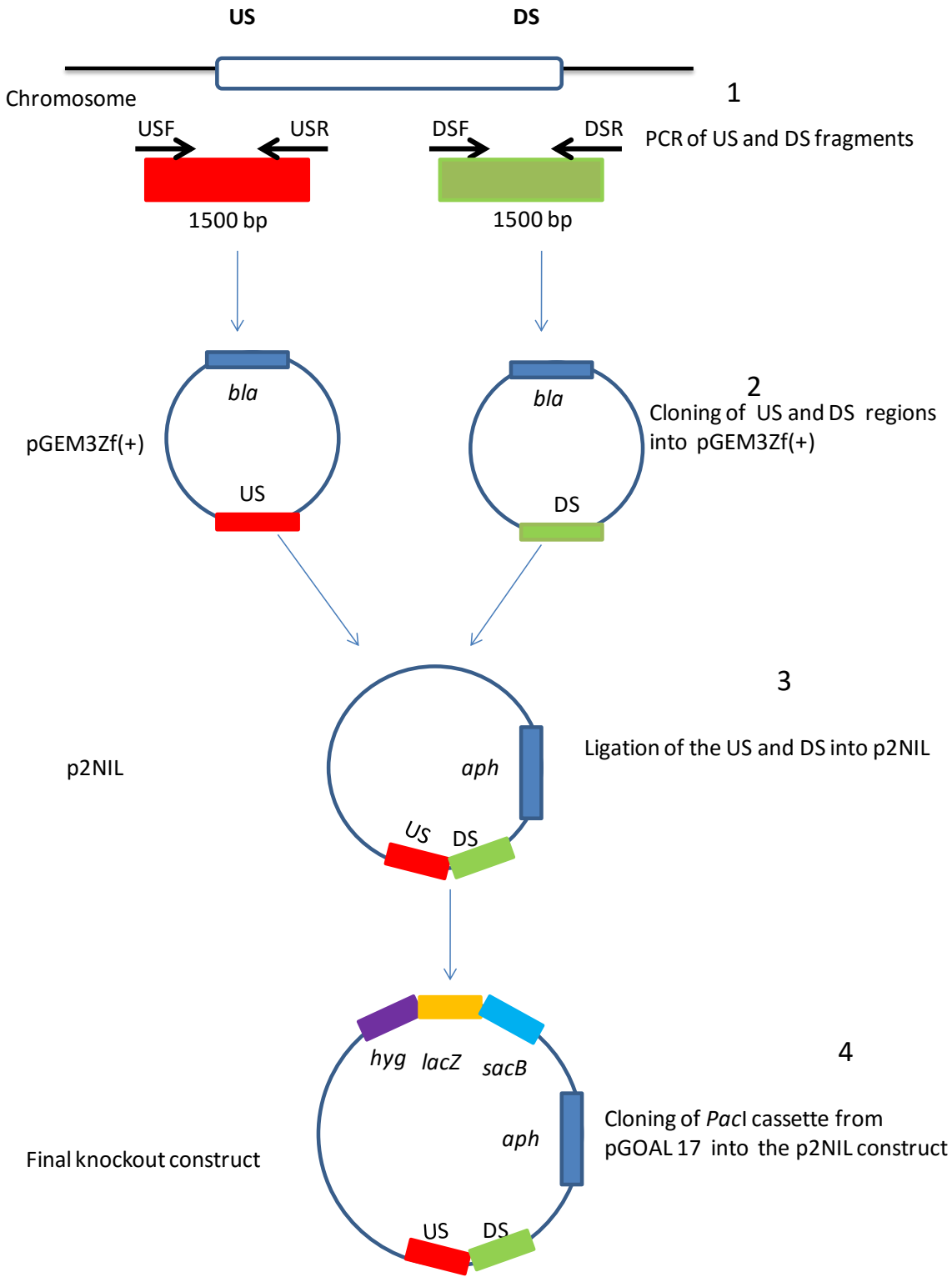

Figure 4. Schematic representation of the construction of knockout constructs using three way cloning.US – upstream region (red), DS – downstream region (green). The *bla* gene confers ampicillin resistance, *aph* gene confers kanamycin resistance and *hyg* gene confers hygromycin resistance. The black arrows represent forward and reverse primers.

2.5.1 Inactivation of the Nth and MutY DNA glycosylases to generate double deletion mutants

Homologous recombination using two-step allelic exchange methodology as described by (Gordhan and Parish, 2001) was used to generate gene deletion mutants. This involved the use of a suicide vector p2NIL (Table 2.2) carrying a truncated version of either the *nth* or *mutY* gene (Table 2.1) which was electroporated into competent *M. smegmatis* cells. Through homologous recombination the non-functional gene and the vector backbone is integrated into the mycobacterial genome, generating a single crossover mutant (SCO) carrying the wildtype gene, truncated gene and marker genes (*aph, sacB* and *lacZ).* The *lacZ* gene, which expresses the β-galactosidase enzyme that degrades X-gal into a blue colour, results in blue colonies which allows for the selection of single cross-over (SCO) homologous recombinants which carrying a copy of the functional gene and a copy of the truncated gene as depicted in Figure 5 (1 and 2). Single cross-overs were allowed to undergo a double cross over event in the presence of sucrose. The basis for this is that colonies retaining the *sacB* cassette will not be viable in the presence of sucrose, since *sacB* expresses levansucrase which converts sucrose to toxic levan thus killing the bacteria. Hence, white sucrose resistant colonies lose all the marker genes together with the vector sequence and are indicative of successful double cross over (DCO) transformants as shown in Figure 5 (3).

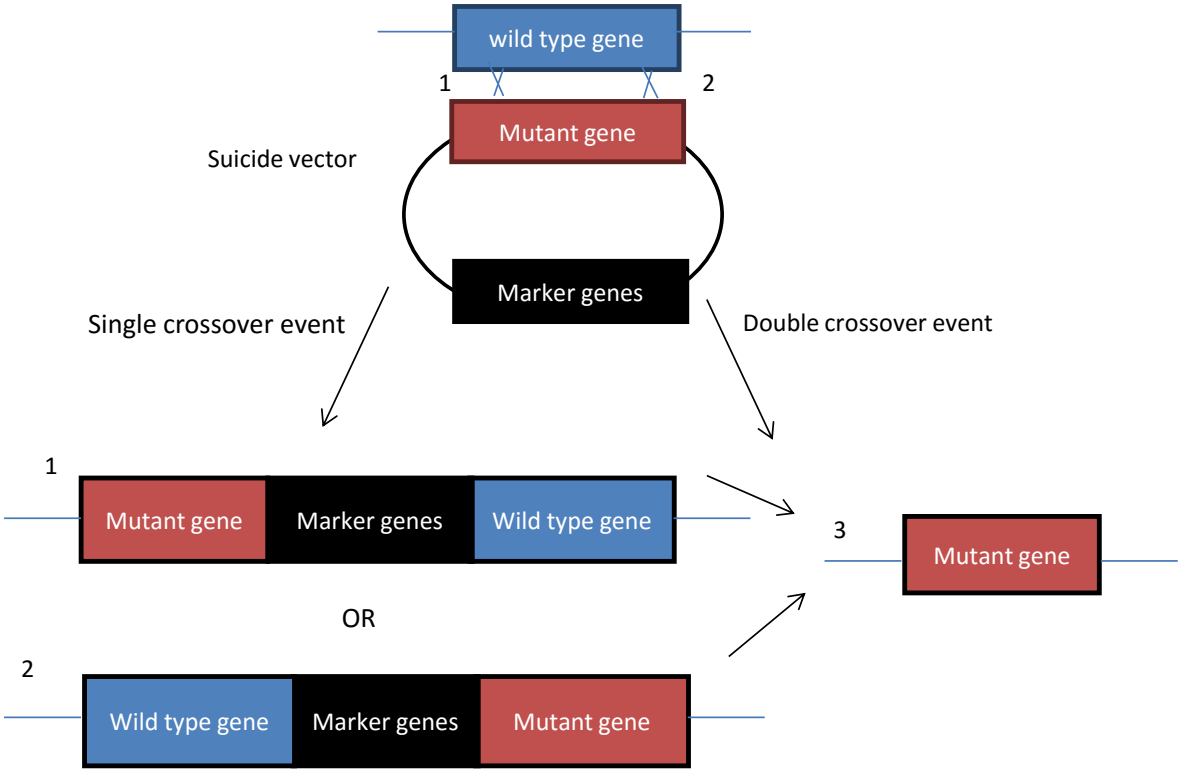

Figure 5. Diagrammatic representation of allelic replacement by homologous recombination**.** Marker genes – *sacB, lacZ, aph*and/or hygromycin resistance. Modified from (Gordhan and Parish, 2001).

2.5.2 Generation of SCO and DCO transformants

The p2NILΔ*mutY*::pGOAL17 and p2NILΔ*nth*::pGOAL19 suicide plasmids were electroporated into mid-logarithmic phase cultures of the Δ*nth* and Δ*mutY* deletion mutant strains respectively and selected on7H10 plates containing kan and X-gal to identify for SCO's. The genotype of the SCO's was confirmed by PCR (Section 2.4.6) and Southern blot analysis (Section 2.4.10). For the PCR, chromosomal DNA was extracted from potential SCO's using the colony boil method (Section 2.4.3) and the DNA amplified using primers that distinguished the mutant and the wild type alleles (Appendix 5.2 Table 5.1).

To generate DCO mutants, one of the PCR confirmed SCO's was selected and grown overnight in 10 ml 7H9 with kan. The overnight culture was inoculated into 20 ml of fresh 7H9 without antibiotics and grown at 37°C overnight to allow for the second crossover to

take place. The cells were serially diluted (10-fold) and100 µl of each of the dilutions (10^0-10^8) were plated on 7H10 supplemented with 2% sucrose and X-gal. Plates were incubated at 37°C and scored for white sucrose resistant colonies, which were potential DCO mutants. Potential DCO's were further confirmed for kan sensitivity by spotting on 7H10 media with and without the antibiotic. The potential confirmed DCO's were screened initially by PCR to distinguish between wild type and mutant alleles (Figures 11 and 12). The PCR confirmed putative mutants together with the SCO and parental stain were further analysed by Southern blot to ensure that the genes upstream and downstream of the deletion were genotypically intact.

2.5.3 Complementation of *M. smegmatis* mutants

To confirm that the phenotypes observed for the double gene knockout mutant strains was due to the loss of the respective DNA glycosylase gene and not due to downstream polar mutations, complementation strains were generated. For complementation, the full length of each functional gene with 350 bp of upstream sequence, carrying the promoter region, was previously amplified and cloned into the integrating vector pTWEETY (Appendix 5.3 Figure 33) to generate pTWEETY::*nth* and pTWEETY::*mutY* (Table 2.1). Both these constructs were created by two previous Masters students (Moolla *et al*., 2014, Hassim *et al*., 2015). As a secondary confirmation these vectors were rescreened in this study by restriction analysis to confirm that the vectors did not rearrange. The appropriate complementation vector was electroporated into the respective mutant strain and the resulting clones were screened by PCR (Figure19) using the colony boil method for DNA extraction. Two complemented strains, Δ*mutY*Δ*nth*::*nth* and Δ*nth*Δm*utY::mutY* were generated (Table 2.1).

2.6 Phenotypic characterization of DNA glycosylase deficient mutant strains

2.6.1 Growth kinetics under normal culture conditions

To determine growth kinetics of the various mutant strains, 1 ml bacterial freezer stocks were grown overnight at 37 ºC in 5 ml 7H9 medium with shaking at 100 rpm. The overnight late log phase culture was diluted into 50 ml of fresh media to a starting OD_{600nm} of 0.02 and growth of the cultures was monitored by OD_{600nm} measurements every 3 hours for a period of 36 hours. Growth was represented graphically as optical density over time.

2.6.2 Mutation frequency

For mutation frequency analysis, bacterial strains were grown overnight in 20 ml 7H9 at 37 ºC to an OD_{600nm} of 0.5 - 0.8. Aliquots (100µl) of 10 fold serial dilutions (10^4-10^7) were spread onto 7H10 media for colony forming unit (CFU) counts. The remaining culture was centrifuged for 15 minutes at 4500 rpm and the pellet re-suspended in 500 µl of fresh 7H9 broth. The cells were spread onto 7H10 supplemented with 200 µg/ml rifampicin (rif) and incubated at 37ºC. The plates were scored after 7 days for rifampicin resistant (rif^R) colonies. Mutation frequency was calculated as total number of rif^R colonies divided by the total number of colony forming units (CFU/ml) per culture.

2.6.3 UV induced mutagenesis

Overnight cultures grown in 100 ml of 7H9 to an OD_{600nm} of 0.6 in a shaking incubator were harvested by centrifuging at 4000 rpm for 15 minutes. The cells were re-suspended in 12 ml of 7H9 and split into two aliquots of 6 ml each. One aliquot was treated with UV at 50 mJ/cm^2 (UV Stratalinker 1800, Stratagene) and the other aliquot was the untreated control. 1

ml of the untreated cells was plated onto 7H10 plates containing 200 µg/ml rif and 0.1 ml for each of the dilutions (10^5-10^8) was plated onto 7H10 for viable colony counts. After UV treatment, damaged cell were added to 50 ml 7H9 and allowed to recover for 6 hours. At 3 and 6 hour time intervals, a 2 ml aliquot was sampled, serially diluted (10^5-10^8) and spread onto 7H10. The plates were incubated at 37ºC for 3 days before scoring. In addition 1ml was spread onto7H10 rif (200 µg/ml) plates and scored after 7 days for rif^R colonies. The induced damaged mutation frequency was calculated as total number of rif^R colonies divided by total population of cells (CFU/ml). The survival of UV treated cultures was scored by counting CFU of the surviving cells and represented graphically as log CFU/ml over time.

2.6.4 Sensitivity to H_2O_2

Bacteria were grown in 30 ml of 7H9 at 37ºC to early log phase (OD_{600nm} 0.35) and hydrogen peroxide (2.0 mM) was added to the cells to induce oxidative stress. At 2, 4 and 6 hour time intervals, 1 ml aliquots were removed, serially diluted (10^0 -10^7) in 7H9 and0.1 ml of each dilution spread onto 7H10 plates. The plates were incubated at 37ºC for 3 days before scoring for CFU's of surviving cells. The surviving cells were represented graphically as log CFU/ml over time.

2.6.5 H_2O_2diffusion susceptibility test

To investigate the sensitivity of the wildtype, single and double mutants and their respective complemented strains to H_2O_2, cultures of each of the strains were grown overnight in 7H9 at 37ºC with shaking to an OD_{600nm} of 0.35. A hundred microliters of the overnight culture was plated on 7H10 and allowed to dry for an hour. Aliquots of 0.5, 1.0 and 1.25 µl of an 880 mM

stock solution of H_2O_2 (0.176, 0.352 and 0.440 mM final concentration in agar plates respectively) was spotted in the centre of the plate and incubated at 37°C for three days. Zones of inhibition were recorded as the distance between the cleared zone and the edge where there was visible bacterial growth.

2.6.6 Mutation rate measurements

A mutation rate measure the likelihood of a cell gaining a mutation during its lifetime and takes into account the possibility of mutations arising either early or late during growth. The Luria-Delbrück fluctuation analysis was used to measure spontaneous mutation rates for the various mutants. This method allows for the number of mutational events to be accurately calculated by using parallel cultures, thereby minimizing variability (Rosche and Foster, 2000). The mutation rate was calculated as described previously by Machowski *et al*., 2007. Briefly, mutation rate is taken as the number of observed mutations per culture (*m*) within the total population (*Nt*). The mutation rates were analysed using either the P naught method (P0) or the Lea-Coulson Maximum Likelihood method (MSS-LC) (Rosche and Foster, 2000). To decide on the method of choice, the number of rif^R mutants per culture (*m*-value) needed to be determined. In order to estimate the *m*-value, the Ma-Sandri-Sarkar Maximum Likelihood Estimator (MSS-MLE) and the *Po* method were combined as explained by the Luria-Delbrück distribution. Using a spreadsheet for calculations generated by Machowski *et al*., 2007, MSS-LC distribution graph/curve was generated (Figure 6). The peak (green arrow) of the curve is the determined as estimated *m*-value which used to calculate the mutation rate.

The P0 method was used when there was a low number of rif^R mutants on selective plates, in this case it was used for analysis of the wildtype, Δ*nth*, *ΔmutY* and their respective complemented strains as the *m*-value was between 0.3 and 2.3. The MSS-LC was used when a high number of rif^R mutants (*m*-value) were obtained on selective plates, which was used

for Δ*nth*Δ*mutY*, Δ*mutY*Δ*nth* and their respective complemented strains as the*m*-values were between 1 to 15. The Mutation rate was calculated using the following formula:$\mu = \frac{m\ X\ In2}{Nt-\text{value}}$. Where *m* is the number of observed mutations per culture and *Nt* the total final number of cells in a culture. Frozen stocks of the parental, mutant and complemented strains were streaked on 7H10 and incubated at 37ºC until single colonies emerged. Single colonies from the respective strains were grown in 7H9 media to late log phase (10^8 cells/ml). A dilution series of the culture was performed and spread on 7H10 media to measure the initial inoculum (N_0). Also, 1 ml of the culture was spread onto 7H10 rifampicin plates to ensure that there were no pre-existing mutants. The cell density was diluted from 10^8cells/ml to 10^2 cells/ml and 2 ml aliquots were dispensed into 30 culture tubes which were incubated at 37°C with constant shaking (100 rpm) for 6 to 7 days until the cultures were in late log phase. The total population size (CFU/ml) was determined by randomly selecting 5 culture tubes out of the 30 and spreading a serial dilution of these on 7H10 plates (*Nt*). The culture from the remaining 25 tubes was plated individually on 7H10 rif (200 µg/ml) to score for spontaneous rif^R mutants (*m*-value). The 7H10 plates were incubated at 37ºC for 3 days for total population size count and 7 days for scoring rif^R mutants.

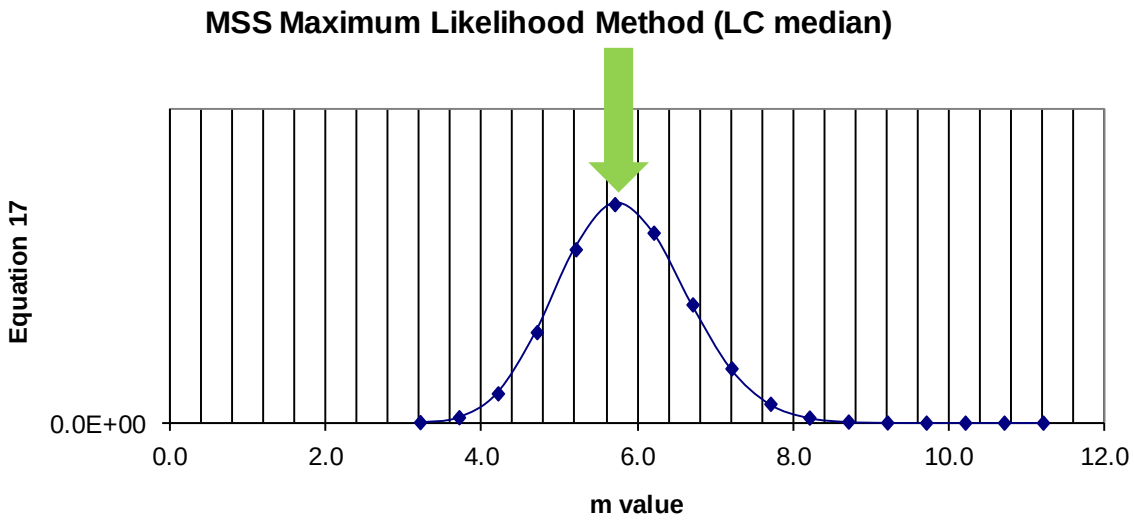

Figure 6. An example of the MSS-LC distribution graph/curve use to estimate the Rif^R mutants per culture (*m*-value).The green arrow represents the peak of the graph which is the estimated *m*-value from the data of the experiment.

2.6.7 Spectral analysis of rifampicin resistant mutants in the *rpoB* region

Most of the spontaneous rifampicin resistant mutations in mycobacteria are associated with mutations within the 81 bp rifampicin resistance-determining region (RRDR) found in the *rpoB* gene (Siu *et al*., 2011). To assess the spectrum of mutations in the rifampicin resistance-determining region (RRDR) of the *rpoB* gene, genomic DNA was extracted using the colony boil method from rifampicin resistant colonies isolated from the fluctuation assay (Section 2.6.6). Primers MSmrBR2 and MSmrBF2 listed in. (Appendix 5.2 Table 5.1) were used to amplify the RRDR of *rpoB* (549 bp). The PCR products were sequenced by DNA Sequencer Central Analytical Facility in Stellenbosch using the sequencing primer MSmrBF1 (Appendix 5.2 Table 5.1) to identify mutations resulting in rif^R.

3. Results

3.1 Bioinformatics of Nth and MutY DNA glycosylases

Bacterial survival in an oxidative environment requires constant adaptation. Bacteria are equipped with proteins and genes that detoxify, scavenge and repair the DNA damage caused by endogenous oxidative stress. When there is damage, glycosylases in the base excision repair (BER) pathway are responsible for locating and removing oxidatively damaged bases. Studies in *E. coli* of the Nth and MutY glycosylases clearly identified a functionally unique role for each enzyme however, some level of structural similarity has been recognized between the two proteins (Thayer *et al*., 1995). Crystal structures of the *E. coli* Nth and MutY DNA glycosylases show that both these proteins have the Helix-hairpin-Helix domain which serve as a DNA binding motif and a highly conserved 4Fe-4S domain, also important for DNA binding (Guan *et al*., 1998, Kuo *et al*., 1992). Previous mycobacterial amino acid alignments of Nth and MutY glycosylases identified that they contain an iron-sulfur cluster with the four cysteine residues and Helix-hairpin-Helix domain (Moolla, *et al*., 2014; Hassim, *et al*., 2015). In *M. tuberculosis*, *M. smegmatis* and *E. coli*, the *nth* gene is in the same chromosomal context (Moolla, *et al*., 2014). Comparisons of the protein crystal structures of the *E. coli* Nth and MutY revealed a 66% similarity between the two enzymes (Michaels *et al*., 1990). Similarly using tertiary structure prediction software (http://zhanglab.ccmb.med.umich.edu/I-TASSER/), the protein structures of both Nth and MutY from *M. smegmatis* were modelled (Figures 7A and 7B). The predicted protein structures showed the presence of the Helix-hairpin-Helix (HhH) motif, the four iron-sulphur (4Fe-4S) cluster for both the glycosylases, which appear to be highly conserved in mycobacteria. The overall folding of the predicted protein structures for both the enzymes are similar, with most of the residues buried inside the globule like structure (Figures 7A and 7B). Interestingly, both proteins in mycobacteria have conserved the helix-hairpin-helix and

the 4Fe-4S DNA binding residues. The one difference between the two enzymes is that at position 120, the tyrosine (Tyr120) in MutY (Figure 7A) is replaced with lysine (Lys) in the Nth DNA glycosylase (Figure 7B), suggesting that the latter enzyme has lyase activity whilst MutY does not (shown in turquoise).

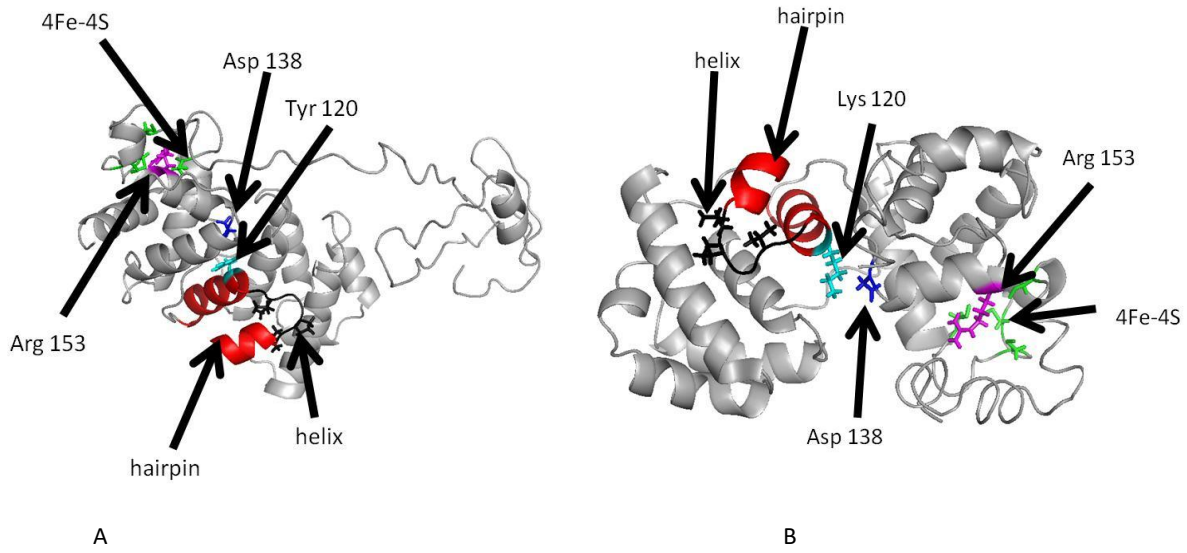

Figure 7. Predicted protein structure of the *M. smegmatis* Nth and MutY DNA glycosylases.Proteins were modelled using the I-TASSER pymol software (http://zhanglab.ccmb.med.umich.edu/I-TASSER/). (A) MutY DNA glycosylase and (B) Nth DNA glycosylase.

Amino acid comparisons of the sequences of the Nth and MutY proteins from *M. tuberculosis*, *E. coli* and *M. smegmatis* was done to confirm the amino acids responsible for lyase activity and to identify residues which may play an important role in determining substrate specificity (Figure 8). A pairwise alignment of the *Nth* and *MutY* glycosylases of *M. smegmatis* demonstrated 17% identical with 28% similar on the primary amino acid level, and for *M. tuberculosis* the proteins are 30% similar with 20% identical. In *E. coli* the Asp 138 residue in both Nth and MutY has been shown to be important for catalytic activity (Yang *et al.*, 2000). The Lys120 residue, has been reported to be essential for AP lyase

activity and cleaves the glycosidic bond by nucleophilc attack, noticeably this residue is replaced with valine in the *E. coli* MutY hence, accounting for the lack of mechanistic lyase activity (Thayer *et al.*, 1995, Guan *et a*l., 1998). The amino acid alignments (Figure 8) show that in both *M. smegmatis* and *M. tuberculosis* the Nth DNA glycosylase has retained the lysine residue at position 120, but in the MutY protein it has been replaced with tyrosine (Tyr120), suggesting that MutY in mycobacteria acts only as a glycosylase and similar to the *E.coli* counterpart does not have lyase activity.

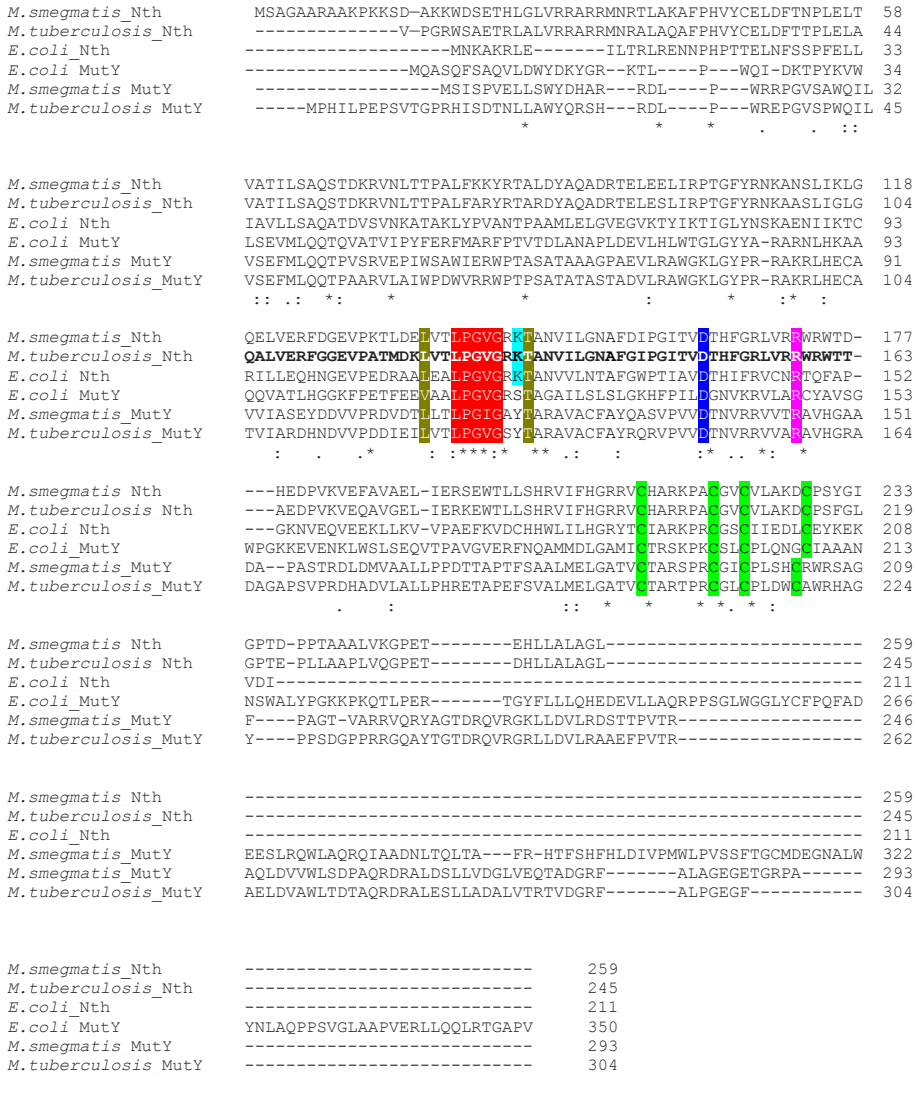

.

Figure 8. Amino acid sequence alignments of the Nth and MutY DNA glycosylases from *M. smegmatis*, *M tuberculosis* and *E. coli*. The helix is shaded dark yellow, the hairpin is shown in red, the aspartic acid residue is in blue (position 148), the arginine residue is shown in pink at position 153, which is conserved in both proteins, the cysteine residues involved in the binding of the 4Fe-4S cluster is shaded in green. The conserved lysine residue in Nth (but not in MutY) at position 120, responsible for lyase activity, is shaded in turquoise.

3.2 Confirmation of existing knockout constructs

In order to ensure that the deletion constructs for *nth* and *mutY* generated in previous studies (Moola *et al* 2014; Hassim *et al* 2015) were correct, DNA from the *E. coli* strains carrying the p2NILΔ*mutY*::pGOAL17 and p2NILΔ*nth*::pGOAL19 knockout vectors, were isolated and digested with various restriction enzymes. Both constructs yielded in the corresponding expected sizes, thus confirming that the knockout vectors were correct (Figures 9 and 10).

A.

Enzyme	Expected sizes(bp)
*Sph*I	14742
*Hind*III	9451, 4525, 739, 27
*Kpn*I	6803, 5197, 1580, 1132, 30
*Pvu*II	7498, 3259, 2557, 819, 363, 144,102
*Nru*I	4954, 4356, 3470, 1061, 412, 270, 219

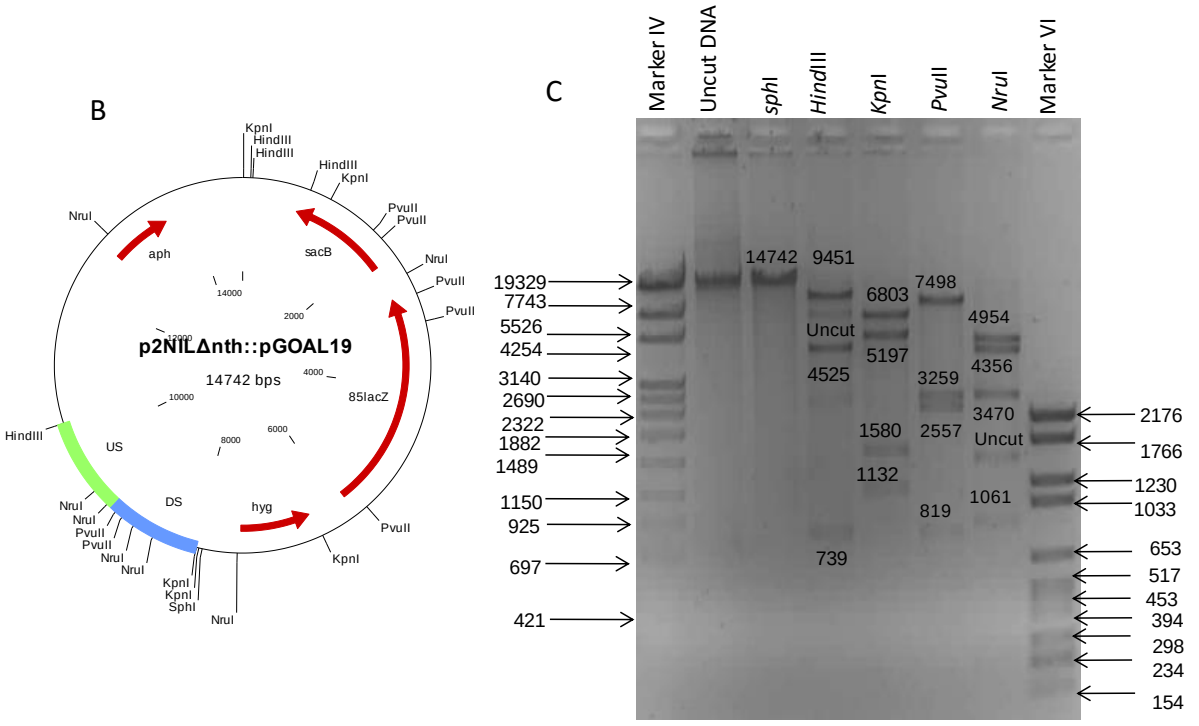

Figure 9. The p2NILΔ*nth*::pGOAL19 deletion construct.(A) Table displaying the different restriction endonucleases used and the expected fragment sizes (bp), (B) Plasmid map of the p2NILΔ*nth*::pGOAL19 vector showing the cloned US and DS regions(shaded in green and blue respectively) and (C) Agarose gel of digested fragments of p2NILΔ*nth*::pGOAL19 vector.

A.

Enzyme	Expected sizes(bp)
Asp 718	7011, 5197, 1132, 1100
Bam HI	7156, 3279, 3072, 1001
Eco RI	5902, 5827, 1863, 766, 150
Pst I	5696, 3949, 3933, 897, 33
Pvu II	7773, 2852, 2557, 819, 363, 144

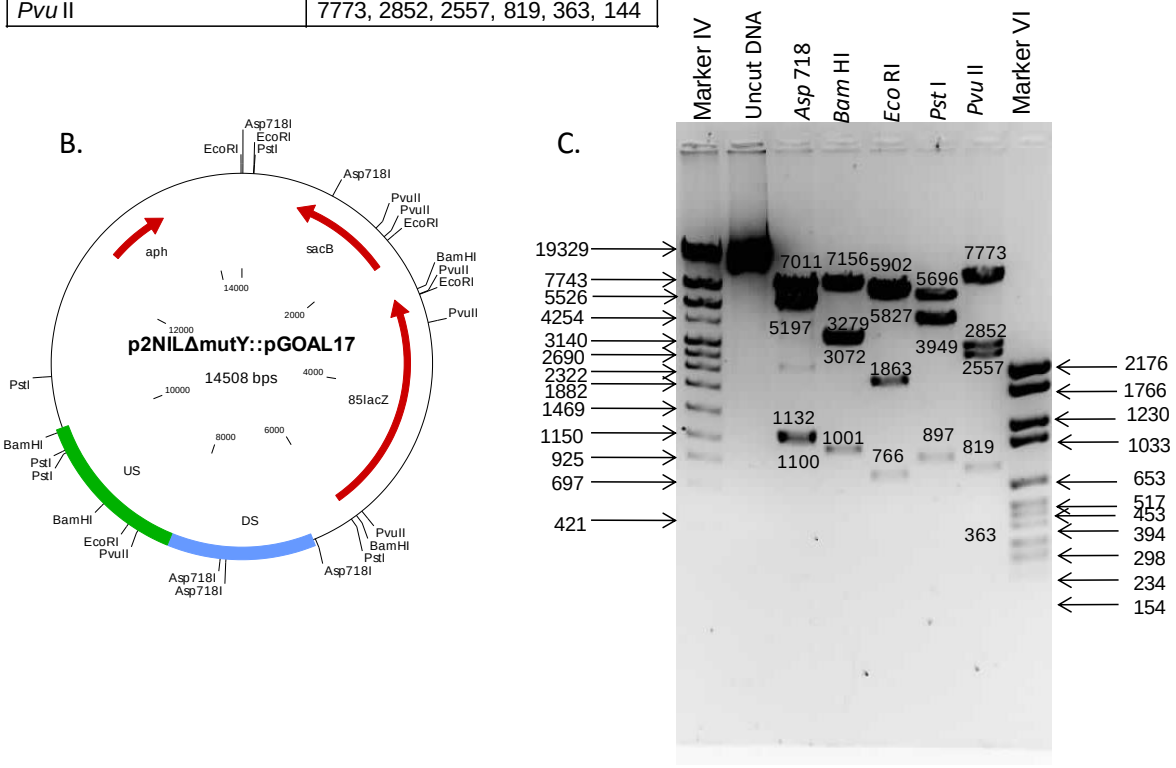

Figure 10. The p2NIL*mutY*::pGOAL17 deletion construct.(A) Table displaying the different restriction endonucleases used and the expected fragment sizes, (B) Plasmid map of the vector showing the cloned US and DS regions (shaded in green and blue respectively) and (C) Agarose gel of digested fragments of the p2NILΔ*mutY*::pGOAL17.

3.3 Generation and identification of single crossover (SCO) and double crossover (DCO) mutants

Suicide vectors p2NILΔ*nth*::pGOAL19 and p2NILΔ*mutY*::pGOAL17 were electroporated into previously generated mutant strains lacking either *mutY* (Δ*mutY*) or *nth* (Δ*nth*) (Moolla, *et a*l., 2014; Hassim, *et al*., 2015) respectively to generate double gene knockout mutant strains. After electroporation, blue transformants (SCO mutants) selected on 7H10 agar plates

supplemented with kanamycin (kan) and X-gal were screened for genotypic confirmation initially by PCR followed by Southern blot analysis (Section 3.3.2). To achieve the second crossover, PCR verified SCO mutants were cultured in non-selective media and plated on 7H10 plates containing 2% sucrose. White, sucrose resistant clones resulting from the loss of the marker genes on the suicide vector during the double cross over event selection were screened by PCR to identify positive double cross over (DCO) clones.

3.3.1 PCR confirmation of double mutants

PCR primers used for screening the *nth* and *mutY* deletion region were designed previously and are listed in (Appendix 5.2 Table 5.1). The primers were designed to bind upstream and downstream of the gene to distinguish the wildtype allele from the mutant allele hence, a smaller PCR product was amplified for the deleted mutant allele. The expected size for the *nth* deletion using the primer set NthF1and NthR1 (Appendix 5.2 Table 5.1) was 270 bp and 833 bp for the wildtype allele. For the *mutY* deletion a 780 bp fragment was expected for the deletion allele and a 1481 bp fragment for the parental allele using the primer set mutYFwd and mutYRev (Appendix 5.2 Table 5.1). The PCR data shown in Figure11 and 12 identified several possible *nth* (6) and *mutY* (7) deletion double mutants in the Δ*mutY* and Δ*nth* background strains respectively.

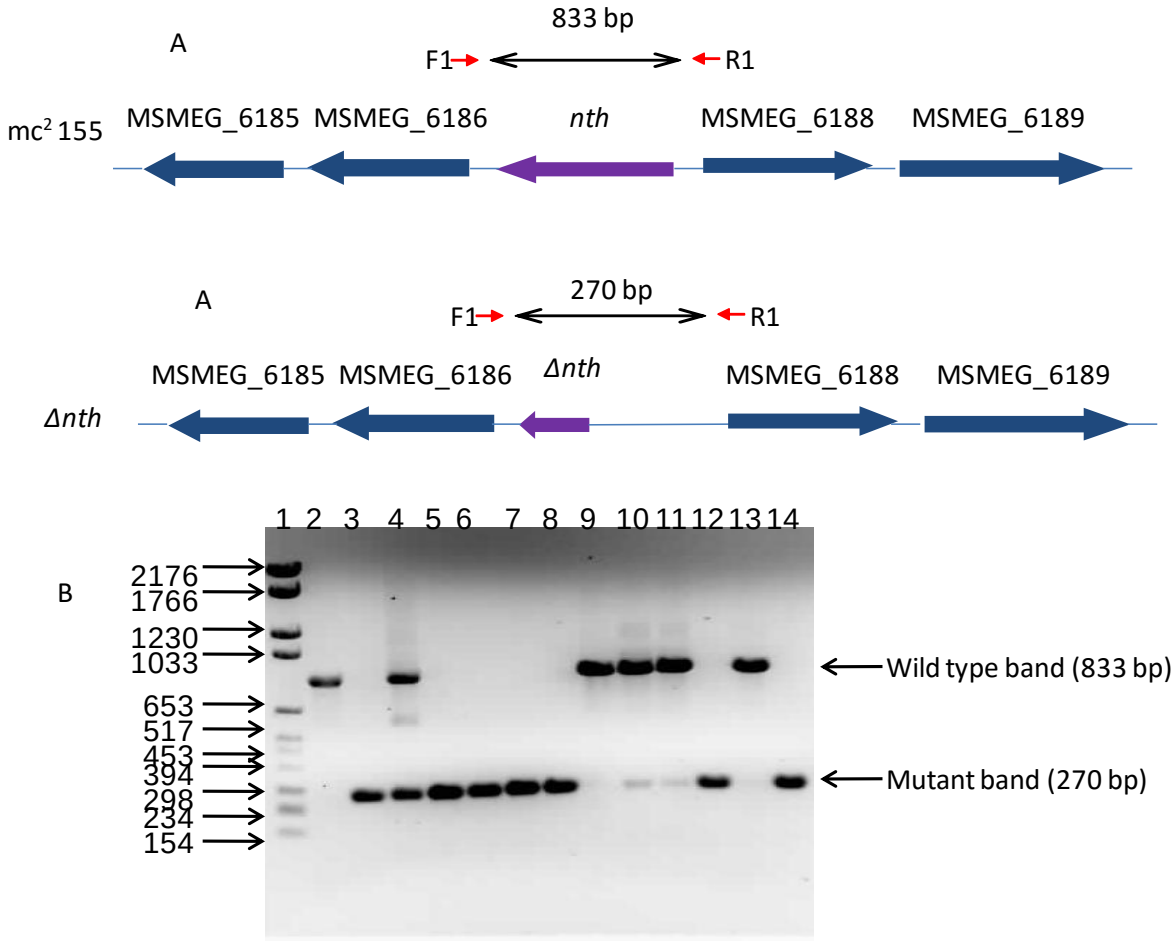

Figure 11. PCR screen for identification of double gene knockout deleted mutant strains using *nth* primers.(A) Schematic diagram showing screening primers (red arrows) with forward primer (F1) located upstream of the gene and reverse primer (R1) located downstream of the gene. (B) Agarose gel showing the PCR screen for deletion of *nth* in the Δ*mutY* deletion mutant. [Lane 1] Marker VI, [Lane 2] mc^{2}155, [Lane 3],p2NILΔ*nth*::pGOAL19 plasmid DNA, [Lane 4] SCO mutant strain, [Lanes 5 to 14], possible DCO Δ*mutY*Δ*nth* clones. Expected sizes, for wild type (mc^2 155) =833 bp and for Δ*nth* =270 bp.

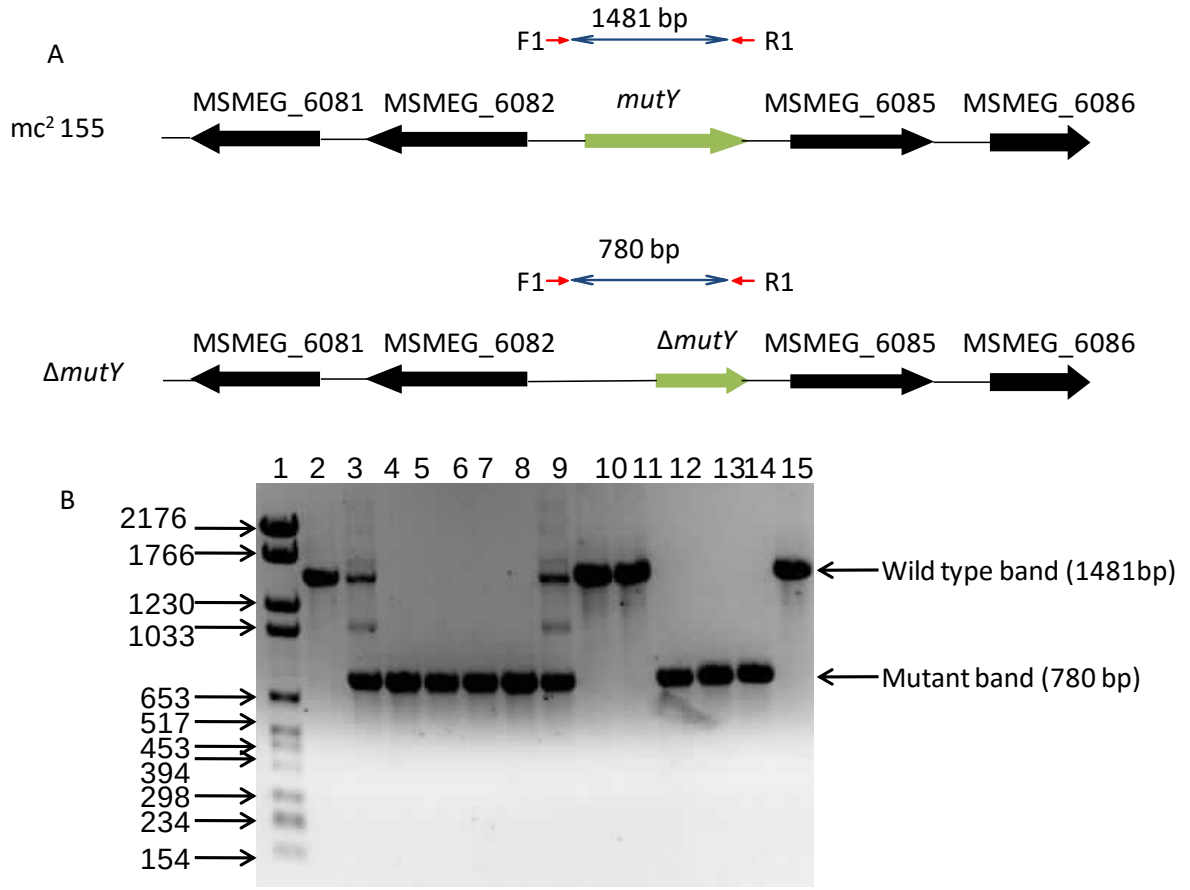

Figure 12. PCR screen for identification of double gene knockout deleted strain using *mutY* primers.(A) Schematic diagram showing screening primers (red) with forward primer (F1) located upstream of the gene and reverse primer (R1) located downstream of the gene. (B) Agarose gel showing the PCR screen for deletion of *mutY* in the Δ*nth* deletion mutant. [Lane 1] Marker VI, [Lane 2] mc^{2}155, [Lane 3] SCO strain, [Lane 4] p2NILΔ*mutY*:pGOAL17, [Lane 5 to 15], possible DCO Δ*nth*Δ*mutY* clones. Expected sizes, for wild type (mc^2 155) = 1481 bp and for the Δ*mutY* =780 bp.

3.3.2 Southern Blot confirmation of double mutants

The PCR confirmed potential mutants where further screened by Southern blot analysis to validate the integrity of the upstream and downstream regions flanking the deletion to ensure that the possible deletion mutants were genetically intact and no chromosomal rearrangement occurred, in addition to confirming integration at the correct site within the genome. To confirm the presence of *nth* in the wildtype and complemented strains and its deletion in the

respective mutant backgrounds; genomic DNA from the parental strain mc^2155, the single Δ*mutY* on Δ*nth* mutant strains, the SCO's obtained during the generation of the double deletion mutants and the possible double deletion mutant strains (Δ*mutY*Δ*nth* and Δ*nth*Δ*mutY*) was extracted. For genotypic confirmation of the Δ*mut*YΔ*nth* mutants, the genomic DNA was digested with *Pst*I for analysis of the region upstream of the deletion and with *Bam*HI to check the downstream region (Figures 13 and 14). Similarly, the presence of *mutY* in the wildtype and complemented strains and its deletion in the mutant strains was assessed by digesting the genomic DNA with *Eco*RI for the upstream region and *Bgl*II for the downstream region from the same strains listed above (Figures 15 and 16).

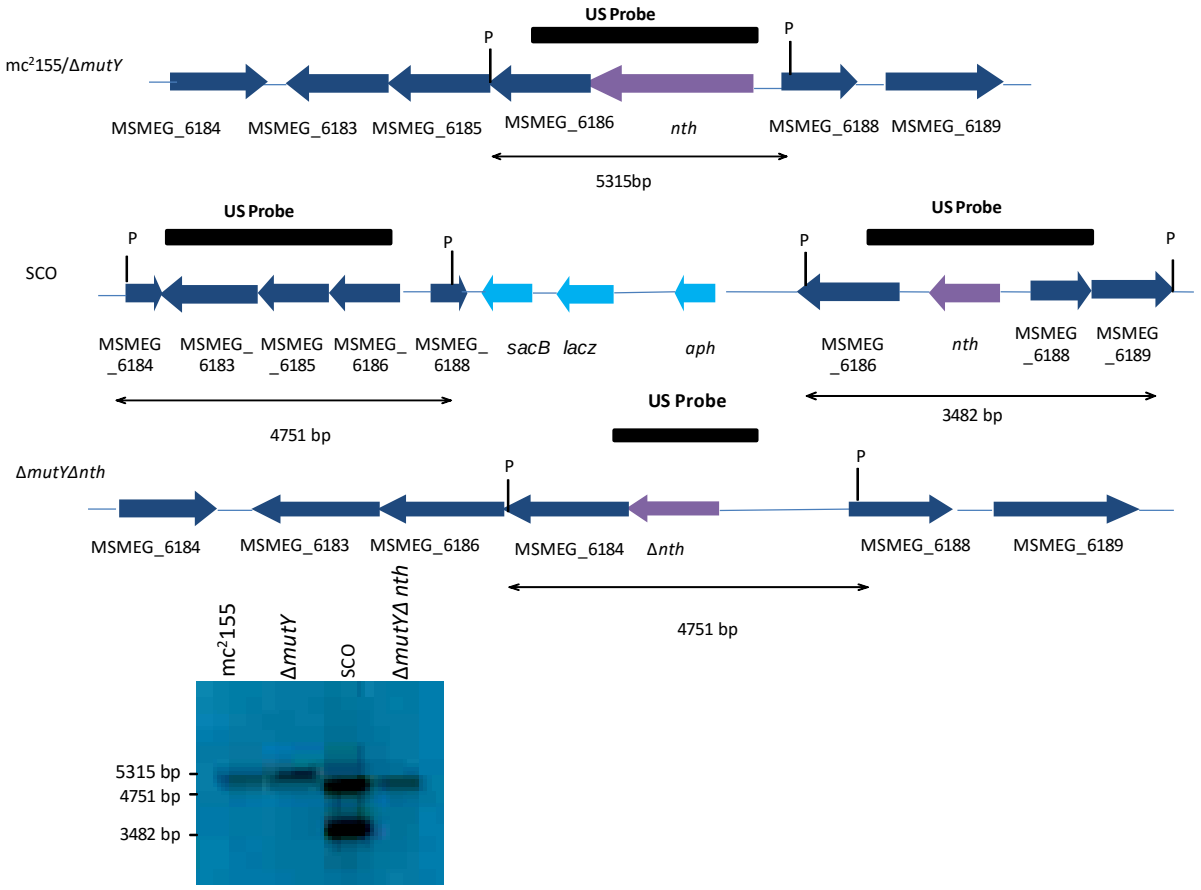

Figure 13. Genotypic characterization of mc^{2}155, Δ*mutY*, SCO and Δ*mutY*Δ*nth* by Southern blot analysis. The genomic map of the relevant locus is shown for mc^{2}155, Δ*mutY*, SCO and Δ*nth*Δ*mutY*. Also shown below is the Southern blot. Chromosomal DNA from mc^{2}155, Δ*mutY*, SCO and Δ*mutY*Δ*nth* was digested with *Pst*I (P). The probe used for hybridization (upstream probe [US]) is shown by the solid black box and the expected sizes are indicated with a black arrow. The *nth* gene is highlighted in purple. Note that in mc^{2}155 and Δ*mutY* the genomic content around Δ*nth* is the same. The single deletion mutant, Δ*mutY* was previously genotyped for genomic integrity (Hassim *et al*., 2015) hence, this region is not shown on the maps.

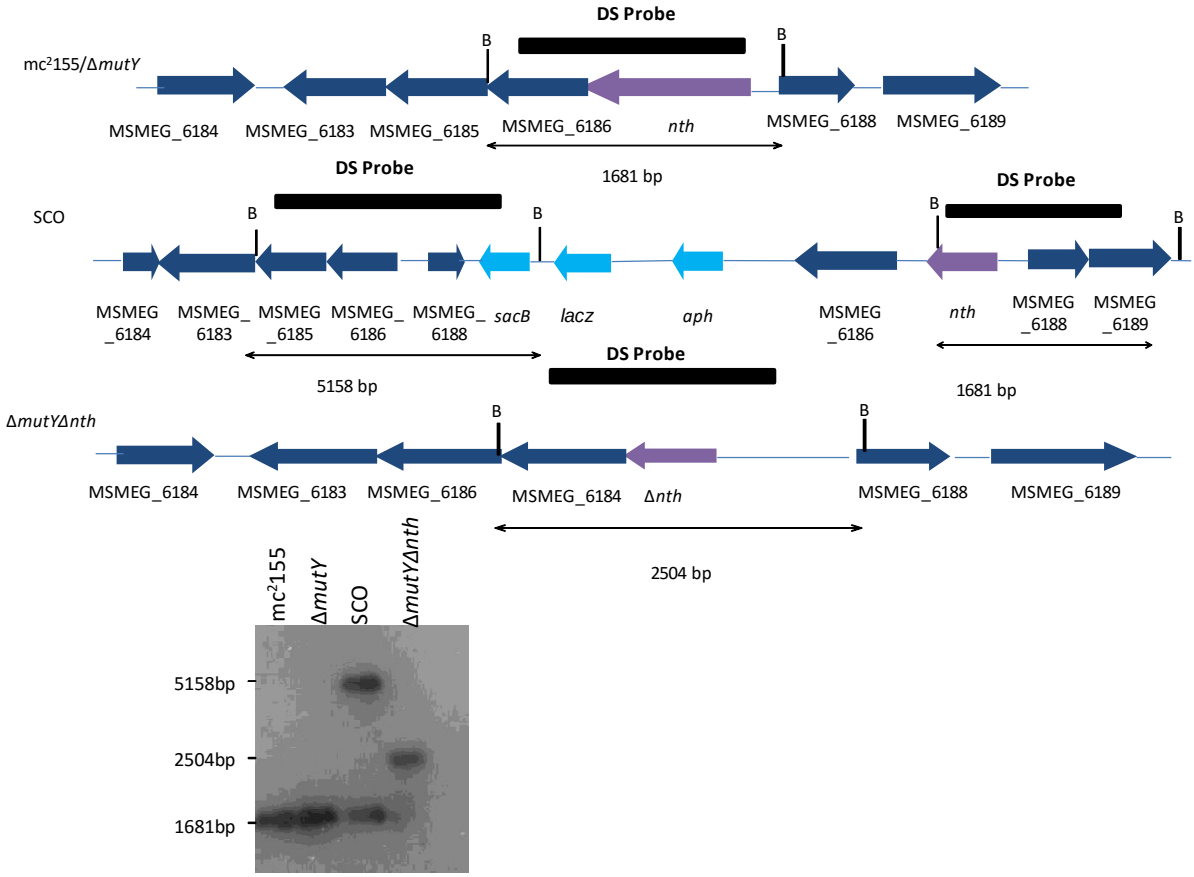

Figure 14. Genotype characterization of mc^{2}155, Δ*mutY*, SCO and Δ*mutY*Δ*nth* by Southern blot analysis. The genomic map of the relevant locus is shown for mc^{2}155, Δ*mutY*, SCO and Δ*nth*Δ*mutY*. Also shown below is the Southern blot. Chromosomal DNA from mc^{2}155, Δ*mutY*, SCO and Δ*mutY*Δ*nth* was digested with *Bam*HI (B). The probe used for hybridization (downstream probe [DS]) is shown by the solid black box and the expected sizes are indicated with a black arrow. The *nth* gene is highlighted in purple. Note that in mc^{2}155 and Δ*mutY* the genomic content around Δ*nth* is the same. The single deletion mutant, Δ*mutY* was previously genotyped for genomic integrity (Hassim *et al*., 2015) hence, this region is not shown on the maps

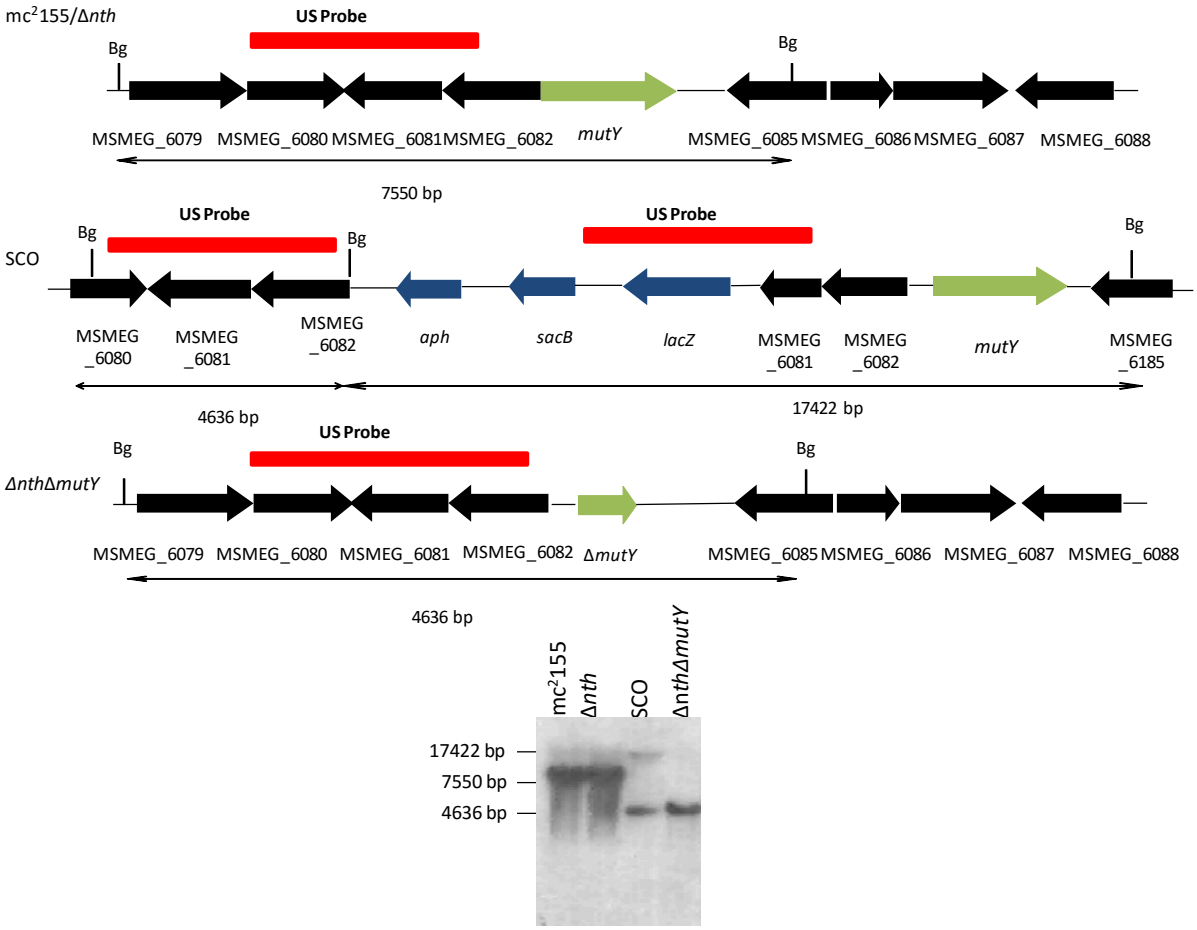

Figure 15. Genotypic characterization of mc^{2}155, Δ*nth*, SCO and Δ*nth*Δ*mutY* by Southern blot analysis. The genomic map of the relevant locus is shown for mc^{2}155, Δ*nth*, SCO and Δ*nth*Δ*mutY*. Also shown below is the Southern blot. Chromosomal DNA from mc^{2}155, Δ*nth*, SCO and Δ*nth*Δ*mutY* was digested with *Bgl*II (Bg). The probe used for hybridization (upstream probe [US]) is shown by the solid red box and the expected sizes are indicated with a black arrow. The *mutY* gene is highlighted in green. Note that the genomic content around mc^{2}155 and *Δnth* is the same. The single deletion mutant, Δ*nth* was previously genotyped for genomic integrity (Moolla *et al*., 2014)hence, this region is not shown on the maps

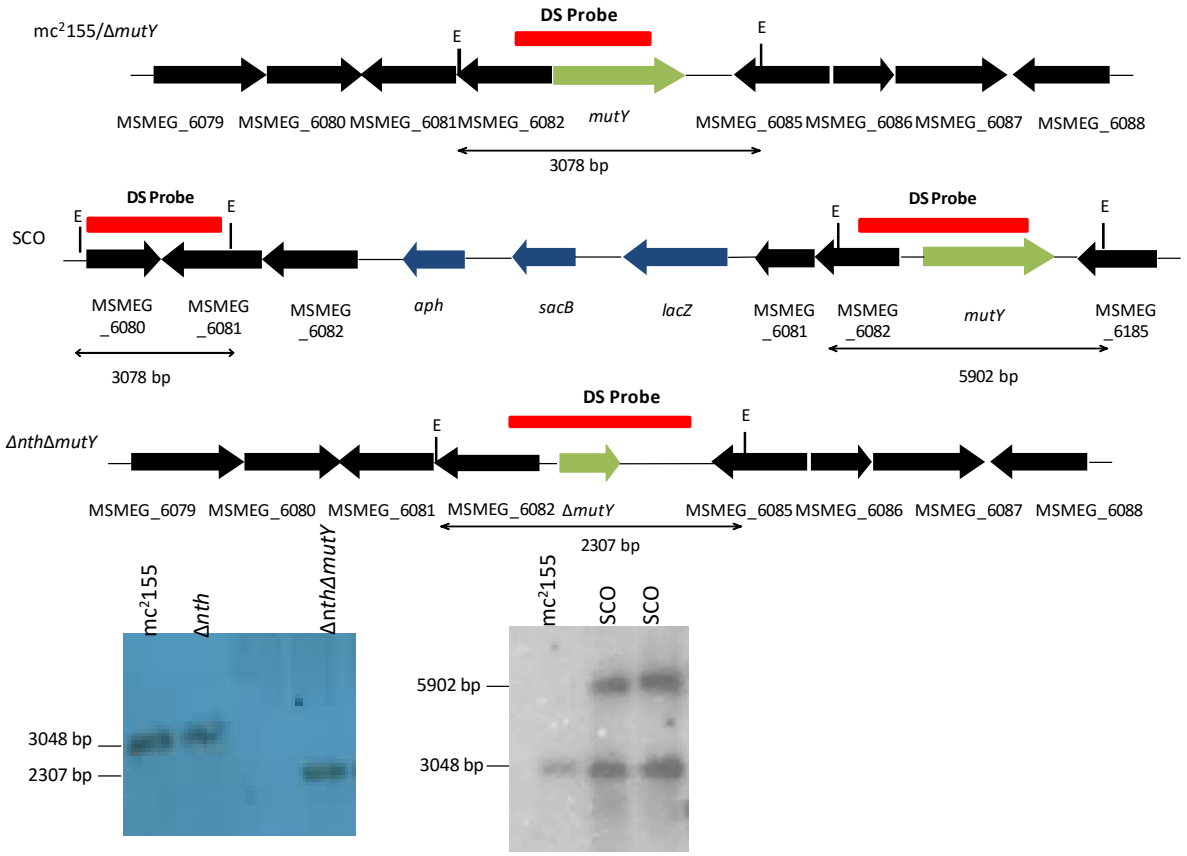

Figure 16. Genotypic characterization of mc^{2}155, Δ*nth*, SCO and Δ*nth*Δ*mutY* by Southern blot analysis. The genomic map of the relevant locus is shown for mc^{2}155, Δ*nth*, SCO and Δ*nth*Δ*mutY*. Also shown below is the Southern blot. Chromosomal DNA from mc^{2}155, Δ*nth*, SCO and Δ*nth*Δ*mutY* was digested with *Eco*RI (E). The probe used for hybridization (downstream probe (DS)) is shown by the solid red box and the expected sizes are indicated with a black arrow. The *mutY* gene is highlighted in green. Note that in mc^{2}155 and Δ*nth* the genomic content around Δ*mutY* is the same. The single deletion mutant, Δ*nth* was previously genotyped for genomic integrity (Moolla *et al*., 2014) hence, this region is not shown on the maps.

3.4 Complementation of the double deletion mutant strains

Complementation of Δ*nth*Δ*mutY* and Δ*mutY*Δ*nth* with *mutY* and *nth* respectively, was accomplished by utilizing previously constructed integrating vectors (Moolla *et al*., 2014, Hassim *et al*., 2015). The pTWEETY::*nth* and pTWEETY::*mutY* (Table 2.2) are integrating vectors carrying a functional copy of the *nth* or *mutY* genes with an additional 350 bp upstream sequence that contains the promoter sequence. To reconfirm genetic integrity of the two integrating vectors, restriction mapping was carried out and the fragments sizes for both pTWEETY::*nth* and pTWEETY::*mutY* were confirmed to be correct, Figures 17 and 18. The complementation vector, pTWEETY::*nth* was electroporated into the double mutant strain Δ*mutY*Δ*nth* to revert the strain to the Δ*mutY* single deletion mutant. Similarly, pTWEETY::*mutY* was integrated into the Δ*nth*Δ*mutY* mutant to obtain the Δ*nth* single deletion mutant genotype. Transformants were screened by PCR (Figures19 a and b), which confirmed the integration of the respective functional gene into the respective deletion mutants as both the functional and deleted alleles were identified. The resulting complemented strains were annotated as Δ*nth*Δ*mutY*::*mutY* and Δ*mutY*Δ*nth*::*nth* (Table 2.1). In both the PCR confirmations non-specific bands were observed. This a common observation due to the high G+C rich content in mycobacteria primers often mis-prime resulting in non-specific products,

A

Enzyme	Expected sizes(bp)
*Eco*RI	6990
HindIII	6029, 961
NruI	4536, 2454
PvuII	4154, 2836
PstI & *ScaI*	4289, 2701
SalI	5320, 1496, 174

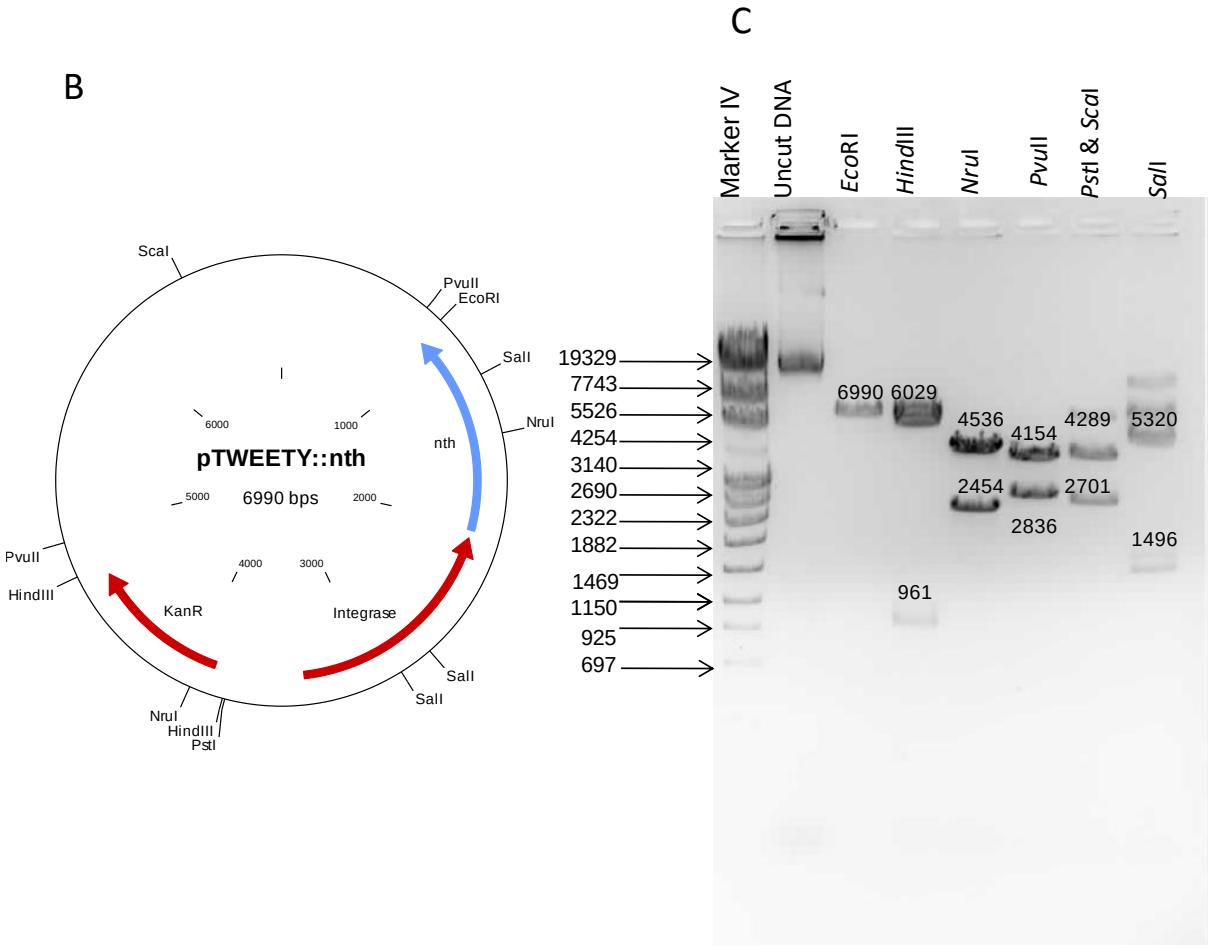

Figure 17. The complemented vector for the *nth* deletion.(A) Table displaying the different restriction endonucleases used and the expected fragment sizes, (B) Plasmid map of the pTWEETY::*nth* vector and (C) Agarose gel of digested fragments of the pTWEETY::*nth* vector.

A

Enzyme	Expected sizes(bp)
*Bgl*II	4296, 3026
*Eco*RI	4466, 2850
*Hind*III	6355, 961
Pst I	7322
Pvu II	2999, 264, 1699

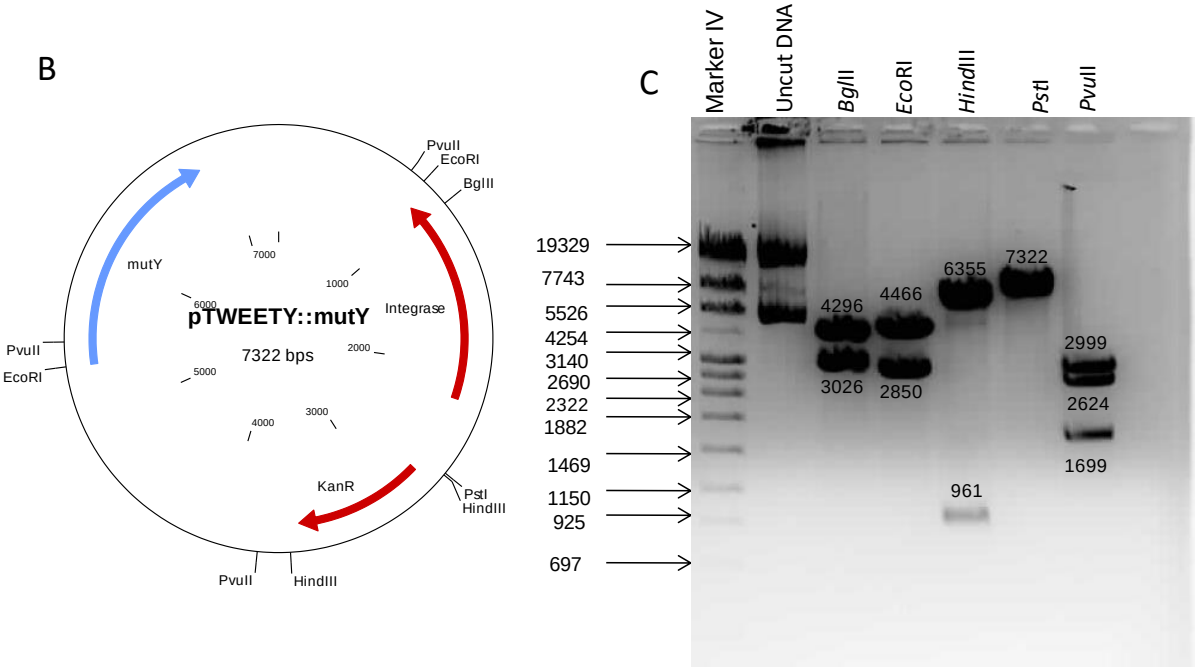

Figure 18. Restriction mapping of the complemented vector for pTWEETY::*mutY*. (A) Table displaying the different restriction endonucleases used and the expected fragment sizes, (B) Plasmid map of the pTWEETY::*mutY* vector and (C) Agarose gel of digested fragments of the pTWEETY::*mutY* vector.

3.4.1 PCR confirmation of complemented strains

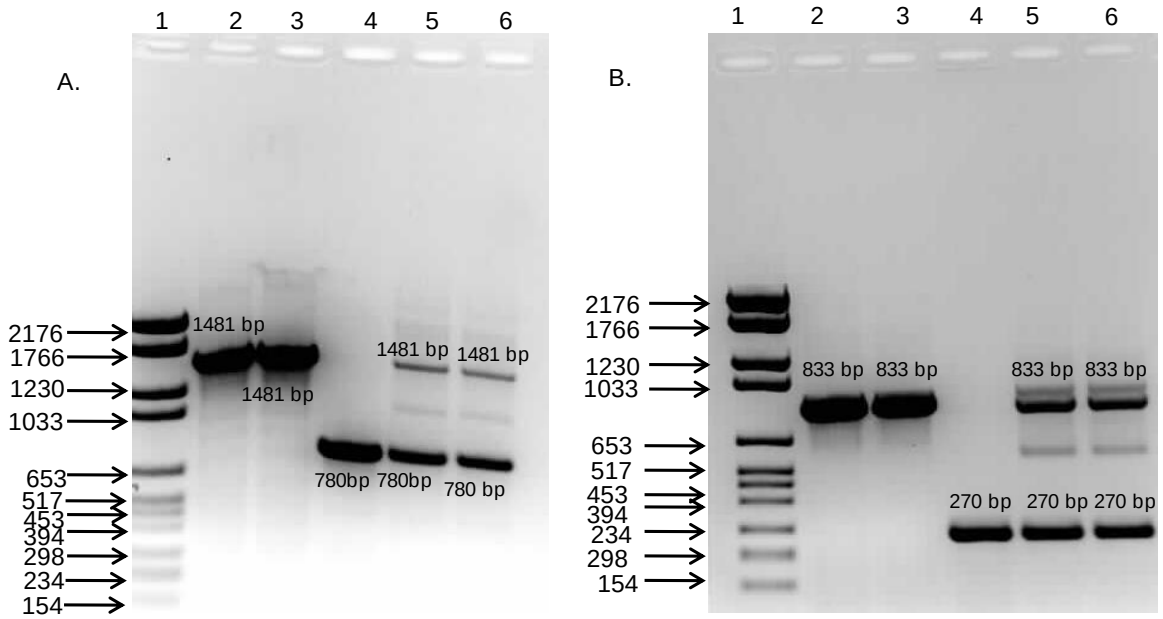

Figure 19. PCR conformation of complemented strains.(A)Complementation of Δ*nth*Δ*mutY* with .Δ*mutY*. [Lane 1] Marker VI, [Lane 2] mc^{2}155, [Lane 3] Δ*nth*, [Lane 4] Δ*nth*Δ*mutY*, [Lane 5 to 6] Δ*nth*Δ*mutY*::*mutY*. Expected sizes, mc^{2}155 (1481 bp) and Δ*nth* (1481 bp),] Δ*nth*Δ*mutY* (780 bp) and Δ*nth*Δ*mutY*::*mutY* (1481 bp and 780 bp). (B)Complementation of Δ*mutY* Δ*nth* with *nth*, [Lane 1] Marker VI, [Lane 2] mc^{2}155, [Lane 3] Δ*mutY*, [Lane 4] Δ*mutY*Δ*nth*, [Lane 5 to 6] Δ*mutY* Δ*nth*::*nth*. Expected sizes, wildtype (833 bp), Δ*mutY* (833), Δ*nth*Δ*mutY* (270 bp) and Δ*mutY*Δ*nth*::*nth* (833 and 270bp).

3.5 Phenotypic characterisation

3.5.1 Growth kinetics

Growth kinetics of mc^{2}155, single mutants, double mutants and complemented strains were assessed under normal culture conditions to evaluate the effect of the combinatorial loss of *nth* and *mutY* in the Δ*mutY*Δ*nth* and Δ*nth*Δ*mutY* strains respectively. Freezer stocks of the

various strains were inoculated in 7H9 media and bacterial growth monitored by measuring the OD_{600nm} at 3 hours intervals over a period of 36 hours. Both the double mutant strains showed comparable growth to the parental strain and the respective single deletion mutants suggesting that Nth and MutY are dispensable for growth in vitro. Furthermore, both the complemented strains also displayed the same growth kinetics as the respective single gene deletion mutants indicating that integration of the functional gene at the *attB* site does not affect the growth kinetics of these strains.

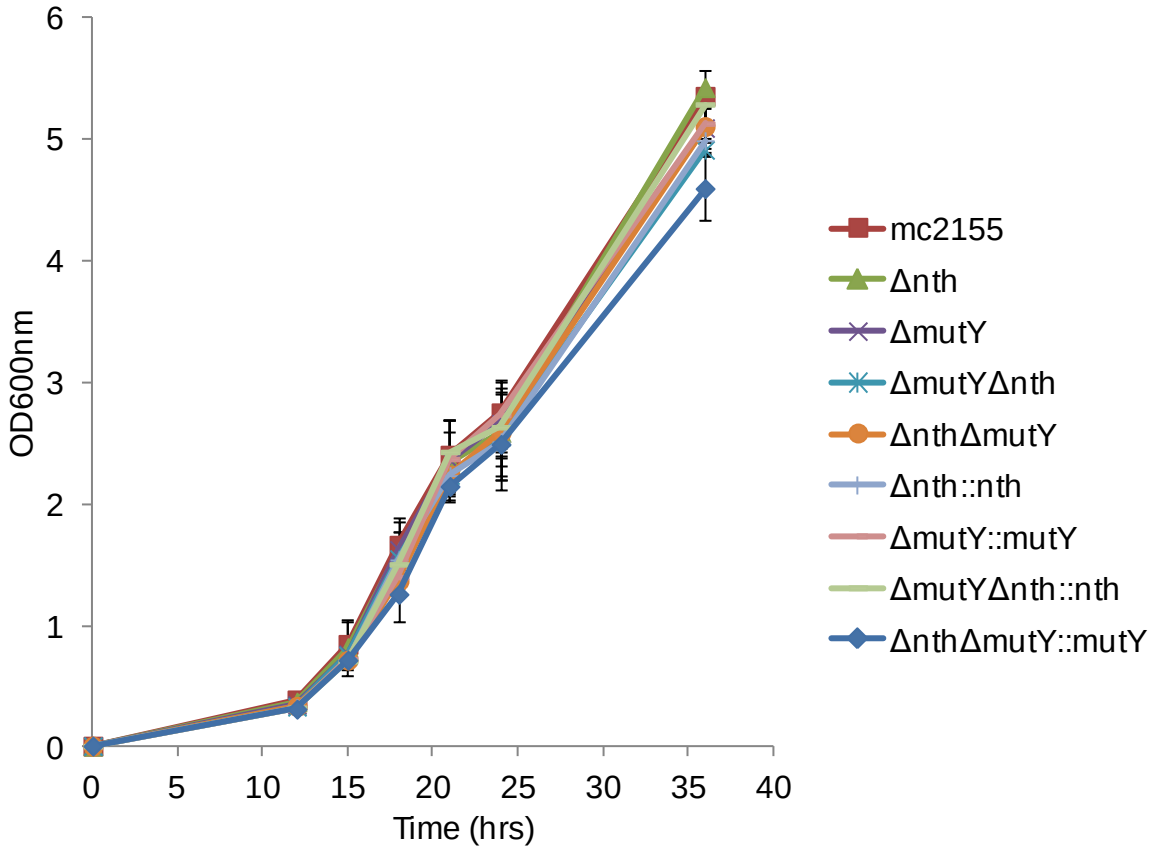

Figure 20. Growth curve of *M. smegmatis* mc^2155, single mutants, double mutants and complemented strains under normal culture conditions. The represented data points are an average of three independent experiments and the standard error for each point is included.

3.5.2 Spontaneous mutation frequency

The parental, mutant and complemented strains were grown overnight to approximately 2 $\times 10^7$ CFU's/ml and 500 µl was plated onto rifampicin (200 µg/ml). The data in Figure 21 and 22 showed that the deletion of *mutY* in the Δ*nth* background (Δ*nth*Δ*mutY*) resulted in an exaggerated increase in the level of spontaneous rif^R mutations. Comparatively, the Δ*nth*, Δ*mutY* and Δ*mutY*Δ*nth* strains showed marginal increase in mutagenesis compared to mc^2155. Both the *nth* complemented strains reduced the mutation frequency to the level of the respective parental strains, whereas the Δ*nth*Δ*mutY*::*mutY* stain showed a slightly more mutants compared to Δ*nth*. A possible interpretation of this observation is that the Nth DNA glycosylase plays a greater role in controlling mutagenesis hence, its deletion, prior to deletion of *mutY* results in exacerbated spontaneous rif^R mutants when compared to the Δ*mutY*Δ*nth* strain, where the order of the deletion of the two glycosylases is reversed. These data suggest a possible hierarchy between the Nth and MutY DNA glycosylases in the maintenance of mycobacterial genome integrity.

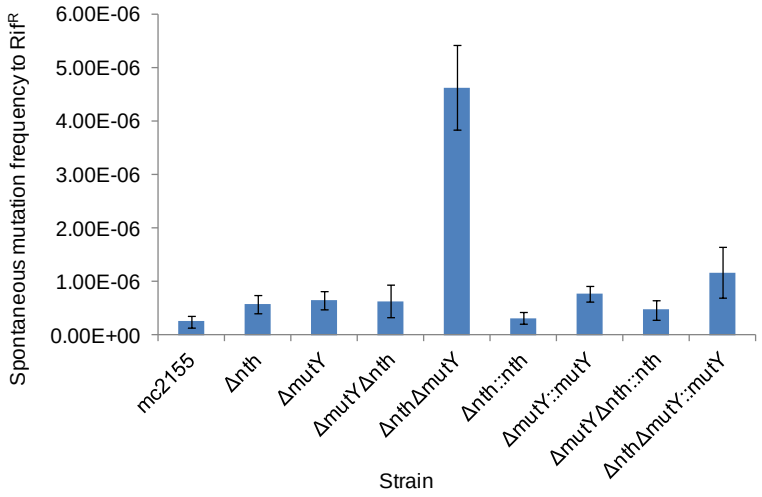

Figure 21. Spontaneous Rif^R mutation for single mutants, double mutants and complemented strains. The error bars represent standard error between 3 biological replicates

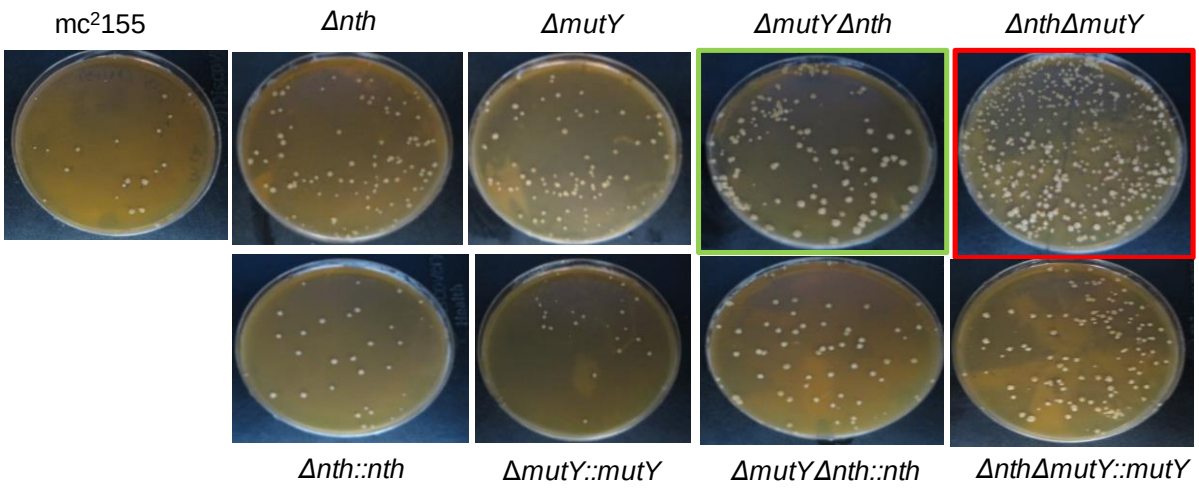

Figure 22. Rifampicin containing plates showing rif^R mutants from spontaneous mutation frequency assay. The plates are representatives of one of 3 experiments. The plates are representatives of one of 3 experiments. The increased rifampicin resistant colonies observed for Δ*nth*Δ*mutY* (red box) was consistent over 3 replicates which is markedly different when compared to the Δ*mutY*Δ*nth* double mutant strain (green).

3.5.3 Effect of H_2O_2on the survival of *M. smegmatis*

Mycobacteria are subjected to host-derived ROS such as hydroxyl radical (•OH) and H_2O_2 which have the ability to causes damage to DNA through oxidative stress. In this study, H_2O_2 was used as a source of inducing oxidative stress *in vitro*. Previous studies at the CBTBR showed that *M. smegmatis* log phase cultures treated with 2.5 mM H_2O_2 resulted in a 4 log reduction in survival after 4 hours (Moolla, *et a*l., 2014; Hassim, *et al*., 2015). Since H_2O_2 is light sensitive and is unstable, variable results are obtained from one experiment to another hence, the optimal H_2O_2 concentration to test the double DNA glycosylase deletion mutants generated in this study together with the previously generated single deletion mutants was optimized. *M. smegmatis* mc^{2}155 was grown to an OD_{600nm} of 0.35 and treated with 1.0, 2.0 and 2.5 mM of H_2O_2. The data in Figure 23 indicate that 1.0 mM of H_2O_2 was insufficient as

it did not display a killing effect after 6 hours of treatment. In contrast, at 2.5 mM all the cells died after two hours of exposure to H_2O_2. Treatment of the bacteria with 2.0 Mm H_2O_2, resulted in approximately 4-5 log killing after 4 hours of exposure to H_2O_2 hence, in this study all further testing was done at 2.0 mM of H_2O_2.

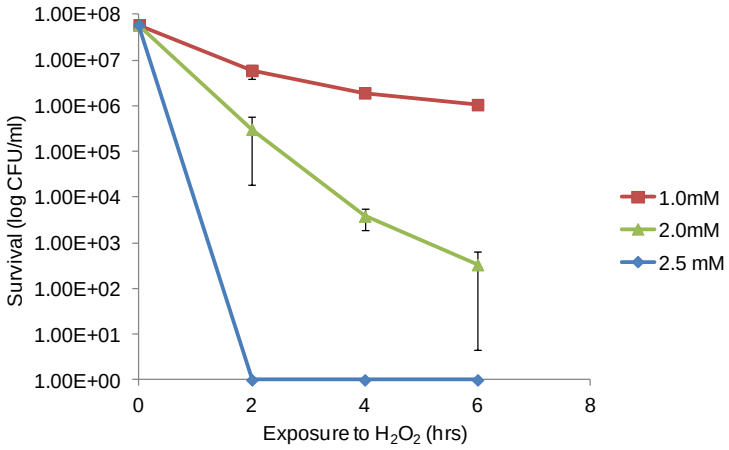

Figure 23. Assessment of mc^{2}155 with three different concentrations of H_2O_2. Early log phase early log phase cultures were treated with 1.0 2.0 and 2.5 mM H_2O_2 and growth was monitored as CFUs/ml over a 6 h period. The error bars represent the standard error between 3 biological replicates.

M. smegmatis mc^{2}155, the double mutants and their complemented strains were grown to an OD_{600nm} of 0.35 followed by treatment with 2.0 mM H_2O_2 and monitored for a period of 6 hours to determine whether the deletion of *nth* and *mutY* in each genetic background would make the strains more prone to oxidative damage. The results from 5 independent experiments showed some variation in the response of the wild type, double knockout mutants and respective complemented strains under oxidative stress conditions (Figure 24 and Appendix 5.4, Figures35 A-D). The variation amongst these experiments is likely linked to the instability of H_2O_2. However, in three out of the five experiments (Figure 24 and Appendix 5.4, Figures 35A and B) both the double deletion mutants showed a 2-3 log kill after 4 hours of exposure to H_2O_2 which was exaggerated after 6 hours compared to the

parental strain. Previously, it was shown the that the Δ*mut*Y mutant was sensitive to oxidative stress (Hassim *et al*., 2015) and therefore, the observed phenotype of Δ*mut*YΔ*nth*::*nth* complemented strain was as expected which was consistent with the previous observation by Hassim *et al* (Hassim *et al.,* 2015). However, the Δ*mut*YΔ*nth*::*nth* complemented strain displayed an increased sensitivity to oxidative stress after 4 hours (Figure 24 and Appendix 5.4 Figures 35A and B) which was surprisingly more than that observed for the double deletion mutants. The reason(s) for this observation is currently unclear. Previously, Moolla *et al* (Moolla *et al*., 2014) showed that loss of the *nth* gene does not affect survival under oxidative stress when compared to mc^2155 and therefore, the Δ*nth*Δ*mutY*::*mutY* complemented strain was expected to display H_2O_2 sensitivity at comparable to wild type levels. The reasons for the differences in these observations are currently unknown but the data clearly indicate that combinatorial loss of Nth together with MutY leads to increased mutagenesis and these two DNA glycosylases possibly co-ordinate their function to control mutagenesis in mycobacteria under oxidative stress conditions. In the other two experiments (Appendix 5, Section 5.4, Figures 35C and D) the double deletion mutant, Δ*mut*YΔ*nth* and both the complemented strains showed the same kill kinetics as the parental strain indicating once again that some hierarchy exists between these DNA glycosylases as deletion of *nth* after the removal of *mutY* does not exaggerate mutagenesis. In both these experiments, the Δ*nth*Δ*mutY* double deletion mutant surprisingly survived the oxidative assault which can be attributed to possible technical experimental error.

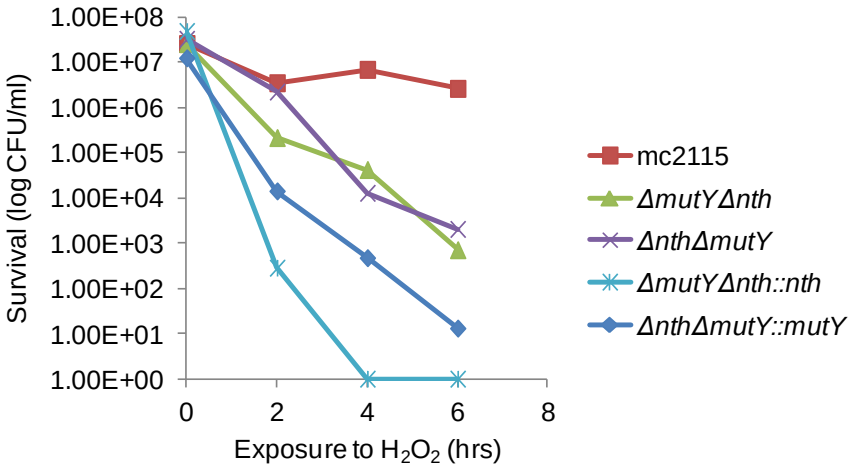

Figure 24. Survival of mc2155, Δ*mutY*Δ*nth* , Δ*nth*Δ*mutY* and complemented strains under oxidative stress condition. Early log phase early cultures were treated with 2.0 mM H_2O_2 and growth was monitored as CFUs/ml over a 6 h period. The graph is a representative of one of five independent experiments. The other four representative graphs are shown in Appendix 5, Section 5.4.

3.5.4 H_2O_2 diffusion susceptibility test

Since the H_2O_2 liquid assay showed variability between experiments, the susceptibility test was performed on solid agar plates. The various mutants and respective parental strains were grown overnight to an OD_{600nm} of 0.35 in 7H9 at 37 ºC. One Hundred microlitres of each culture was plated onto 7H10 plates and left at room temperature to allow the bacteria to be absorbed into the plate. Different concentrations of H_2O_2, 0.18, 0.35 and 0.44 mM (0.5, 1.0 and 1.25 µl) were spotted onto the centre of the 7H10 agar plates that had been inoculated with the test microorganism. Lower concentrations of H_2O_2 were used in this assay as with2.5 mM of H_2O_2 there was complete killing (data not shown). Diffusion of H_2O_2 in an outward manner from the spot creates a concentration gradient and after three days of incubation, the diameter of the zone of inhibition was measured. The control was 7H10 plates with the test organism without H_2O_2 and the total numbers of cells (colony forming units CFU/ml) were

also calculated by spreading dilutions from the cultures onto 7H10. In this assay the loss of *nth* and *mutY* either individually or in combination did not significantly increase susceptibility to H_2O_2, compared to the wildtype strains (Figure 25). These data are in contrast to the liquid assay in wherein the both the double mutants strains showed susceptibility to H_2O_2compared to the mc^2155. It is possible that H_2O_2in solid media is unable to generate sufficient oxidative stress to cause DNA damage resulting in variable kill kinetics in the two different assay systems.

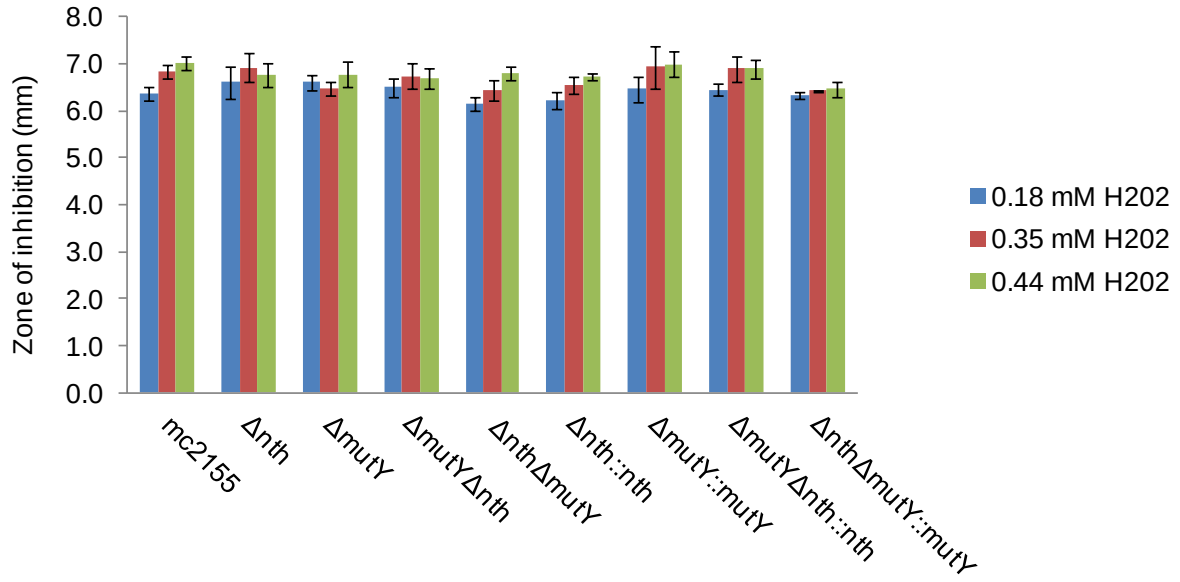

Figure 25. H_2O_2 diffusion susceptibility assay of *M. smegmatis* and its derivative mutant and complemented strains. The graph represents the mean diameters of the bacterial zones of inhibition from three replicate experiments.

3.5.5 UV induced mutagenesis

Moolla *et al* (Moolla *et al*., 2014) demonstrated that deletion of *nth* resulted in increased UV induced mutagenesis to rifampicin. Similarly, the *M. smegmatis* wildtype, single mutants, double mutants and the complemented strains generated in this study were tested for

enhanced UV induced mutagenesis. To determine the optimal UV energy that will result in mutagenesis, experiments were carried out using the wild type strain grown to an OD_{600mn} of 0.6 and were treated with different UV fluences, 25, 50 and 70 mJ/cm^2 as described by (Boshoff *et al*., 2003) (Figures 26Aand 26B). At all three wavelengths the cells displayed similar survival with about 1× 10^7 cells recovered post UV exposure. There was a corresponding increase in rif^R mutants at all three wavelengths as well and for all downstream experiments a UV fluence, of 50 mJ/cm^2 was used to induce mutagenesis.

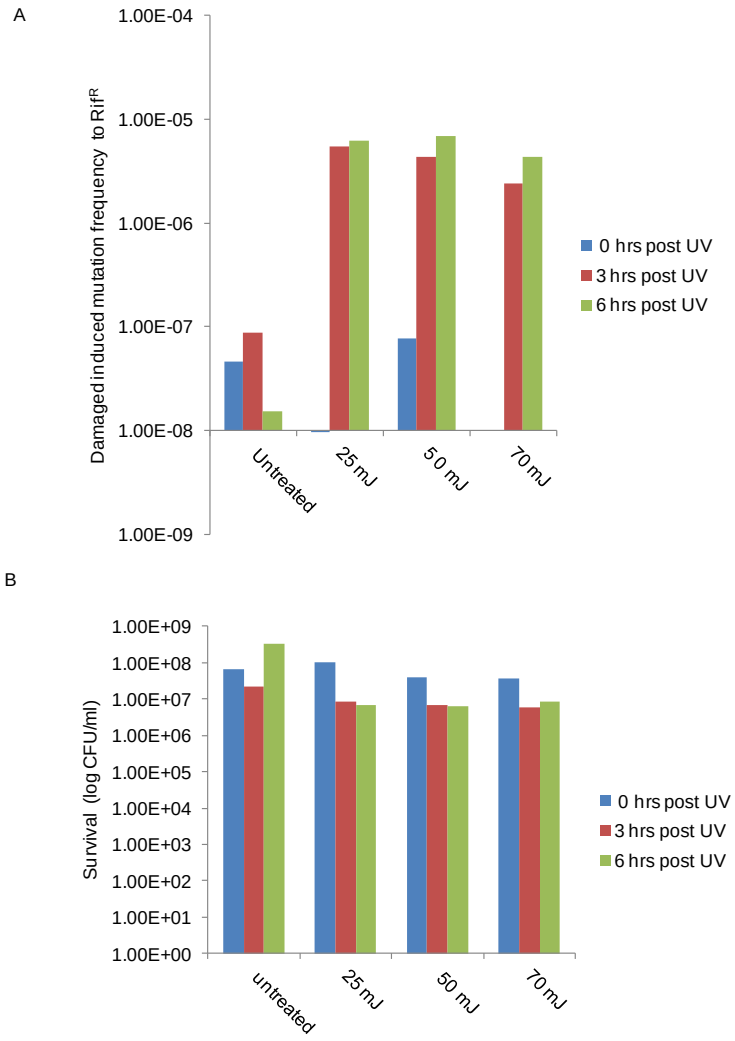

Figure 26. Effect of different UV energies (25, 50, and 70 mJ/cm^2). (A) UV induced mutation frequency of *M. smegmatis* mc^2 155 to rifampicin. (B) Survival of *M. smegmatis* mc^{2}155 after UV treatment.

All cultures were therefore, treated with 50 mJ/cm^2 and after treatment, cultures were inoculated into 50 ml 7H9 and allowed to recover for 3 and 6 hours before plating on 7H10. The single *nth* deletion mutant showed an increased mutation frequency to rifampicin resistance after 3 hours of recovery from UV in 7H9 compared to mc^{2}155 (Figure 27) which is consistent with the observation of Moolla *et al* (Moolla *et al*., 2014), who demonstrated an increase in mutation frequency to rifampicin after 3 hours and marginal increase after 6 hours of recovery. In Figure 27, the Δ*mutY* deletion show a lower induced frequency of rif^R compared to mc^{2}155 and Δ*nth.* It is possible that the intact *nth* gene can repair the damage caused by UV in this mutant strain or uses a different repair mechanism.

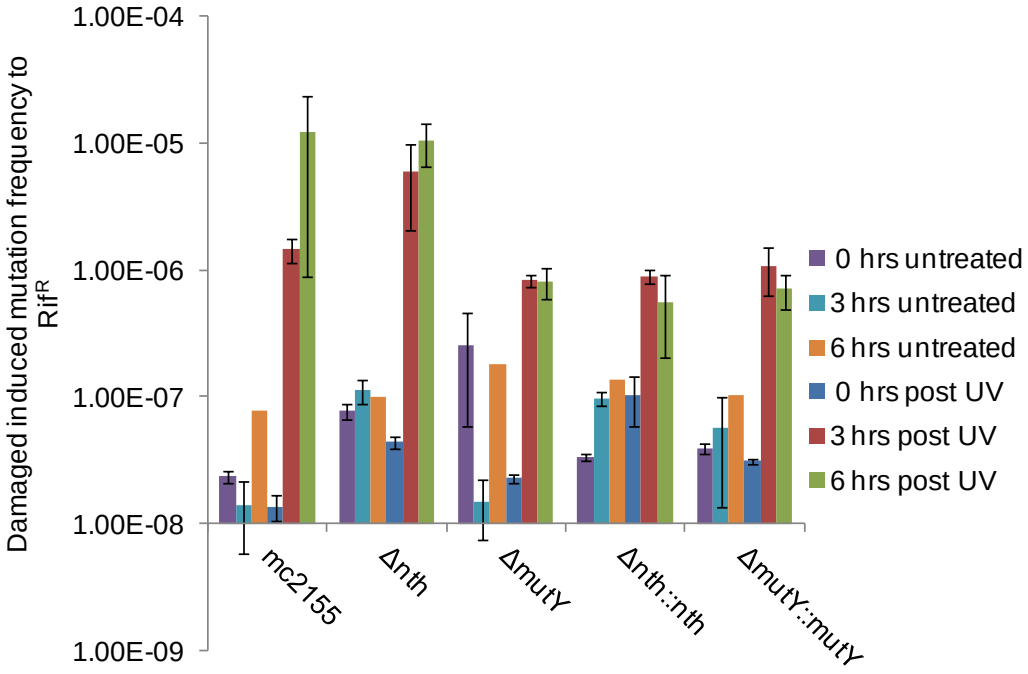

Figure 27. UV induced mutation frequency to rifampicin of mc^2 155, Δ*nth*, Δ*mutY*, Δ*nth*::*nth* and Δ*mutY*::*mutY*. Results represent an average of three independent experiments.

Subsequently the mutation frequency to rifampicin resistance after UV induced damage was assessed for the two double deletion mutants, Δ*mutY*Δ*nth* and Δ*nth*Δ*mutY* to determine

whether combinatorial loss of two DNA glycosylases will enhance mutagenesis. The rif^R frequencies were not elevated when the double mutants were exposed to UV when compared to mc^2155. However, in this instance the complemented Δ*nth*Δ*mutY*::Δ*mutY* strain restored phenotype of Δ*nth* at 3 hours of recovery from UV (Figure 28). The Δ*mutY*Δ*nth*::Δ*nth* complemented strain (Figure 28) did not restore the phenotype and the rif^R mutation frequency remained at the same level as the mutant strain. The elevated UV induced rif^R frequency observed for the Δ*nth* single deletion mutant and restoration of the phenotype in the complemented Δ*nth*Δ*mutY*::*mutY* strain at 3 hours of UV recovery suggests that *nth* is clearly involved in the repair of UV induced DNA damage. These data are consistent with the observation of Moolla *et al* (Moolla *et al*., 2014). Deletion of *mutY* did not show an equivalent amount of mutagenesis as the *nth* deletion mutant (Figure 27) suggesting that *mutY* is not involved in the repair of DNA damaged by UV. As the double mutants do not show elevated UV induced mutagenesis, it is possible that other repair systems maybe involved in maintaining mycobacterial genome integrity.

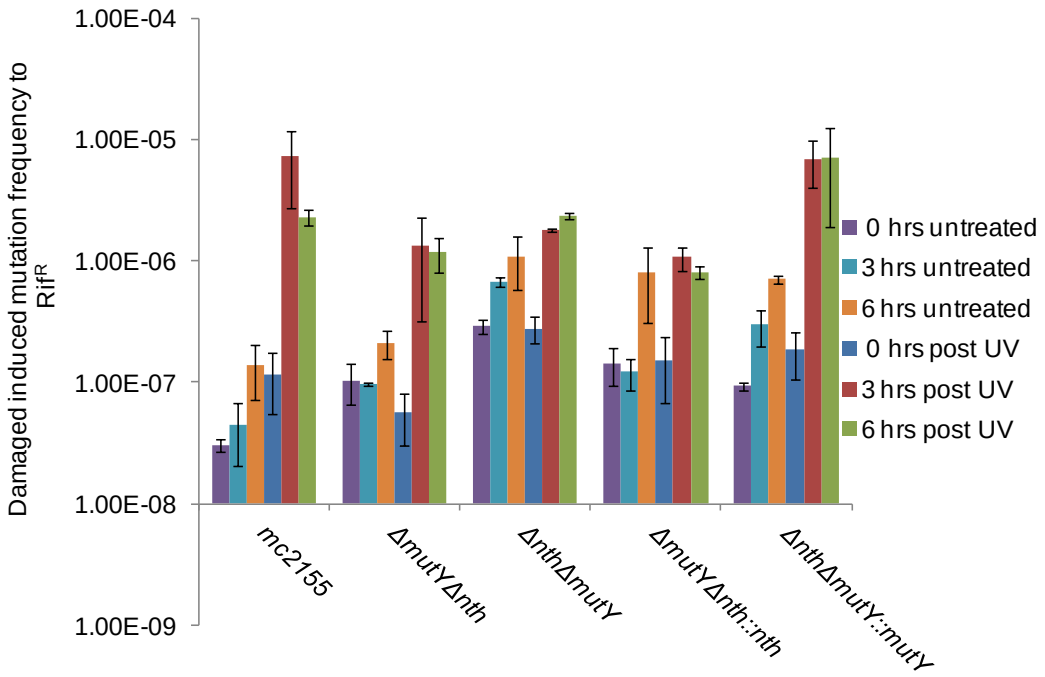

Figure 28. UV damaged induced mutation frequency of mc^{2}155, Δ*mutY*Δ*nth*, Δ*nth*Δ*mutY*, Δ*mutY*Δ*nth*::*nth* and Δ*nth*Δ*mutY*::*mutY* to rifampicin. Results represent an average of three independent experiments.

3.5.6 Mutation rates of Nth and MutY DNA glycosylases

Rates of mutation (μ) to rifampicin resistance were estimated by the fluctuation assay based on the use of the Luria and Delbruck analysis (Rosche and Foster, 2000). Mutation rate determinations are more accurate and reproducible compared to mutation frequency since they estimate the rate at which an organism will sustain a resistance confirming mutation to an antibiotic such as rifampicin during its lifetime. To investigate the combined role of Nth and MutY glycosylases on spontaneous mutation rates to rifampicin, the parental, Δ*nth*, Δ*mutY*, Δ*mutY*Δ*nth*, Δ*nth*Δ*mutY* and the respective complemented strains were tested in triplicate in the fluctuation assay as described in the materials and methods (Section 2.6.6). Mutation rate calculations demonstrated (Table 3.1) that the individual loss of Nth or MutY did not result in an increased spontaneous mutation rate to rifampicin, which was in

concordance with two previous assessments of these mutant strains under these conditions (Moola *et al.* 2014; Hassim *et al.* 2015). However, in experiment 1 (Table 3.1; highlighted in blue) the *nth* deficient mutant strain displayed a 3.4 fold increase in mutation rate to rifampicin which could be attributed to technical differences and/or errors during the experimental procedure. Interestingly, the combined loss of Nth and MutY, regardless of the genetic order in which these respective genes were deleted, resulted in an overall increased mutation rate compared to the parental strain as well as the individual single deletion mutants Δ*nth* and Δ*mutY*, suggesting that these glycosylases play an important role in maintaining genome integrity in mycobacteria. However, the deletion of *mutY* in an *nth* deficient background, Δ*nth*Δ*mutY* (highlighted in red) showed an exacerbated mutation rate compared to the Δ*mutY*Δ*nth* (highlighted in orange) mutant wherein the *nth* was deleted in the Δ*mutY* mutant background. The Δ*nth*Δ*mutY* mutant displayed between 2.2-2.5 fold differences in mutation rates compared to the Δ*mutY*Δ*nth* mutant (Table 3.1). From these data it is clear that the two double mutants have different phenotypic characteristics that may be associated with genotypic changes in their respective genomes which may require whole genome sequencing to elucidate further. The complemented strains for the double deletion mutants showed variable levels of complementation between the three experiments, but in all cases, a reduction in mutation rate was observed. The lack of full complementation may be due to the fact that functional gene is not integrated in the exact genomic context (Table 3.1). From comparisons of the two double deletion mutants, based on the phenotypic analysis carried out in this study, it seems that the Δ*nth*Δ*mutY* mutant has a less stable genome when compared to the Δ*mutY*Δ*nth* mutant, as it consistently displayed a more exaggerated phenotype in response to oxidative stress and had a greater propensity to accumulate rif^R mutations. This suggests that loss of *mutY* subsequent to *nth* seems to result in catastrophic lesions in *M. smegmatis*, which cannot be repaired by other DNA glycosylases of the base excision repair

pathway. The Nth glycosylase is also likely the more dominant of the two DNA glycosylases in controlling mutations under oxidative stress conditions.

Table 3.1: Spontaneous mutation rates to rifampicin of the single and double deletion mutants in the *nth* and *mutY* DNA glycosylases and their respective complemented strains.

	Experiment 1		Experiment 2		Experiment 3	
Stains	**Mutation rate**	**Fold increase**	**Mutation rate**	**Fold increase**	**Mutation rate**	**Fold increase**
mc^2155	4.21E-09	1	5.77-09	1	4,46E-09	1
Δnth	1.43E-08	3.40	5,40E-09	0.94	5.73E-09	1.28
ΔmutY	6.57E-09	1.56	2,03E-09	0.35	3,65E-09	0.82
ΔmutYΔnth	1.20E-08	2.9	1.03E-08	1.79	1.52E-08	3.42
ΔnthΔmutY	1.92E-08	4.6	4.37E-08	7.57	2.51E-08	5.63
Δnth::nth	1.12E-08	2.66	4,21E-09	0.70	4,18E-09	0.9
Δ*mutY::mutY*	7.25E-09	1.72	2,94E-09	0.51	4,99E-09	1,12
ΔmutYΔnth::nth	1.10E-08	2.60	6.12E-09	1.06	1.31E-08	2.93
ΔnthΔmutY::mutY	1.19E-08	2.8	2.61E-08	4.52	1.47E-08	3.29

3.5.7 Mutation spectrum

Rifampicin resistance arises mainly through the acquisition of mutations in the Rifampicin Resistance Determining Region (RRDR) within the 81-bp region of the *rpoB* gene (Figure 29) and the most common mutations occur at positions, 513, 522, 526, and 531 (Figure 29; highlighted in orange boxes). The RRDR region from genomic DNA isolated from 8-10 randomly selected rifampicin-resistant isolates from the fluctuation assay for mc^2155, Δ*nth*, Δ*mutY*, Δ*nth*Δ*mutY*, Δ*mutY*Δ*nth* and their respective complemented strains was sequenced using the primer MsmrpoBF1 (Appendix 5.2, Table5.1). In the wildtype strain from 10

isolates 7 different mutations were revealed within the 81-bp region of *rpoB* gene, with the highest percentage of mutations observed in His526 →Arg (CAC→ CGC) (30%), followed by Ser531 →Leu (TCG →TGG) (Table 3.2). No mutations were found within the 81-bp *rpoB* segment for two rif^R isolates, presumably the mutations occurred outside the sequenced region. In the Δ*nth* mutant there was an increase in C→T mutations at Ser531 → Leu (TCG→ TTG) from 20% in mc^2155 to 30%. Also, there was an increase in mutation at Ser531 → Trp (TCG → TGG) from 10% in the mc^2155 wildtype to 20% in the mutant (Table 3.2). In a previous study within the laboratory, the Δ*mutY* mutant spectrum displayed increased C→A transversions at Gln513 → Lys (CAG →AGG) (Hassim *et al.*, 2015). Similarly in this study Δ*mutY* mutant yielded in increased C→A transversions (44.4%) at the same position. This phenotype was reversed in the complemented strain (Table 3.2). Interestingly, the deletion of *nth* in Δ*mutY* (Δ*mutY*Δ*nth*) yielded in the highest mutation frequency (33%) at the Asp516→Tyr (GAC →TAC). This point mutation was unique to this mutant and was absent in the other complemented strains (Table 3.2). The prevalence of the Asp516 substitution in Δ*mutY*Δ*nth* was unexpected because the mutation occurred in the amino acid which is not common within the RRDR region. The deletion of *mutY* in Δ*nth* (Δ*nth*Δ*mutY*) presented an increase in His526 → Tyr mutations and this was in concordance with the increased C→T transitions (Ser531→Leu), which also formed the major mutations in the *nth* single deletion mutant (Table 3.2). There was also an increase of 20% in C → A mutations at Gln513 →Lys (CAG→AGG) when compared to mc^2155. The increase in C→T and C→A transitions in the Δ*nth*Δ*mutY* was expected as the Nth and MutY DNA glycosylases are responsible for repairing these mutational changes.

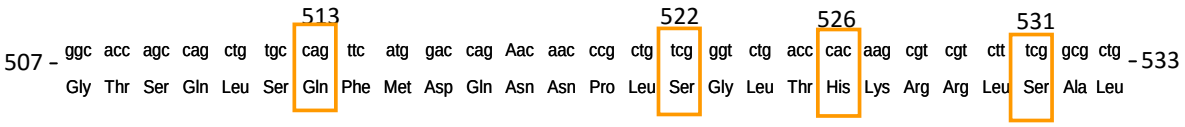

Figure 29. The 81 bp RRDR region of the *rpoB* gene. The common areas where mutations occur are highlighted in orange boxes.

Table: 3.2. Mutation patterns and percentage distribution of the rifampicin resistant mutations found in the RRDR region. The total number of sequenced rif^{R} mutants for each strain is shown in brackets. The common amino acids where mutations occur are in blue and the least common are in black. Values are given as a percentage.

Mutation	Amino acid change	mc^{2}155(10)	Δ*nth* (10)	Δ*mutY* (9)	Δ*mutY* Δ*nth* (9)	Δ*nth* ΔmutY (10)	Δ*nth* ::*nth(8)*	Δ*mutY* ::*mutY* (9)	Δ*mutY* Δ*nth*::*nth* (10)	Δ*nth* ΔmutY::*mutY* (10)
CAC → GAC	His526 → Asp	10	-	-	-	-	-	-	-	-
TCG→ TGG	Ser531→ Trp	10	20	-	-	-	-	-	-	-
CAC→ TAC	His526 → Ser	10	-	-	-	10	-	-	-	-
CAC→CGC	His526 → Arg	30	10	11.1	22.2	10	-	11.1	10	10
CGT→TGT	Leu 521→Cys	10	-	-	-	-	-	-	-	-
TCG→ TTG	Ser531→Leu	20	30	11.1	-	10	12.5	33.3	-	10
CAC→TAC	His526→Tyr	10	-	-	11.1	40	-	11.1	20	10
CGT→CAT	Arg528→His	-	10	-	-	-	-	11.1	-	-
CAG→AAG	Gln513→Lys	-	10	44.4	11.1	20	-	-	-	-
CAC→CCC	His526 → Pro	-	-	11.1	-	-	62.5	11.1	60	40
CTG→GTG	Leu511 →Val	-	-	22.2	11.1	-	-	-	-	-
CAC→ACC	His526 → Ans	-	-	-	-	10	-	-	-	-
CAC→ACC	His526 → Leu	-	-	-	-	-	-	11.1	-	-
CAG→CCG	Gln513→Pro	-	-	-	-	-	-	11.1	-	-
GGT→GAT	Gln513→Asp	-	-	-	-	-	-	-	-	10
GAC→TAC	Asp516→Tyr	-	-	-	33.3	-	-	-	-	-
CGT→TGT	Arg529→Cys	-	-	-	11.1	-	-	-	-	-
Unknown		-	20	-	-	-	25	11.1	10	20

4.0 Discussion

The ability to rapidly repair DNA damage caused by reactive oxygen and nitrogen intermediates in the host environment using robust DNA repair systems is essential for *M. tuberculosis* to survive in hostile conditions within phagocytic cells. Consequently, to counter these threats *M. tuberculosis* is armed with efficient repair systems such as base excision repair (BER) and the GO repair system. The key enzymes within the BER pathway are the DNA glycosylases. Our interest in these repair pathways stemmed from a need to understand the importance and functioning of the DNA glycosylase enzymes in mycobacteria, more specifically, the role of Nth, Fpg, Nei and MutY in controlling mutations within this species. A key question which remained unanswered is whether genes involved in BER work independently or interdependently. According to previous findings in our laboratory, there is strong evidence of overlapping functions between these DNA glycosylase genes as well as a backup function in the event of extensive DNA damage. The study by Moolla *et al* demonstrated that the Nth and Nei DNA glycosylases functioned synergistically and probably compensate for each other under oxidative stress conditions in order to maintain genomic integrity (Moolla *et al*., 2014). Similarly, the loss of MutY together with the Fpg DNA glycosylases displayed an exaggerated reduction in survival under oxidative stress conditions and an increased spontaneous mutation rate to rifampicin, suggesting a co-operative interaction between these two proteins for genome maintenance (Hassim *et al*., 2015). These findings highlighted that Nth and MutY have an antimutator role and the Fpg/Nei family of DNA glycosylases play more of a backup role during DNA repair under oxidative stress conditions. Hence, in this study, we attempted to understand if there was functional association or overlap between the Nth and MutY DNA glycosylases in the BER pathway. To our knowledge the combined loss of these DNA glycosylases for the maintenance of genome

integrity under stressful conditions has not been previously investigated in *E.coli* or in any mycobacterial species.

The Nth and MutY glycosylases are members of a sequence related family involved in the BER pathway with MutY forming part of the GO system. Panels of single DNA glycosylase gene knockout mutants were available from previous studies (Moolla *et al*., 2014, Hassim *et al*., 2015) hence, these were used to generate the two double mutants that lacked both Nth and MutY in different genetic lineages. The *mutY* gene was deleted in a mutant strain that had the *nth* gene deletion (Moolla *et al*., 2014) and in the second double mutant *nth* was deleted in a *mutY* deletion mutant that was previously generated (Hassim *et al*., 2015). In this study, the individual and combined roles of the *M. smegmatis* Nth and MutY DNA glycosylases was assessed under normal growth culture conditions and under different stress conditions to determine whether the loss of these enzymes had an impact on survival of the mutant strains. Loss of key DNA repair enzymes is assumed to increase mutations hence, the changes in spontaneous mutation rates to rifampicin was measured for each of the combinatorial deletion mutants. Collectively, the data presented here have afforded greater insight into the functioning of the BER pathway in mycobacteria and clearly show that both Nth and MutY are required to prevent mutations in the mycobacterial genome.

As previously shown (Moolla *et al*., 2014, Hassim *et al*., 2015), the single *nth* or *mutY* deletion mutants which were used as control strains in this study showed the same *in vitro* growth kinetics as the parental strain under normal culture conditions. The combined loss of these DNA glycosylases did not affect growth as both the double mutants displayed the same doubling times as the single deletion mutants and the parental wild type strain, mc^2155. These data suggest that the two glycosylases are not essential for growth under *in vitro* culture

conditions or that there is not enough spontaneous DNA damage generated under these conditions to cause growth defects.

In previous studies, 2.5 mM H_2O_2 was used to generate *in vitro* oxidative stress conditions however, in this study under these conditions this led to complete killing of the parental strain after 2 hours of exposure. Hence, the H_2O_2 concentration was optimized, and with 2.0 mM H_2O_2 a 5 log reduction (10^3 viable cells) was observed for the wildtype strain after 4 hours of exposure. Subsequently, assessment of the parental mc^2155, the double mutant strains and their respective complemented strains were tested with 2.0 mM H_2O_2 and the data revealed variable killing rates between biological repeat experiments. This discrepancy between experiments could be attributed to the instability of H_2O_2, which is affected by a range of external sources, one of which is light. Interestingly, based on the 5 biological repeats there was a consistent trend of almost equivalent decreased survival for both the double deletion mutants after 6 hours of exposure to H_2O_2 compared to mc^2155 in three of the experiments. However, the complemented strains were unable to restore the defect and in fact showed a greater reduction in survival compared to the mutant strains. In two of the experiments the Δ*mutY*Δ*nth* mutant showed enhanced survival under oxidative stress suggesting that there may be other protective mechanisms that may have been triggered in this mutant to allow it to combat the effects of oxidative stress. Due of the variation in biological replicates in the liquid assay, we employed a more stable H_2O_2 spotting assay to test for sensitivity of the strains. In contradiction to the trend we saw in the liquid assay of H_2O_2, the Δ*mutY*Δ*nth* mutant showed no difference in survival when compared to the single mutants or mc^2155 wildtype. The differences in the results might be due to H_2O_2 being more effective in the liquid assay in comparison to the spotting assay since the strains take approximately 3-5 days

to grow on the plate and by this time the H_2O_2 could lose its effectiveness as it is light sensitive.

The phenotypic differences between the two double mutants (*ΔmutYΔnth* and *ΔnthΔmutY*) could be as a result of a compensatory mutation that may have been introduced during the generation of the single *mutY* mutant. In order to understand the phenotypic differences manifested between these two double mutant strains from different genetic lineages, whole genome sequencing will be required, however that is beyond the scope of this project.

In *E.coli*, the involvement of Nth in the repair of DNA damage caused by UV has long been suspected since it was initially discovered using UV-irradiated DNA substrates (Radman, 1976). The Nth protein in *E.coli* is a key enzyme responsible for the removal of oxidized pyrimidines (Bauche and Laval, 1999, Zharkov and Grollman, 2002). To determine the exact role of Nth in the repair of UV induced lesions in mycobacteria, Moolla *et al* (Moolla *et al*., 2014) assessed the Δ*nth* single mutant for UV (250 mJ/cm^2) induced mutagenesis. The single Δ*nth* mutant, 3 hours post UV treatment, demonstrated increased mutation frequencies compared to the parental mc^{2}155 strain, suggesting its role in controlling UV induced mutagenesis. Similarly, in this study the single deletion mutants of *nth* together with the two combinatorial double deletion mutants, were tested for increased mutagenesis under UV (50 mJ/cm^2) induced conditions. The data for the single *nth* deletion mutant showed an almost 10 fold increase in mutagenesis compared to the parental strain after 3 hours of recovery post UV which was in accordance to previously observed data (Moolla *et* al., 2014). However, there was only a marginal change in mutation frequency for the *nth* deletion mutant after 6 hours, which was not significantly different to the parental strain. Moreover, the complemented strain Δ*nth*Δ*mutY*::*mutY* when exposed to UV showed the same mutation

frequencies as the single *nth* mutant confirming that Nth plays an important role in repairing UV induced DNA damage. In contrast the *mutY* single deletion mutant or either of the two double deletion mutants showed no increased mutagenesis after 3 and 6 hours post UV treatment compared to the parental strain. A likely explanation for the reduced induced frequencies could be the suppression of UV induced mutations by *mutY* or its non-involvement in the repair of damage caused by UV. Consistent with this hypothesis is the observation of no change in UV induced mutagenesis in a *Helicobacter pylori mutY* deficient mutant compared to the parental strain, suggesting that MutY may not play a role in UV induced mutagenesis (Huang *et al*., 2006).

A compromised DNA repair system impacts on the integrity of the genome resulting in increased mutations. The various single and double mutants (mc^2155, Δ*nth,* Δ*mutY* and Δ*mutY*Δ*nth,* Δ*nth*Δ*mutY*) were assessed for changes in spontaneous mutation frequency and rates to rifampicin. The single *nth* or *mutY* deletion mutants and the Δ*mutY*Δ*nth* double mutants yielded in a two fold increase in spontaneous mutation frequency when compared to mc^2155 wildtype. In contrast, the double mutant strain (Δ*nth*Δ*mutY*), that showed an enhanced survival trend under oxidative stress conditions also showed a significant elevation in (3 fold higher) in spontaneous rifampicin mutagenesis compared to the single deletion mutants and the double mutant Δ*mutY*Δ*nth*. The striking difference in mutation frequency between the two double mutants is somewhat surprising given the fact that both these strains are devoid of the same DNA glycosylases and therefore, should be genetically identical. The only difference is the order in which they were inactivated and thus it is highly likely that during the generation of the Δ*mutY*Δ*nth* double mutant, compensatory mutation(s) may have been introduced within the genome, which may have imparted a fitness advantage to this mutant. In previous studies, the loss of *mutY* did not show an increase in mutation rates

(Kurthkoti *et al*., 2010, Hassim *et al*., 2015) however, reassessment of the *mutY* deletion mutant in this study, revealed a two-fold higher mutation frequency when compared to the wildtype. The variation between these experiments might be due to mutations occurring early during culture growth, leading to the propagation of the same mutation during the life-cycle, a phenomenon known as a "jackpot phenotype"(Luria and Delbrück, 1943). The mutation frequency data for the various mutants and parental strain was further confirmed with mutation rate measurements using the Luria-Delbrück fluctuation assay. Mutation rate determinations are more accurate and reproducible compared to mutation frequency as the estimate the rate at which an organism will sustain a resistance mutation to an antibiotic during its lifetime. In contrast to the spontaneous mutation frequency, assessment of spontaneous mutation rates to rifampicin showed no increase in mutation rate for the single Δ*nth* and Δ*mutY* mutants compared to mc^2155 which is consistent with previous findings (Moolla *et al*., 2014, Hassim *et al*., 2015). Once again the Δ*nth*Δ*mutY* double mutant strain showed a dramatic increase (4.6 to 7.6 fold) in mutation rate but a comparable significant increase was not observed for the Δ*mutY*Δ*nth* mutant (1.8 to 3.4 fold). The collective data obtained in this study clearly shows that Nth could be classified to have a more important an antimutator role for genome stability in mycobacteria compared to MutY.

More than 90% of rifampicin resistance in *M. tuberculosis* strains is due to mutations acquired within an 81 bp region within the *rpoB* gene (Ramaswamy and Musser, 1998). The mutations consist of nucleotide changes, deletions and insertions (Yue *et al*., 2003) In mycobacteria the most common codons which sustain mutations are at position 512,522, 526 and 531 (Höfling *et al*., 2005, Hillemann *et al*., 2005). In order to identify the mutational changes responsible for rifampicin resistance the 81 bp RRDR region was sequenced for several rifampicn resistant colonies obtained for mc^2155 wildtype, the single mutants, double

mutants and their respective complemented strains from the fluctuation assay. Previous studies showed that deletion of *mutY* leads to increased C → A mutations in *M. smegmatis* (, Kurthkoti *et al.,* 2010, Hassim *et al.,* 2015). Similarly, in this study the *mutY* deletion mutant showed a 34% increase in C →A mutations compared to the mc^2155 wildtype strain. Since damaged pyrimidine bases and oxidised cytosines are generally recognized by the Nth glycosylase, in the absence of this enzyme it is expected that there will be an increase in the C→T or G→A mutations (Guo *et al*., 2010). Consistent with this, in the single *nth* deletion mutant the majority of mutations were C→T changes, with a combined total of 40%. In the double mutants, which are devoid of the *nth* and *mutY* DNA glycosylases, an increase in C → A and A → C mutations attributed to the deletion of *mutY,* and C→T or G→A mutations due to the absence of *nth* was as expected. Interestingly, in the Δ*mutY*Δ*nth* mutant there was a unique mutation at codon 516 (G →T), which was not present in any of the strains analysed in this study. The Δ*nth*Δ*mutY* strain showed an increased frequency of C→T transitions compared to the wildtype but this was comparable to the single *nth* mutant. There was also a marginal increase in C → A transversions which could be attributed to the loss of *mutY*. The two double mutants (Δ*mutY*Δ*nth* and Δ*nth*Δ*mutY*) also displayed a diverse spectrum of rif^R mutations once, again suggesting that the two mutants generated from different lineages have genetic variances.

In conclusion, this study further highlights key insight regarding the importance of Nth and MutY DNA glycosylases in the BER pathway in maintaining genome integrity. Based on the data obtained, it is clear that the combinatorial loss of Nth and MutY does have an additive impact on the survival of *M. smegmatis* under oxidative stress conditions, compared to the individual enzymes respectively. Based on the phenotypic differences observed for the two double mutants, it is possible that initial loss of *nth* which has been shown to have

antimutator properties (Moolla *et al*., 2014) may be predisposing the mycobacteria to catastrophic levels of DNA damage hence, subsequent deletion of *mutY* exaggerates genomic instability. As *mutY* does not have scission activity removal, of MutY first does not have a severe genotoxic impact on the genomic DNA as the remaining Fpg/Nei and Nth DNA glycosylases are able to act on any mutations arising under oxidative stress. Moreover, these results may suggest a functional hierarchy between the various DNA glycosylases in the BER system with Nth predominating over MutY as an antimutator.

4.1 Future studies

As the oxidative stress inducing agent H_2O_2 used in this study had limitations, it is important that future studies focus on testing and optimizing more stable compound for generating oxidative stress. Testing the panel of deletion mutants under improved conditions may shed further insight on the association and interplay of these various DNA glycosylases during DNA repair. In the absence of Nth and MutY it would also be interesting to measure the expression levels of Fpg and Nei under normal culture conditions as well as under oxidative stress conditions to assess whether these DNA glycosylases display a backup function. Whole genome sequencing of the two double mutants will identify genomic differences in terms of compensatory mutations that may be contributing to the phenotypic difference observed for the two strains. In addition, perhaps other DNA repair genes in the BER pathway may be identified to play a role in genome maintenance.

5. Appendix

5.1 Media preparation and solutions

5.1.1 *Mycobacterium smegmatis*

Middlebrook 7H9

4.9 g powder, 0.2% glycerol, 0.05% Tween 80 (filter sterilized) and 0.2% glucose

Middlebrook 7H10

19 g powder, 0.085 % NaCl, 0.2% glucose, 0.2% glycerol

5.1.2 *Escherichia coli*

Luria-Bertani Broth (LB)

5g yeast extract, 10g tryptone, 10g NaCl.

All media were made up to 1000 ml and autoclaved at 121˚C for 10 min.

5.2 PCR and sequencing primers

Table 5.1.Primers used in this study, with description and expected sizes.

Oligonucleotide name	Sequence 5' – 3'	Description	Expected (bp)	Reference
NthF1 NthR1	GTCAGCCGTGGTCAGTACC CGAGACGCTCATCGTGTG	Confirmation of wildtype and DCO	Wildtype (833) DCO (270)	(Moolla *et al*., 2014)
mutYFwd mutYRev	GCCTCGAATTCGTCGACCAC CGTGACACCGTCGGACTAC	Confirmation of wildtype and DCO	Wildtype (1481) DCO (780)	(Hassim *et al*., 2015)
NthUsF1 NthUsR1	AAGCTTGTGTGCGTGCTGGCCAAG AGATCTCACACCGGTGATCGTCTT	Nth upstream deletion region	1185	(Moolla *et al*., 2014)
NthDsF2 NthDsR2	AGATCTACGACGCACGAGACCCAG *GGTACC*AGCTGGGCGATCTCTTCC	Nth Downstream deletion region	1170	(Moolla *et al*., 2014)
MutYUSF MutYUSR	GGCCAAGCTTAGCTGATCGTTCGCGACTAC GGCCAGATCTGCATGGTCGTACCAACTCCAA	mutY Downstream deletion region	1932	(Hassim *et al*., 2015)
MutYDSF MutYDSR	GGCCAGATCTGACTCGCTGCTGGTGGAC GGCCGCGGCCGCGCTTCTGCGCAAGAGGTTA	mutY Downstream deletion region	1775	(Hassim *et al*., 2015)
MsmrpoBF2 MsmrpoBR2	TGGTGCGTCTGCACGAGGGTC ATCTGGTCGGTGACCACACCG	RRDR region	549	(Hassim *et al*., 2015)
MsmrpoBF1	GCAGACCCTGATCAACATCC	RRDR sequencing primer	451	(Hassim *et al*., 2015)

5.3 Vectors maps used in this study and previous studies

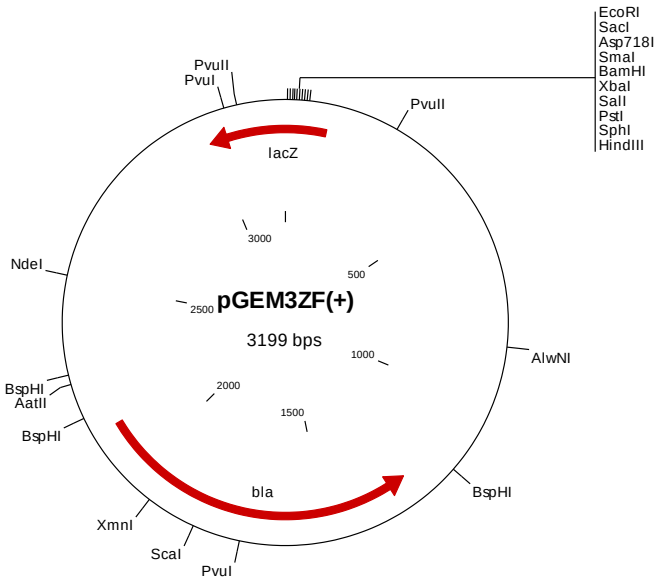

Figure 30 GEM3Zf(+).Vector used for cloning upstream and downstream fragments to generate the *nth* and *mutY* deletion knockout constructs (Moolla *et al*., 2014 and Hassim *et al*., 2015). The plasmid was also used as a positive control for *E.coli* transformations.

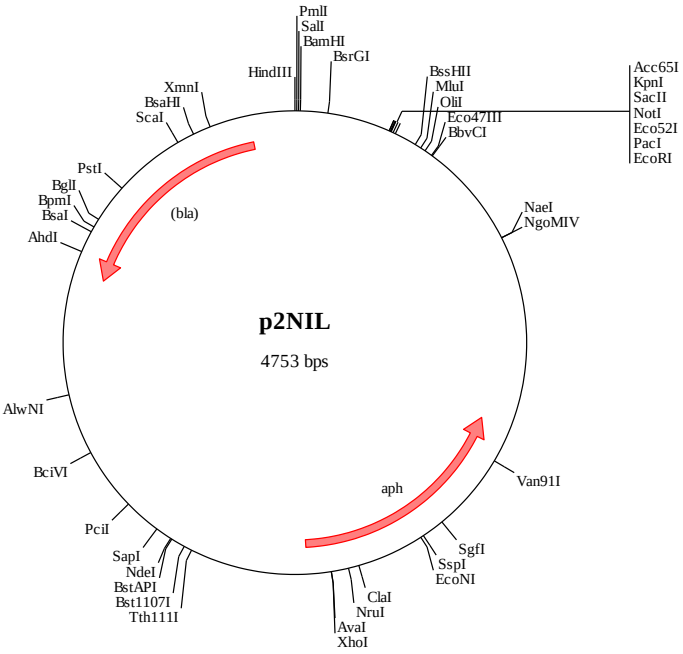

Figure 31. p2NIL suicide vector The suicide vector used in 3 way cloning, where the upstream and downstream fragments for the *nth* and *mutY* deletion constructs were simultaneously ligated into p2NIL (Parish and Stoker, 2000).

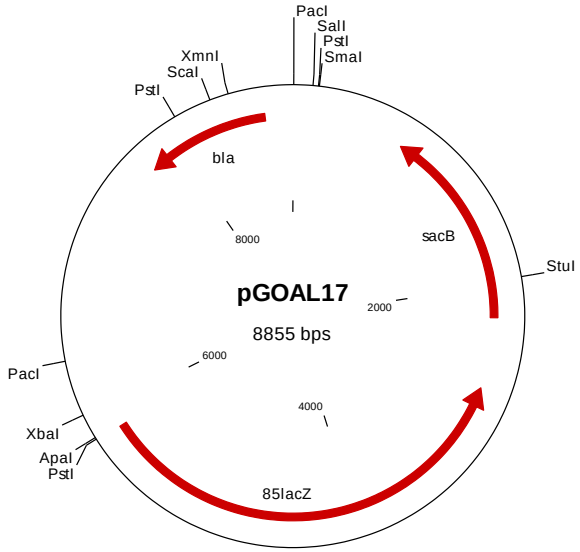

Figure 32. pGOAL17. The vector with the Pac cassette (*sacB*, *lacZ*,) which was inserted into p2NIL vector carrying the *mutY* deletion allele to generate p2NILΔ*mutY*::pGOAL17 (Hassim *et al.*, 2015).

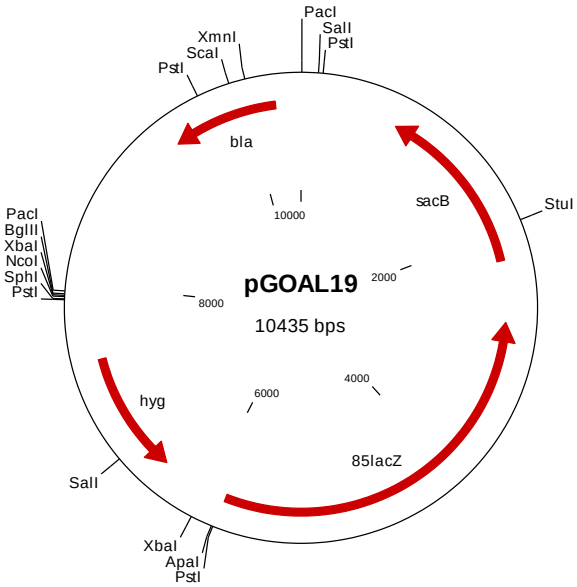

Figure 33. pGOAL19. The vector with the Pac cassette (*sacB*, *lacZ*, and *hyg*) which was inserted into the p2NILvector carrying the*nth* deletion allele to generate p2NILΔ*nth*::pGOAL19 (Moolla *et al.*, 2014).

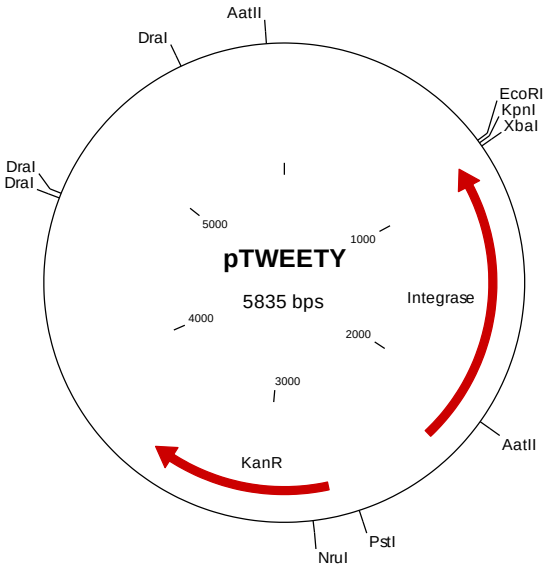

Figure 34. pTWEETY. Vector used for constructing the all the complementation vectors.

5.4: Effect of hydrogen peroxide (H_2O_2) on the survival of *M. Smegmatis*

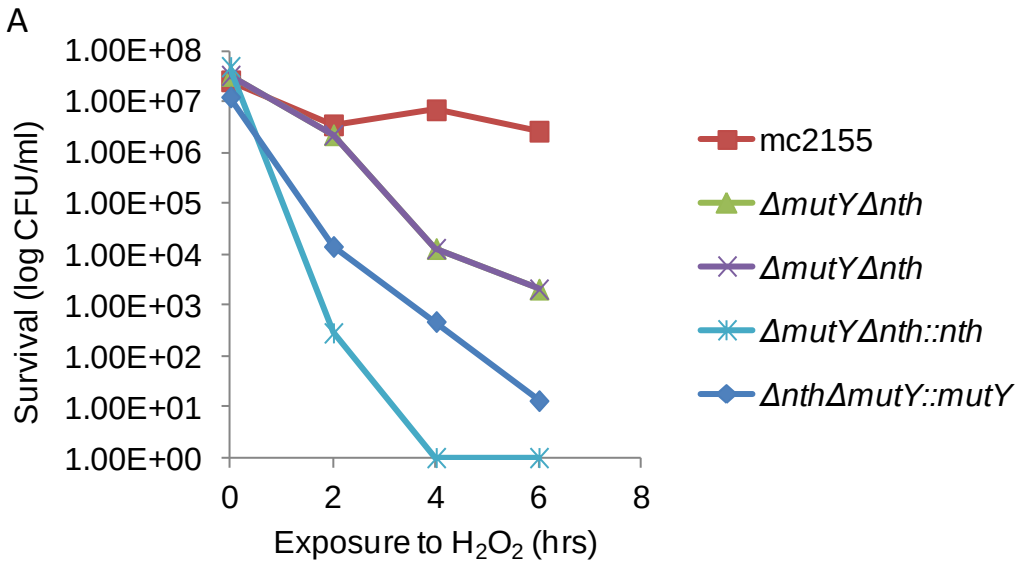

B

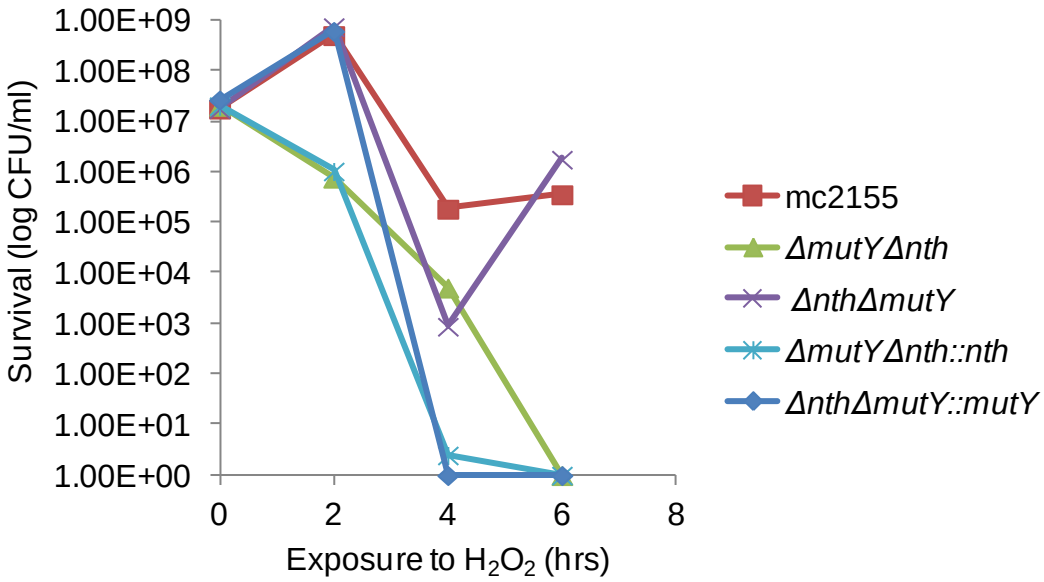
1.00E+09
1.00E+08
1.00E+07
1.00E+06
1.00E+05
1.00E+04
1.00E+03
1.00E+02
1.00E+01
1.00E+00
Survival (log CFU/ml)
0
2
4
6
8
Exposure to H2O2 (hrs)
mc2155
ΔmutYΔnth
ΔnthΔmutY
ΔmutYΔnth::nth
ΔnthΔmutY::mutY

C

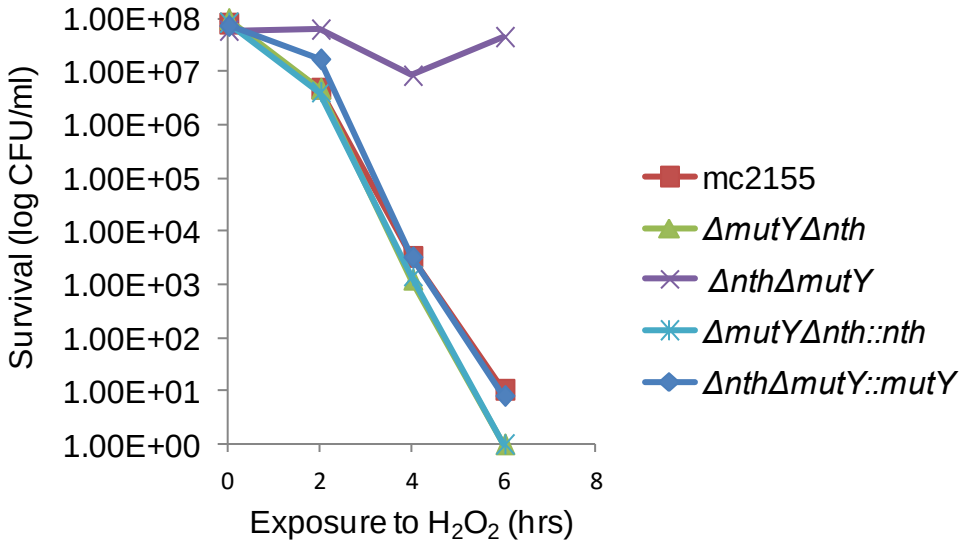
1.00E+08
1.00E+07
1.00E+06
1.00E+05
1.00E+04
1.00E+03
1.00E+02
1.00E+01
1.00E+00
Survival (log CFU/ml)
0
2
4
6
8
Exposure to H2O2 (hrs)
mc2155
ΔmutYΔnth
ΔnthΔmutY
ΔmutYΔnth::nth
ΔnthΔmutY::mutY

D

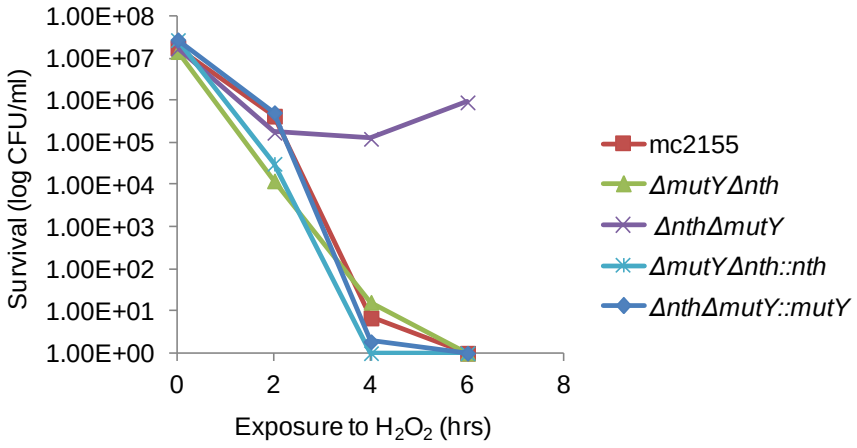

Figure 35. Survival of the mc^{2}155, Δ*mutY*Δ*nth*, Δ*mutY*Δ*nth* and complemented strains under oxidative stress conditions. Early log phase cultures were treated with 2.0 mM H_2O_2 and growth was monitored as CFUs/ml over a 6 h period.

5.5 DNA molecular weight markers

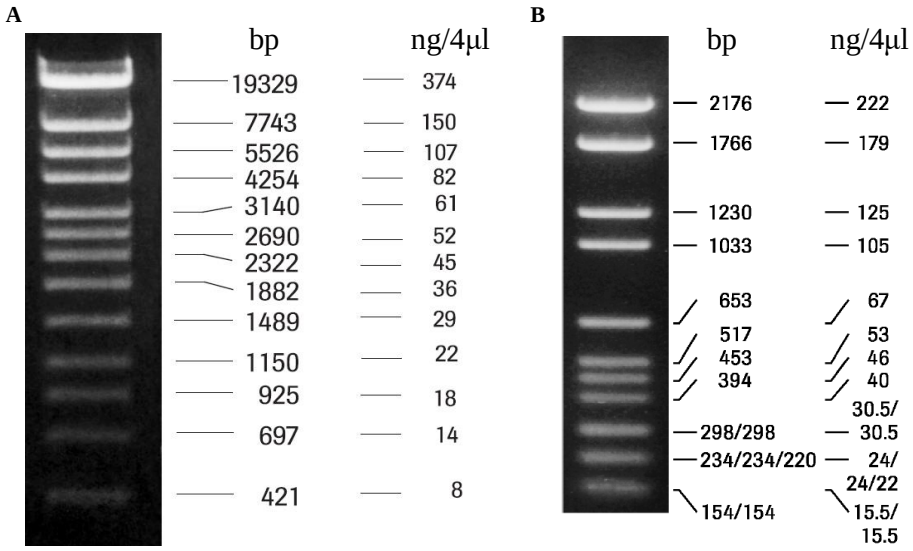

Figure 36. The DNA molecular weight markers. A. Marker λIV. B. Marker λVI used in this study (Roche Biochemicals)

6. References

AHMAD, S. (2011) Pathogenesis, immunology, and diagnosis of latent *Mycobacterium tuberculosis* infection. *Clinical and Developmental Immunology,* doi:10.1155/2011/814943

AKIRA, S., UEMATSU, S. & TAKEUCHI, O. (2006) Pathogen recognition and innate immunity. *Cell,* 124**,** 783-801.

ANDREWS, J. R., SHAH, N. S., GANDHI, N., MOLL, T. & FRIEDLAND, G. (2007) Multidrug-resistant and extensively drug-resistant tuberculosis*:* implications for the HIV epidemic and antiretroviral therapy rollout in South Africa. *Journal of Infectious Diseases,* 196**,** S482-S490.

ASAD, N. R., ASAD, L. M. B. O., ALMEIDA, C. E. B. D., FELZENSZWALB, I., CABRAL-NETO, J. B. & LEITÃO, A. C. (2004) Several pathways of hydrogen peroxide action that damage the *E. coli* genome. *Genetics and Molecular Biology,* 27**,** 291-303.

AUNG, K., VAN DEUN, A., DECLERCQ, E., SARKER, M., DAS, P., HOSSAIN, M. & RIEDER, H. (2014) Successful '9-month Bangladesh regimen 'for multidrug-resistant *tuberculosis* among over 500 consecutive patients. *The International Journal of Tuberculosis and Lung Disease,* 18**,** 1180-1187.

BABIOR, B. M. (1999) NADPH oxidase: an update. *Blood,* 93**,** 1464-1476.

BARRY, C. E., BOSHOFF, H. I., DARTOIS, V., DICK, T., EHRT, S., FLYNN, J., SCHNAPPINGER, D., WILKINSON, R. J. & YOUNG, D. (2009) The spectrum of latent tuberculosis: rethinking the biology and intervention strategies. *Nature Reviews Microbiology,* 7**,** 845-855.

BAUCHE, C. & LAVAL, J. (1999) Repair of oxidized bases in the extremely radiation-resistant bacterium *Deinococcus radiodurans*. *Journal of bacteriology,* 181**,** 262-269.

BÉBIEN, M., LAGNIEL, G., GARIN, J., TOUATI, D., VERMÉGLIO, A. & LABARRE, J. (2002) Involvement of superoxide dismutases in the response of *Escherichia coli* to selenium oxides. *Journal of bacteriology,* 184**,** 1556-1564.

BOSHOFF, H. I., REED, M. B., BARRY, C. E. & MIZRAHI, V. (2003) DnaE2 polymerase contributes to in vivo survival and the emergence of drug resistance in *Mycobacterium tuberculosis*. *Cell,* 113**,** 183-193.

BOUTRY, C., DELPLACE, B., CLIPPE, A., FONTAINE, L. & HOLS, P. (2013) SOS response activation and competence development are antagonistic mechanisms in *Streptococcus thermophilus*. *Journal of bacteriology,* 195**,** 696-707.

BRENT, R. & PTASHNE, M. (1981) Mechanism of action of the *lexA* gene product. *Proceedings of the National Academy of Sciences,* 78**,** 4204-4208.

BREWER, T. F. (2000) Preventing tuberculosis with bacillus Calmette-Guerin vaccine: a meta-analysis of the literature. *Clinical Infectious Diseases,* 31**,** S64-S67.

BRIDGE, G., RASHID, S. & MARTIN, S. A. (2014) DNA mismatch repair and oxidative DNA damage: implications for cancer biology and treatment. *Cancers,* 6**,** 1597-1614.

BUCHMEIER, N., LIBBY, S., XU, Y., LOEWEN, P., SWITALA, J., GUINEY, D. & FANG, F. (1995) DNA repair is more important than catalase for *Salmonella* virulence in mice. *Journal of Clinical Investigation,* 95**,** 1047-1053.

CAAMANO, J. & HUNTER, C. A. (2002) NF-κB family of transcription factors: central regulators of innate and adaptive immune functions. *Clinical microbiology reviews,* 15**,** 414-429.

CADET, J., DELATOUR, T., DOUKI, T., GASPARUTTO, D., POUGET, J.-P., RAVANAT, J.-L. & SAUVAIGO, S. (1999) Hydroxyl radicals and DNA base damage. *Mutation Research/Fundamental and Molecular Mechanisms of Mutagenesis,* 424**,** 9-21.

CADET, J. & WAGNER, J. R. (2014) Oxidatively generated base damage to cellular DNA by hydroxyl radical and one-electron oxidants: Similarities and differences. *Archives of biochemistry and biophysics,* 557**,** 47-54.

CALVER, A. D., MURRAY, M., STRAUSS, O. J., STREICHER, E. M., HANEKOM, M., LIVERSAGE, T., MASIBI, M., VAN HELDEN, P. D., WARREN, R. M. & VICTOR, T. C. (2010) Emergence of increased resistance and extensively drug-resistant tuberculosis despite treatment adherence, South Africa. *Emerging infectious diseases,* 16**,** 264-271.

CHAO, M. C. & RUBIN, E. J. (2010) Letting sleeping dogs lie: does dormancy play a role in tuberculosis? *Annual review of microbiology,* 64**,** 293-311.

CHAWLA, M., PARIKH, P., SAXENA, A., MUNSHI, M., MEHTA, M., MAI, D., SRIVASTAVA, A. K., NARASIMHULU, K., REDDING, K. E. & VASHI, N. (2012) *Mycobacterium tuberculosis* WhiB4 regulates oxidative stress response to modulate survival and dissemination in vivo. *Molecular microbiology,* 85**,** 1148-1165.

CHEN, L., XIE, Q.-W. & NATHAN, C. (1998) Alkyl hydroperoxide reductase subunit C (AhpC) protects bacterial and human cells against reactive nitrogen intermediates. *Molecular cell,* 1**,** 795-805.

CHHABRA, N., ASERI, M., DIXIT, R. & GAUR, S. (2012) Pharmacotherapy for multidrug resistant tuberculosis. *Journal of pharmacology & pharmacotherapeutics,* 3**,** 98-104.

COLDITZ, G. A., BREWER, T. F., BERKEY, C. S., WILSON, M. E., BURDICK, E., FINEBERG, H. V. & MOSTELLER, F. (1994) Efficacy of BCG vaccine in the prevention of tuberculosis: meta-analysis of the published literature. *The Journal of the American Medical Association,* 271**,** 698-702.

COLE, S. T., BROSCH, R., PARKHILL, J., GARNIER, T., CHURCHER, C., HARRIS, D., GORDON, S. V., EIGLMEIER, K., GAS, S., BARRY, C. E., 3RD, TEKAIA, F., BADCOCK, K., BASHAM, D., BROWN, D., CHILLINGWORTH, T., CONNOR, R., DAVIES, R., DEVLIN, K., FELTWELL, T., GENTLES, S., HAMLIN, N., HOLROYD, S., HORNSBY, T., JAGELS, K., KROGH, A., MCLEAN, J., MOULE, S., MURPHY, L., OLIVER, K., OSBORNE, J., QUAIL, M. A., RAJANDREAM, M. A., ROGERS, J., RUTTER, S., SEEGER, K., SKELTON, J., SQUARES, R., SQUARES, S., SULSTON, J. E., TAYLOR, K., WHITEHEAD, S. & BARRELL, B. G. (1998) Deciphering the biology of *Mycobacterium tuberculosis* from the complete genome sequence. *Nature,* 393**,** 537-544.

CORBETT, E. L., WATT, C. J., WALKER, N., MAHER, D., WILLIAMS, B. G., RAVIGLIONE, M. C. & DYE, C. (2003) The growing burden of *tuberculosis*: global trends and interactions with the HIV epidemic. *Archives of Internal Medicine,* 163**,** 1009-21.

COX, H., KEBEDE, Y., ALLAMURATOVA, S., ISMAILOV, G., DAVLETMURATOVA, Z., BYRNES, G., STONE, C., NIEMANN, S., RÜSCH-GERDES, S. & BLOK, L. (2006) Tuberculosis recurrence and mortality after successful treatment: impact of drug resistance. *PLoS Med,* 3**,** 1836-1843.

DARWIN, K. H. & NATHAN, C. F. (2005) Role for nucleotide excision repair in virulence of *Mycobacterium tuberculosis*. *Infection and immunity,* 73**,** 4581-4587.

DAVID, S. S., O'SHEA, V. L. & KUNDU, S. (2007) Base-excision repair of oxidative DNA damage. *Nature,* 447**,** 941-950.

DAVIS, E., SEDGWICK, S. & COLSTON, M. (1991) Novel structure of the *recA* locus of *Mycobacterium tuberculosis* implies processing of the gene product. *Journal of bacteriology,* 173**,** 5653-5662.

DAVIS, E. O., DULLAGHAN, E. M. & RAND, L. (2002) Definition of the mycobacterial SOS box and use to identify LexA-regulated genes in *Mycobacterium tuberculosis*. *Journal of bacteriology,* 184**,** 3287-3295.

DE OLIVEIRA, A. H. S., DA SILVA, A. E., DE OLIVEIRA, I. M., HENRIQUES, J. A. P. & AGNEZ-LIMA, L. F. (2014) MutY-glycosylase: An overview on mutagenesis and activities beyond the GO system. *Mutation Research/Fundamental and Molecular Mechanisms of Mutagenesis,* 769**,** 119-131.

DEMPLE, B. & HARRISON, L. (1994) Repair of oxidative damage to DNA: enzymology and biology. *Annual review of biochemistry,* 63**,** 915-948.

DEN HENGST, C. D. & BUTTNER, M. J. (2008) Redox control in actinobacteria. *Biochimica et Biophysica Acta (BBA)-General Subjects,* 1780**,** 1201-1216.

DENVER, D. R., SWENSON, S. L. & LYNCH, M. (2003) An evolutionary analysis of the helix-hairpin-helix superfamily of DNA repair glycosylases. *Molecular biology and evolution,* 20**,** 1603-1611.

DERETIC, V., PHILIPP, W., DHANDAYUTHAPANI, S., MUDD, M., CURCIC, R., GARBE, T., HEYM, B., VIA, L. & COLE, S. (1995) *Mycobacterium tuberculosis* is a natural mutant with

an inactivated oxidative-stress regulatory gene: implications for sensitivity to isoniazid. *Molecular microbiology,* 17**,** 889-900.

DILLINGHAM, M. S., SPIES, M. & KOWALCZYKOWSKI, S. C. (2003) RecBCD enzyme is a bipolar DNA helicase. *Nature,* 423**,** 893-897.

DIXON, D. A. & KOWALCZYKOWSKI, S. C. (1995) Role of the *Escherichia coli* recombination hotspot, χ, in RecABCD-dependent homologous pairing. *Journal of Biological Chemistry,* 270**,** 16360-16370.

DOOLEY JR, S. W., CASTRO, K., HUTTON, M., MULLAN, R., POLDER, J. & SNIDER JR, D. (1990) Guidelines for preventing the transmission of *tuberculosis* in health-care settings, with special focus on HIV-related issues. *Recommendations and reports: Morbidity and mortality weekly report. Recommendations and reports/Centers for Disease Control,* 39**,** 1-29.

DOS VULTOS, T., MESTRE, O., TONJUM, T. & GICQUEL, B. (2009) DNA repair in *Mycobacterium tuberculosis* revisited. *FEMS microbiology reviews,* 33**,** 471-487.

DOYLE, J. J. (1987) A rapid DNA isolation procedure for small quantities of fresh leaf tissue. *Phytochem bulletin* 19**,** 11-15.

EHRT, S., GUO, X. V., HICKEY, C. M., RYOU, M., MONTELEONE, M., RILEY, L. W. & SCHNAPPINGER, D. (2005) Controlling gene expression in mycobacteria with anhydrotetracycline and Tet repressor. *Nucleic Acid Res,* 33 (2), 1-11

EHRT, S. & SCHNAPPINGER, D. (2009) Mycobacterial survival strategies in the phagosome: defence against host stresses. *Cellular microbiology,* 11**,** 1170-1178.

FARNELL, D. A. (2011) Nucleotide excision repair in the three domains of life. *Western Undergraduate Research Journal: Health and Natural Sciences,* 2**,** doi:15206/wujr hns

FINE, P. E. (1995) Variation in protection by BCG: implications of and for heterologous immunity. *The Lancet,* 346**,** 1339-1345.

FLYNN, J. L. & CHAN, J. 2001. Tuberculosis: latency and reactivation. *Infection and immunity,* 69**,** 4195-4201.

FRAGA, C. G., SHIGENAGA, M. K., PARK, J.-W., DEGAN, P. & AMES, B. N. (1990) Oxidative damage to DNA during aging: 8-hydroxy-2'-deoxyguanosine in rat organ DNA and urine. *Proceedings of the National Academy of Sciences,* 87**,** 4533-4537.

FRIEDBERG, E. C., WALKER, G. C., SIEDE, W. & WOOD, R. D. (2005) *DNA repair and mutagenesis, American Society for Microbiology Press,* Second Edition Washington, DC.

FRIEDEN, T. R. & SBARBARO, J. A. (2007) Promoting adherence to treatment fortuberculosis: the importance of direct observation. *Bulletin of the World Health Organization,* 85**,** 407-409.

FROMME, J. C., BANERJEE, A. & VERDINE, G. L. (2004) DNA glycosylase recognition and catalysis. *Current opinion in structural biology,* 14**,** 43-49.

FU, L. & FU-LIU, C. 2002. Is Mycobacterium tuberculosis a closer relative to Gram-positive or Gram–negative bacterial pathogens? *Tuberculosis,* 82**,** 85-90

GANDHI, N. R., NUNN, P., DHEDA, K., SCHAAF, H. S., ZIGNOL, M., VAN SOOLINGEN, D., JENSEN, P. & BAYONA, J. (2010) Multidrug-resistant and extensively drug-resistant *tuberculosis*: a threat to global control of tuberculosis. *The Lancet,* 375**,** 1830-1843.

GENGENBACHER, M. & KAUFMANN, S. H. 2012. *Mycobacterium tuberculosis*: success through dormancy. *FEMS microbiology reviews,* 36**,** 514-532.

GOGOS, A., CILLO, J., CLARKE, N. D. & LU, A.-L. (1996) Specific recognition of A/G and A/7, 8-dihydro-8-oxoguanine (8-oxoG) mismatches by *Escherichia coli* MutY: removal of the C-terminal domain preferentially affects A/8-oxoG recognition. *Biochemistry,* 35**,** 16665-16671.

GORDHAN, B. G. & PARISH, T. (2001) Gene replacement using pretreated DNA**.** . IN PARISH, T. & STOKER, N. G. (Eds.) *Mycobacterium tuberculosis protocols.* Totowa, New Jersey, Humana Press.

GREEN, J. & PAGET, M. S. (2004) Bacterial redox sensors. *Nature Reviews Microbiology,* 2**,** 954-966.

GROS, L., SAPARBAEV, M. K. & LAVAL, J. (2002) Enzymology of the repair of free radicals-induced DNA damage. *Oncogene,* 21**,** 8905-8925.

GUAN, Y., MANUEL, R. C., ARVAI, A. S., PARIKH, S. S., MOL, C. D., MILLER, J. H., LLOYD, R. S. & TAINER, J. A. (1998) MutY catalytic core, mutant and bound adenine structures

define specificity for DNA repair enzyme superfamily. *Nature Structural & Molecular Biology,* 5**,** 1058-1064.

GUO, Y., BANDARU, V., JARUGA, P., ZHAO, X., BURROWS, C. J., IWAI, S., DIZDAROGLU, M., BOND, J. P. & WALLACE, S. S. (2010) The oxidative DNA glycosylases of *Mycobacterium tuberculosis* exhibit different substrate preferences from their *Escherichia coli* counterparts. *DNA repair,* 9**,** 177-190.

GÜTHLEIN, C., WANNER, R. M., SANDER, P., DAVIS, E. O., BOSSHARD, M., JIRICNY, J., BÖTTGER, E. C. & SPRINGER, B. (2009) Characterization of the mycobacterial NER system reveals novel functions of the uvrD1 helicase. *Journal of bacteriology,* 191**,** 555-562.

GUTTERIDGE, J. M. & HALLIWELL, B. (2010) Antioxidants: molecules, medicines, and myths. *Biochemical and biophysical research communications,* 393**,** 561-564.

HAILER, M. K., SLADE, P. G., MARTIN, B. D. & SUGDEN, K. D. (2005) Nei deficient *Escherichia coli* are sensitive to chromate and accumulate the oxidized guanine lesion spiroiminodihydantoin. *Chemical research in toxicology,* 18**,** 1378-1383.

HALL, R. G., II, R. D. L. & GUMBO, T. (2009) Treatment of active pulmonary tuberculosis in adults: current standards and recent advances: insights from the Society of Infectious Diseases Pharmacists. *Pharmacotherapy,* 29**,** 1468-1481.

HANAHAN, D. (1983) Studies on transformation of Escherichia coli with plasmids. *Journal of molecular biology,* 166**,** 557-580.

HARDING, C. V. & BOOM, W. H. (2010) Regulation of antigen presentation by *Mycobacterium tuberculosis*: a role for Toll-like receptors. *Nature Reviews Microbiology,* 8**,** 296-307.

HASSIM, F., PAPADOPOULOS, A. O., KANA, B. D. & GORDHAN, B. G. (2015) A combinatorial role for MutY and Fpg DNA glycosylases in mutation avoidance in *Mycobacterium smegmatis*. *Mutation Research/Fundamental and Molecular Mechanisms of Mutagenesis,* 779**,** 24-32.

HAZRA, T. K., MULLER, J. G., MANUEL, R. C., BURROWS, C. J., LLOYD, R. S. & MITRA, S. (2001) Repair of hydantoins, one electron oxidation product of 8-oxoguanine, by DNA glycosylases of *Escherichia coli*. *Nucleic acids research,* 29**,** 1967-1974.

HEGDE, M. L., HAZRA, T. K. & MITRA, S. (2008) Early steps in the DNA base excision/single-strand interruption repair pathway in mammalian cells. *Cell research,* 18**,** 27-47.

HILLEMANN, D., KUBICA, T., AGZAMOVA, R., VENERA, B., RÜSCH-GERDES, S. & NIEMANN, S. (2005) Rifampicin and isoniazid resistance mutations in *Mycobacterium tuberculosis* strains isolated from patients in Kazakhstan. *The International Journal of Tuberculosis and Lung Disease,* 9**,** 1161-1167.

HÖFLING, C., PAVAN, E., GIAMPAGLIA, C., FERRAZOLI, L., AILY, D., DE ALBUQUERQUE, D. & RAMOS, M. (2005) Prevalence of katG Ser315 substitution and *rpoB* mutations in isoniazid-resistant *Mycobacterium tuberculosis* isolates from Brazil. *The International Journal of Tuberculosis and Lung Disease,* 9**,** 87-93.

HORSBURGH JR, C. R. (2004) Priorities for the treatment of latent *tuberculosis* infection in the United States. *New England Journal of Medicine,* 350**,** 2060-2067.

HUANG, S., KANG, J. & BLASER, M. J. (2006) Antimutator role of the DNA glycosylase mutY gene in *Helicobacter pylori*. *Journal of bacteriology,* 188**,** 6224-6234.

JACOBS, A. L. & SCHÄR, P. (2012) DNA glycosylases: in DNA repair and beyond. *Chromosoma,* 121**,** 1-20.

JICK, S. S., LIEBERMAN, E. S., RAHMAN, M. U. & CHOI, H. K. (2006) Glucocorticoid use, other associated factors, and the risk of tuberculosis. *Arthritis Care & Research,* 55**,** 19-26.

KARIM, S. S. A., CHURCHYARD, G. J., KARIM, Q. A. & LAWN, S. D. (2009) HIV infection and tuberculosis in South Africa: an urgent need to escalate the public health response. *the Lancet,* 374**,** 921-933.

KEUGOUNG, B., FOUELIFACK, F. Y., FOTSING, R., MACQ, J., MELI, J. & CRIEL, B. (2014) A systematic review of missed opportunities for improving tuberculosis and HIV/AIDS control in Sub-saharan Africa: what is still missed by health experts? *The Pan African medical journal,* doi: 11604/pomj.

KISKER, C., KUPER, J. & VAN HOUTEN, B. (2013) Prokaryotic nucleotide excision repair. *Cold Spring Harbor perspectives in biology,* 5**,**1-18

KUABAN, C., NOESKE, J., RIEDER, H., AÏT-KHALED, N., ABENA FOE, J. & TRÉBUCQ, A. (2015) High effectiveness of a 12-month regimen for MDR-TB patients in Cameroon. *The International Journal of Tuberculosis and Lung Disease,* 19**,** 517-524.

KUO, C.-F., MCREE, D. E., FISHER, C. L., O'HANDLEY, S. F., CUNNINGHAM, R. P. & TAINER, J. A. (1992) Atomic structure of the DNA repair [4Fe-4S] enzyme endonuclease III. *Science,* 258**,** 434-440.

KURTHKOTI, K., KUMAR, P., JAIN, R. & VARSHNEY, U. (2008) Important role of the nucleotide excision repair pathway in *Mycobacterium smegmatis* in conferring protection against commonly encountered DNA-damaging agents. *Microbiology,* 154**,** 2776-2785.

KURTHKOTI, K., SRINATH, T., KUMAR, P., MALSHETTY, V. S., SANG, P. B., JAIN, R., MANJUNATH, R. & VARSHNEY, U. (2010) A distinct physiological role of MutY in mutation prevention in mycobacteria. *Microbiology,* 156**,** 88-93.

KURTHKOTI, K. & VARSHNEY, U. (2011) Base excision and nucleotide excision repair pathways in mycobacteria. *Tuberculosis,* 91**,** 533-543.

KURTHKOTI, K. & VARSHNEY, U. (2012) Distinct mechanisms of DNA repair in mycobacteria and their implications in attenuation of the pathogen growth. *Mechanisms of ageing and development,* 133**,** 138-146.

KUZMINOV, A. (1999) Recombinational Repair of DNA Damage in*Escherichia coli* and Bacteriophage λ. *Microbiology and molecular biology reviews,* 63**,** 751-813.

LAGE, C., GONÇALVES, S. R., SOUZA, L. L., DE PÁDULA, M. & LEITÃO, A. C. (2010) Differential survival of *Escherichia* coli *uvrA, uvrB,* and *uvrC* mutants to psoralen plus UV-A (PUVA): Evidence for uncoupled action of nucleotide excision repair to process DNA adducts. *Journal of Photochemistry and Photobiology B: Biology,* 98**,** 40-47.

LAVAL, J., JURADO, J., SAPARBAEV, M. & SIDORKINA, O. (1998) Antimutagenic role of base-excision repair enzymes upon free radical-induced DNA damage. *Mutation Research/Fundamental and Molecular Mechanisms of Mutagenesis,* 402**,** 93-102.

LITTLE, J. W., MOUNT, D. W. & YANISCH-PERRON, C. R. (1981) Purified lexA protein is a repressor of the *recA* and *lexA* genes. *Proceedings of the National Academy of Sciences,* 78**,** 4199-4203.

LOMAX, M. E., SALJE, H., CUNNIFFE, S. & O'NEILL, P. (2005) 8-OxoA inhibits the incision of an AP site by the DNA glycosylases Fpg, Nth and the AP endonuclease HAP1. *Radiation research,* 163**,** 79-84.

LONGO, D. L., HORSBURGH JR, C. R., BARRY III, C. E. & LANGE, C. (2015) Treatment of tuberculosis. *New England Journal of Medicine,* 373**,** 2149-2160.

LÖNNROTH, K. & RAVIGLIONE, M. (2008) Global epidemiology of tuberculosis: prospects for control. *Seminars in respiratory and critical care Medicine.*

LU, A.-L. & CHANG, D.-Y. (1988) A novel nucleotide excision repair for the conversion of an A/G mismatch to C/G base pair in E. coli. *Cell,* 54**,** 805-812.

LU, A.-L., LI, X., GU, Y., WRIGHT, P. M. & CHANG, D.-Y. (2001) Repair of oxidative DNA damage. *Cell biochemistry and biophysics,* 35**,** 141-170.

LUO, W., MULLER, J. G., RACHLIN, E. M. & BURROWS, C. J. (2000) Characterization of spiroiminodihydantoin as a product of one-electron oxidation of 8-oxo-7, 8-dihydroguanosine. *Organic letters,* 2**,** 613-616.

LURIA, S. E. & DELBRÜCK, M. (1943) Mutations of bacteria from virus sensitivity to virus resistance. *Genetics,* 28**,** 491-511.

MA, Z., LIENHARDT, C., MCILLERON, H., NUNN, A. J. & WANG, X. (2010) Global tuberculosis drug development pipeline: the need and the reality. *The Lancet,* 375**,** 2100-2109.

MACHOWSKI, E. E., BARICHIEVY, S., SPRINGER, B., DURBACH, S. I. & MIZRAHI, V. (2007) In vitro analysis of rates and spectra of mutations in a polymorphic region of the Rv0746 PE_PGRS gene of *Mycobacterium tuberculosis*. *Journal of bacteriology,* 189**,** 2190-2195.

MAKI, H. & SEKIGUCHI, M. (1992) MutT protein specifically hydrolyses a potent mutagenic substrate for DNA synthesis. *Nature,* 355 273-275.

MANIATIS, T., FRITSCH, E. F. & SAMBROOK, J. (1982) *Molecular cloning: a laboratory manual*, Cold Spring Harbor Laboratory Cold Spring Harbor, NY.

MARKKANEN, E., DORN, J. & HÜBSCHER, U. (2013) MUTYH DNA glycosylase: the rationale for removing undamaged bases from the DNA. *Front Genet,* 4**,** 1-20

MASAOKA, A., TERATO, H., KOBAYASHI, M., OHYAMA, Y. & IDE, H. (2001) Oxidation of thymine to 5-formyluracil in DNA promotes misincorporation of dGMP and subsequent elongation of a mismatched primer terminus by DNA polymerase. *Journal of Biological Chemistry,* 276**,** 16501-16510.

MCILLERON, H., WASH, P., BURGER, A., NORMAN, J., FOLB, P. I. & SMITH, P. (2006) Determinants of rifampin, isoniazid, pyrazinamide, and ethambutol pharmacokinetics in a cohort of *tuberculosis* patients. *Antimicrobial agents and chemotherapy,* 50**,** 1170-1177.

MICHAELS, M. & MILLER, J. H. (1992) The GO system protects organisms from the mutagenic effect of the spontaneous lesion 8-hydroxyguanine (7, 8-dihydro-8-oxoguanine). *Journal of bacteriology,* 174**,** 6321.

MICHAELS, M. L., PHAM, L., NGHIEM, Y., CRUZ, C. & MILLER, J. H. (1990) MutY, an adenine glycosylase active on GA mispairs, has homology to endonuclease III. *Nucleic acids research,* 18**,** 3841-3845.

MITCHISON, D. (1985) The action of antituberculosis drugs in short-course chemotherapy. *Tubercle,* 66**,** 219-225.

MIZRAHI, V. & ANDERSEN, S. J. (1998) DNA repair in *Mycobacterium tuberculosis*. What have we learnt from the genome sequence? *Molecular microbiology,* 29**,** 1331-1339.

MOGENSEN, T. H. (2009) Pathogen recognition and inflammatory signaling in innate immune defenses. *Clinical microbiology reviews,* 22**,** 240-273.

MOOLLA, N., GOOSENS, V. J., KANA, B. D. & GORDHAN, B. G. (2014) The contribution of Nth and Nei DNA glycosylases to mutagenesis in *Mycobacterium smegmatis*. *DNA repair,* 13**,** 32-41.

MUTTUCUMARU, D. N. & PARISH, T. (2004) The molecular biology of recombination in mycobacteria: what do we know and how can we use it? *Current issues in molecular biology,* 6**,** 145-158.

NG, V. H., COX, J. S., SOUSA, A. O., MACMICKING, J. D. & MCKINNEY, J. D. (2004) Role of KatG catalase-peroxidase in mycobacterial pathogenesis: countering the phagocyte oxidative burst. *Molecular microbiology,* 52**,** 1291-1302.

OLSEN, I., BALASINGHAM, S. V., DAVIDSEN, T., DEBEBE, E., RØDLAND, E. A., VAN SOOLINGEN, D., KREMER, K., ALSETH, I. & TØNJUM, T. (2009) Characterization of the major formamidopyrimidine-DNA glycosylase homolog in *Mycobacterium tuberculosis* and its linkage to variable tandem repeats. *FEMS Immunology & Medical Microbiology,* 56**,** 151-161.

PARISH, T. & STOKER, N. G. (2000) Use of a flexible cassette method to generate a double unmarked *Mycobacterium tuberculosis* tlyA plcABC mutant by gene replacement. *Microbiology,* 146**,** 1969-1975.

PFAFFENEDER, T., SPADA, F., WAGNER, M., BRANDMAYR, C., LAUBE, S. K., EISEN, D., TRUSS, M., STEINBACHER, J., HACKNER, B. & KOTLJAROVA, O. (2014) Tet oxidizes thymine to 5-hydroxymethyluracil in mouse embryonic stem cell DNA. *Nature chemical biology,* 10**,** 574-581.

PHAM, T. T., JACOBS-SERA, D., PEDULLA, M. L., HENDRIX, R. W. & HATFULL, G. F. (2007) Comparative genomic analysis of mycobacteriophage Tweety: evolutionary insights and construction of compatible site-specific integration vectors for mycobacteria. *Microbiology,* 153**,** 2711-2723.

PRAKASH, A., DOUBLIÉ, S. & WALLACE, S. S. (2012) The Fpg/Nei family of DNA glycosylases: substrates, structures and search for damage. *Progress in molecular biology and translational science,* 110**,** 71.

RADMAN, M. (1976) An endonuclease from *Escherichia coli* that introduces single polynucleotide chain scissions in ultraviolet-irradiated DNA. *Journal of Biological Chemistry,* 251**,** 1438-1445.

RAMAKRISHNAN, L. (2012) Revisiting the role of the granuloma intuberculosis.*Nature Reviews Immunology,* 12**,** 352-366.

RAMASWAMY, S. & MUSSER, J. M. (1998) Molecular genetic basis of antimicrobial agent resistance in *Mycobacterium tuberculosis*: 1998 update. *Tubercle and Lung disease,* 79**,** 3-29.

RANA, F., HAWKEN, M., MWACHARI, C., BHATT, S., ABDULLAH, F., POWER, C., GITHUI, W., PORTER, J. & LUCAS, S. (2000) Autopsy study of HIV-1-positive and HIV-1-negative adult medical patients in Nairobi, Kenya. *JAIDS Journal of Acquired Immune Deficiency Syndromes,* 24**,** 23-29.

RASTOGI, R. P., KUMAR, A., TYAGI, M. B. & SINHA, R. P. (2010) Molecular mechanisms of ultraviolet radiation-induced DNA damage and repair. *Journal of nucleic acids,* 2010, 1-32.

RODRIGUES, L. C., DIWAN, V. K. & WHEELER, J. G. (1993) Protective effect of BCG against tuberculous meningitis and miliary tuberculosis: a meta-analysis. *International journal of epidemiology,* 22**,** 1154-1158.

ROSCHE, W. A. & FOSTER, P. L. (2000) Determining mutation rates in bacterial populations. *Methods,* 20**,** 4-17.

ROWLAND, R. & MCSHANE, H. (2011) *Tuberculosis* vaccines in clinical trials. *Expert review of vaccines,* 10**,** 645-658.

SAGBAKKEN, M. FRICH, J. C., BJUNE, G. A. & PORTER, J. D. (2013) Ethical aspects of directly observed tr-eatment for *tuberculosis:* a cross-cultural comparison. *Bio Med Central medical ethics,* 14**,** 1-10

SAKUMI, K., FURUICHI, M., TSUZUKI, T., KAKUMA, T., KAWABATA, S., MAKI, H. & SEKIGUCHI, M. (1993) Cloning and expression of cDNA for a human enzyme that hydrolyzes 8-oxo-dGTP, a mutagenic substrate for DNA synthesis. *Journal of Biological Chemistry,* 268**,** 23524-23530.

SANCAR, A. (1996) DNA excision repair. *Annual review of biochemistry,* 65**,** 43-81.

SANDERS, L H., SUDHAKARAN, J. & SUTTON, M. D. (2009) The FO system prevents ROD-induced mutagenesis and killing in *Psuedomonas aeruginosa*. *FEMS Microbiology Letters,* 294, 89-96

SANDER, P., PAPAVINASASUNDARAM, K., DICK, T., STAVROPOULOS, E., ELLROTT, K., SPRINGER, B., COLSTON, M. J. & BÖTTGER, E. C. (2001) *Mycobacterium bovis* BCG *recA* Deletion Mutant Shows Increased Susceptibility to DNA-Damaging Agents but Wild-Type Survival in a Mouse Infection Model. *Infection and immunity,* 69**,** 3562-3568.

SASINDRAN, S. J. & TORRELLES, J. B. (2011) *Mycobacterium tuberculosis* infection and inflammation: what is beneficial for the host and for the bacterium. *Front Microbiol,* 2.

SHUCK, S. C., SHORT, E. A. & TURCHI, J. J. (2008) Eukaryotic nucleotide excision repair: from understanding mechanisms to influencing biology. *Cell research,* 18**,** 64-72.

SILVA MIRANDA, M., BREIMAN, A., ALLAIN, S., DEKNUYDT, F. & ALTARE, F. (2012) The t*uberculous* granuloma: an unsuccessful host defence mechanism providing a safety shelter for the bacteria? *Clinical and Developmental Immunology,* 2012, doi:10.1155/139127

SINGH, H., KAUR, K. & GIRISH, P. (2012) Multidrug-resistant tuberculosis; a pharmacological view based on revised national tuberculosis control programme DOTS-plus guidelines. *Journal of Pharmaceutical Sciences,* 2**,** 62-68.

SIU, G. K. H., ZHANG, Y., LAU, T. C., LAU, R. W., HO, P.-L., YEW, W.-W., TSUI, S. K., CHENG, V. C., YUEN, K.-Y. & YAM, W.-C. (2011) Mutations outside the rifampicin resistance-determining region associated with rifampicin resistance in *Mycobacterium tuberculosis*. *Journal of antimicrobial chemotherapy,* 66**,** 730-733.

SKORVAGA, M., THEIS, K., MANDAVILLI, B. S., KISKER, C. & VAN HOUTEN, B. (2002) The β-hairpin motif of UvrB is essential for DNA binding, damage processing, and UvrC-mediated incisions. *Journal of biological chemistry,* 277**,** 1553-1559.

SNAPPER, S., MELTON, R., MUSTAFA, S., KIESER, T. & WR JR, J. (1990) Isolation and characterization of efficient plasmid transformation mutants of *Mycobacterium smegmatis*. *Molecular microbiology,* 4**,** 1911-1919.

SOUTHERN, E. M. (1975) Detection of specific sequences among DNA fragments separated by gel electrophoresis. *Journal of molecular biology,* 98**,** 503-517.

SPRINGER, B., MASTER, S., SANDER, P., ZAHRT, T., MCFALONE, M., SONG, J., PAPAVINASASUNDARAM, K., COLSTON, M., BOETTGER, E. & DERETIC, V. (2001) Silencing of Oxidative Stress Response in *Mycobacterium tuberculosis*: Expression Patterns

of ahpC in Virulent and Avirulent Strains and Effect of*ahpC* Inactivation. *Infection and immunity,* 69**,** 5967-5973.
STEENKEN, S. & JOVANOVIC, S. V. (1997) How easily oxidizable is DNA? One-electron reduction potentials of adenosine and guanosine radicals in aqueous solution. *Journal of the American Chemical Society,* 119**,** 617-618.
STOOPS, J. K., ARORA, R., ARMITAGE, L., WANGER, A., SONG, L., BLACKBURN, M. R., KRUEGER, G. R. & RISIN, S. A. 2010. Certain surfactants show promise in the therapy of pulmonary tuberculosis. *In Vivo,* 24**,** 687-694.
STORZ, G. & IMLAYT, J. A. (1999) Oxidative stress. *Current opinion in microbiology,* 2**,** 188-194.
SUVARNAPUNYA, A. E., LAGASSE, H. & STEIN, M. A. (2003) The role of DNA base excision repair in the pathogenesis of *Salmonella enterica serovar Typhimurium*. *Molecular microbiology,* 48**,** 549-559.
TAJIRI, T., MAKI, H. & SEKIGUCHI, M. (1995) Functional cooperation of MutT, MutM and MutY proteins in preventing mutations caused by spontaneous oxidation of guanine nucleotide in *Escherichia coli*. *Mutation Research/DNA Repair,* 336**,** 257-267.
TCHOU, J., MICHAELS, M., MILLER, J. & GROLLMAN, A. (1993) Function of the zinc finger in *Escherichia coli* Fpg protein. *Journal of Biological Chemistry,* 268**,** 26738-26744.
THAYER, M., AHERN, H., XING, D., CUNNINGHAM, R. & TAINER, J. (1995) Novel DNA binding motifs in the DNA repair enzyme endonuclease III crystal structure. *The EMBO Journal,* 14**,** 4108-1412.
TOUATI, D. (1988) Molecular genetics of superoxide dismutases. *Free Radical Biology and Medicine,* 5**,** 393-402.
TUDEK, B. (2003) Imidazole ring-opened DNA purines and their biological significance. *Journal of Biochemistry and Molecular Biology*. 36, 12-19
VAN HOUTEN, B., EISEN, J. A. & HANAWALT, P. C. (2002) A cut above: discovery of an alternative excision repair pathway in bacteria. *Proceedings of the National Academy of Sciences,* 99**,** 2581-2583.
VLASITS, J., JAKOPITSCH, C., SCHWANNINGER, M., HOLUBAR, P. & OBINGER, C. (2007) Hydrogen peroxide oxidation by catalase-peroxidase follows a non-scrambling mechanism. *Federation of European Biochemical Societies letters,* 581**,** 320-324.
VON SONNTAG, C. & SCHUCHMANN, H.-P. (1994) [4] Suppression of hydroxyl radical reactions in biological systems: Considerations based on competition kinetics. *Methods in enzymology,* 233**,** 47-56.
WALLACE, S. S. (1998) Enzymatic processing of radiation-induced free radical damage in DNA. *Radiation research,* 150**,** S60-S79.
WALLACE, S. S., BANDARU, V., KATHE, S. D. & BOND, J. P. (2003) The enigma of endonuclease VIII. *DNA repair,* 2**,** 441-453.
WHO (2015) Global Tuberculosis Report 2015. World Health Organization, Geneva, Switzerland. *Available at www. who. int/tb/publications/global_report/en/.*
WHO (2009) Global tuberculosis control: epidemiology, strategy, financing. *World Health Organization, Report ZOO9.* World Health Organization, Geneva, Switzerland. Available at *http:/www.who.int/tb/publications/global report/ZOO9/en/index. html*.
WHO (2002) Tuberculosis. Tuberculosis fact sheet Number 104. World Health Organization, Geneva, Switzerland. Available at *http://www.who.int/medicinecentre/factsheets/who104*
WILLIAMS, S. D. & DAVID, S. S. (1998) Evidence that MutY is a monofunctional glycosylase capable of forming a covalent Schiff base intermediate with substrate DNA. *Nucleic acids research,* 26**,** 5123-5133.
WOODWORTH, J. S. & BEHAR, S. M. (2006) *Mycobacterium tuberculosis*-specific CD8+ T cells and their role in immunity. *Critical Reviews in Immunology,* 26, 317-352.
YANG, H., FITZ-GIBBON, S., MARCOTTE, E. M., TAI, J. H., HYMAN, E. C. & MILLER, J. H. (2000) Characterization of a Thermostable DNA Glycosylase Specific for U/G and T/G Mismatches from the Hyperthermophilic ArchaeonPyrobaculum aerophilum. *Journal of bacteriology,* 182**,** 1272-1279.

YUE, J., SHI, W., XIE, J., LI, Y., ZENG, E. & WANG, H. (2003) Mutations in the *rpoB* gene of multidrug-resistant *Mycobacterium tuberculosis* isolates from China. *Journal of clinical microbiology,* 41**,** 2209-2212.

ZAHRT, T. C. & DERETIC, V. (2002) Reactive nitrogen and oxygen intermediates and bacterial defenses: unusual adaptations in *Mycobacterium tuberculosis*. *Antioxidants and Redox Signaling,* 4**,** 141-159.

ŽGUR-BERTOK, D. (2013) DNA damage repair and bacterial pathogens. *PLoS Pathog,* 9**,** e1003711.

ZHARKOV, D. O. & GROLLMAN, A. P. (2002) Combining structural and bioinformatics methods for the analysis of functionally important residues in DNA glycosylases 1, 2. *Free Radical Biology and Medicine,* 32**,** 1254-1263.

ZHARKOV, D. O., SHOHAM, G. & GROLLMAN, A. P. (2003) Structural characterization of the Fpg family of DNA glycosylases. *DNA repair,* 2**,** 839-862.

ZHENG, M., ÅSLUND, F. & STORZ, G. (1998) Activation of the OxyR transcription factor by reversible disulfide bond formation. *Science,* 279**,** 1718-1722.

ZHENG, M., WANG, X., TEMPLETON, L. J., SMULSKI, D. R., LAROSSA, R. A. & STORZ, G. (2001) DNA microarray-mediated transcriptional profiling of the *Escherichia coli* response to hydrogen peroxide. *Journal of bacteriology,* 183**,** 4562-4570.

ZIGNOL, M., HOSSEINI, M. S., WRIGHT, A., LAMBREGTS–VAN WEEZENBEEK, C., NUNN, P., WATT, C. J., WILLIAMS, B. G. & DYE, C. (2006) Global incidence of multidrug-resistant tuberculosis. *Journal of Infectious Diseases,* 194**,** 479-485.

ZUMLA, A. (2015) Tackling the Tuberculosis Epidemic in sub-Saharan Africa–unique opportunities arising from the second European Developing Countries Clinical Trials Partnership (EDCTP) programme 2015-2024. *International Journal of Infectious Diseases,* 32**,** 46-49.